Refinement of the national TEM reference model at Lyngby

June 2012 (update from Nov. 2011)

GeoFysikSamarbejdet
AARHUS UNIVERSITY

Table of contents

NOTES ON THE UPDATES OF JUNE 2012

After the redaction of the first version of this report (November 2011), Sorø SkyTEM data were reprocessed (it appeared that some lines were too cut regarding the couplings) and reinverted to update the report of the survey. During this reprocessing hold in February 2012 it was found that the coil response contained in the original *.bia file was not accurate enough. A new estimation of the coil response had given a much better fit of the early gates over the entire survey, especially above forest areas where the coil response has a more important impact due to the higher flight altitude and the lower earth response. This improvement is clearly observed in Figure 31 where the global data residual is clearly better with no more high residual areas compared to the first version.

This update of the coil response lead us to run all inversion tests again. So all figures regarding Sorø data have been updated in this new version of the report, i.e. Figure 1, Figures 20-31 and Figures 33-52 in Appendix 3.

The update does not change the conclusion on the impact of the supplementary time shift of -1.1 μs which induces a higher resistive top layer closer to the value obtained by ERT (Figure 21). However the effect of the starting model (50 or 100 Ωm) becomes almost invisible (which actually gives more confidence on the stability of the inversion process). The figures corresponding to a starting model of 50 Ωm could have been removed, but have been kept so that it does not change the numbering of the figures between the two versions of the report.

The effect of considering gate 5 or 6 as the first gate is still visible for areas where the top 20 m is quite resistive (Figures 23 & 24). In conductive areas, considering only one more gate does not bring real supplementary information. The resistive first layer appears more resistive and closer to the ERT values with the supplementary gate 5, which confirms the interest of considering earliest gates as possible to obtain the best near-surface resolution, especially where the conductivity is not very high. One may notice that the elevation has slightly changed between the two versions of the report for the SkyTEM sections. It is because a refined digital elevation model was applied during the reprocessing of the data. The difference of elevation between ERT and SkyTEM in the North part of profile 1 is due to the fact that the two datasets are not exactly on the same line, despite the distance between the two is less than 100 m.

In Figure 26 with the 2nd profile, the thin slightly less resistive second layer observed with the ERT is now not clearly visible with the new

coil response. However, such small resistivity contrast close to the surface is not expected to be resolved with transient AEM method mainly sensitive to conductors and to differences of conductivity. Moreover, in the first version of the report this second layer appeared much more conductive compared to ERT when considering the gate 5 and the old inaccurate coil response. Now the resistivity is in the same range as the one from ERT in the first 15 m. The application of the new shift still greatly reduces the presence of a conductive top layer, even if there is still a small section at the center of the profile where the resistivity is still more conductive compared to ERT.

For the borehole comparison in Figures 27 & 28, the top layer in the South part of the section is clearly more resistive with the new time shift. It has to be noted that a new version of the lateral constraints for smooth inversion has been applied. It allows the limitation of the effect of resistivity interfaces following the topography by dividing and sharing the constraints between the layers having common elevations. Without these new constraints the top resistive layer on the South part of the profile appears more conductive because of the lateral constraints propagating the conductive first layer closer to a lake and present in the North part of the profile.

Regarding the mean resistivity maps of Figures 1, 29-30, and 33-52, even if the resistivity of the first meters appear lower with the new coil response (with the old or new time shifts), the application of the new time shift still increases the resistivity of the first 5 m and provides values which are closer to the ERT ones. A smaller search radius (now 350 m) for the map kriging has been used to give a better representation of the data after the removing of the couplings. It results also in larger holes in some places compared to the first version. One remarks that almost no difference can be observed between the two time shifts for depths below 20 m (Figures 37-52), which confirms that the application of this new time shift has an effect only on the top first 20 m.

1. SUMMARY

Investigations at the national TEM test site have revealed that the reference model has too low resistivities in the upper 15 m of the model. This is based on a detailed three-dimensional characterization of the site by means of the ERT method and of an electrical conductivity log to clarify any anisotropy at the Lyngby site.

The refinement of the reference model in the upper 15 m showed that there are higher resistivities in the first 5 m of the reference model (Table 1) compared to the original model. Additionally the refinement showed that the anisotropy coefficient at the site is low and the site is homogeneous with small lateral variations, making the site suitable for a one-dimensional model and hence calibration of the ground based and airborne TEM systems.

The fact that the reference model has been changed in the upper part of the model does not influence the deeper part of the model, and consequently the deeper layers in older surveys are mapped correctly.

The refinement of the reference model means that a time shift has to be added to the old time shifts that have already been set in the geometry files used for the Aarhus Workbench. The time shift for different TEM configurations is compiled in Tables Table 2-Table 5. The time shift is about **-1.1 μs** for every ground or airborne system, for both Low and High moments (a slightly higher uncertainty exists for the HM, since this small time shift has almost no effect on this moment).

With this new shift, a better correspondence with ERT measurements has been obtained for the very near-surface (see the example of the Sorø survey in Chapter 6), with higher and more likely resistivities for the first 5 m of the ground (Figure 1).

	Resistivity	Thickness	Depth
Layer 1	33.5	2.1	2.1
Layer 2	46.8	11.0	13.1
Layer 3	155.2	19.6	32.6
Layer 4	9.8	23.0	55.5
Layer 5	2.4	61.1	116.7
Layer 6	270.6	148.3	265.0
Layer 7	3		

Table 1. Refined reference model for the National TEM test site at Lyngby, Aarhus.

Moment	**Difference of time shift**	New/Old factor shift
SLM	**-1.1 µs**	1.0
HM	**-1.1 µs**	1.0

Table 2. Comparison between the old and new calibration shifts for the WalkTEM/TEM40 setup (40m by 40m loop).

Moment	**Difference of time shift**	New/Old factor shift
SLM	**-1.12 µs**	1.0
HM	**-1.18 µs**	1.0

Table 3. Comparison between the old and new calibration shifts for the SkyTEM loop of 132 m² (NiCA project, June 2011).

Moment	**Difference of time shift**	New/Old factor shift
SLM	**-1.09 µs**	1.0
HM	**-1.03 µs**	1.0

Table 4. Comparison between the old and new calibration shifts for the SkyTEM loop of 314 m² (Sorø survey, May 2009).

Moment	**Difference of time shift**	New/Old factor shift
SLM	**-1.13 µs**	1.0
HM	**-1.25 µs**	1.0

Table 5. Comparison between the old and new calibration shifts for the SkyTEM loop of 494 m² (Tønder survey, September 2008).

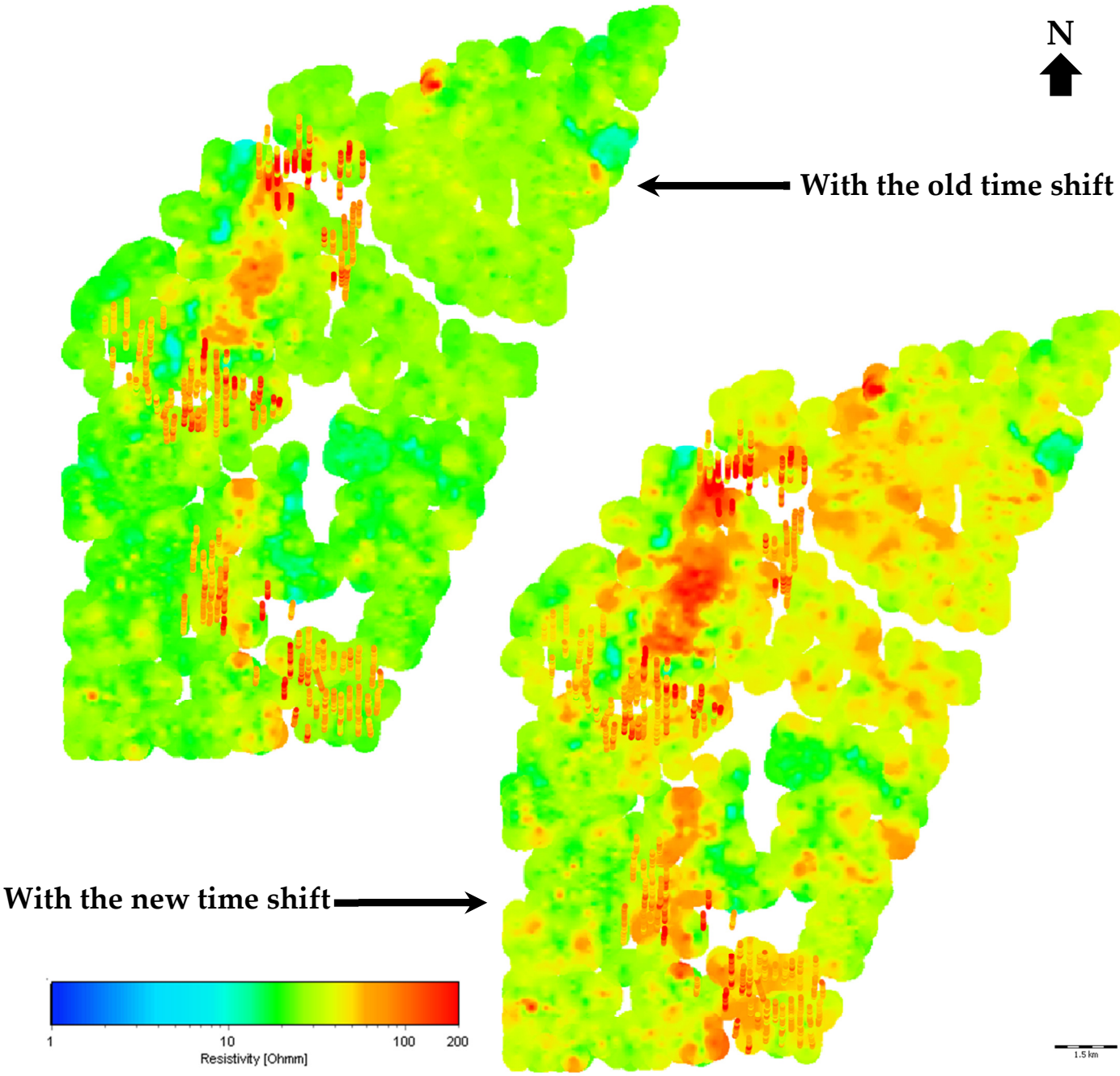

Figure 1. Mean resistivity map for depth 0-5 m - SCI smooth bias inversion on Sorø SkyTEM data with the old and the new time shifts. Inversion parameters: vertical constraint = 2, lat. const.=1.35, starting model of 100 Ωm, and first gate 5$_{old}$. The colored points correspond to the mean resistivity obtain from a SCI smooth inversion of ERT data.

2. INTRODUCTION

The Danish national Transient Electromagnetic (TEM) test site at Lyngby near Aarhus was used for the first time in 2001. The test site was established to ensure that any TEM system used in the Danish groundwater mapping campaign is capable of reproducing the reference model at the test site, so that soundings made with different instruments would end up with the same geophysical model and thereby the same geological model. GeoFysikSamarbejdet[1] (GFS), with Aarhus University (AU) as its scientific partner, was in charge of establishing the test site reference model and developing the calibration procedures.

In 2009, the test site was extended from being a point with a single reference model to include two crossing lines, which opened the test site for calibration, validation and tests for airborne TEM system under survey conditions.

In recent years, the SkyTEM system has undergone rapid developments in terms of inversion methodology, instrumentation and processing schemes. This has resulted in an improved near-surface resolution, with the first usable gate at 6 μs or less. The original test site reference model, which was defined in 2001, was made with focus on the deeper part of the geology, since 1- 2 years ago the first usable gate was at ~18 μs. As a consequence, in 2011 it was decided to make a detailed three-dimensional characterization of the resistivity structure in the upper 15 m of the ground with the electrical resistivity tomography (ERT) method (also known as MEP in Denmark) and supplement with electrical conductivity logs (EC-log) to refine the reference model at the test site, so that the meticulous calibration procedures and standards could be withheld.

This report documents the refining of the reference model and the extension of the national TEM site. The reference model presented in this report is the new reference model to be used for calibrating TEM systems capable of making spot measurements (this includes ground

[1] GFS is a cooperation between the Department of Geoscience, Aarhus University and the Danish Nature Agency. The cooperation dates back to 1999 when it started as a cooperation with the counties. GFS and Aarhus University develop geophysical equipment, field methodologies and data processing software for the methods used in the hydrogeophysical investigations in Denmark. These methods are primarily DC electrical resistivity/induced polarization and time-domain electromagnetics

based TEM systems and SkyTEM). The inversion results of the two profiles presented in this report, the 2009 extension of the test site, are the reference models for the two test lines. New calibration according to the new and refined reference model has been applied and tested on SkyTEM data acquired in Sorø (2009), showing the resistivity change of the first 15 m compared to the old calibration. Finally, other SkyTEM systems have been calibrated with the new reference model.

This report being also of great international interest is written in English.

GeoFysikSamarbejdet 2011

The following scientists have contributed to the report:

Cyril Schamper, post doc

Jesper Pedersen, geophysicist,

Nikolaj Foged, senior geophysicist,

Anders Vest Christiansen, senior researcher,

Kurt Sørensen, professor,

Esben Auken, associate professor.

3. HISTORY OF THE NATIONAL TEM TEST SITE

The Danish national TEM test site at Lyngby, Aarhus was established in 2001 (Figure 2). The test site was established to ensure that any TEM system used in the Danish groundwater campaign is capable of reproducing the reference model at the test site within narrow limits, so that soundings made with different instruments would end up with the same geophysical model and thereby the same geological model. GFS, with the Department of Geoscience, Aarhus University as its scientific partner, was in charge of establishing the test site and defining calibration procedures and requirements to the TEM systems.

Figure 2. Aerial photo showing the National Test site at Lyngby, Aarhus. The dark brown square marks the location of the test site, which is a 40x40 m area. Aerial photo © COWI A/S.

The test site is placed at a location with a relatively high TEM response compared to the noise level as well as relatively homogenous lateral conditions. The conductive top layer is dense clay till, which makes yearly variations small since only the top centimeters are influenced by wet and dry periods.

In 2001, all TEM equipments used in Denmark were Geonics PROTEM systems in combination with the TEM47 transmitter (PROTEM47). GFS defined guidelines for configuration and measuring schemes so that, in principle, all nine Geonics PROTEM47 system from five different consulting companies, should give the same TEM-response. However, this was not the case for the first test where most of the instruments gave significantly different sounding curves. The discrepancies were caused partly by different generations of the PROTEM47-system partly by electronic malfunctioning. With GFS as an objective intermediary, the instrument problems were sorted out with Geonics, and several instruments were updated with new preamplifier components.

In 2002, the test was repeated with a much better consistency for the different instruments. However, minor shifts in data level and small inconsistencies for the very early time gates were still observed. Based on these responses, an average response was calculated and appointed to be the reference response. The reference response is valid for the PROTEM47 system with has a well documented setup including a detailed description of waveform, instrument low-pass filter, geometry etc.

A calibration procedure was developed. The calibration assigns a unique time-shift and a data level shift for the individual TEM systems. After calibration, the different systems could reproduce the reference response within 3% at all time gates. The range of the time shift for the different instruments was up to 0.5 μs and the shift factor up to 9%. The different time-shifts come from variations in transmitter-receiver delays and minor variations in waveforms and low-pass filter cut-off frequencies. The factor shift is assumed to come from inaccurate current measurements by the transmitter.

Over the years, the test site has been used to calibrate TEM instruments not only from Denmark, but also from France, Germany, Switzerland, Australia and the US.

In 2009, the test site was extended from being a square of 40x40 m, to consist of two crossing lines with a reference model for every 40 m, which makes validation and tests possible for airborne TEM systems under production conditions (See Chapter 5).

Due to the vast development of the SkyTEM system in recent years, it is now possible to measure very early gates, thereby achieving a high resolution of the near-surface geology. Therefore a detailed knowledge of the resistivity structure in the upper 15 m is needed. In 2011, it was thus decided to make a detailed three-dimensional mapping of the test site, in order to get a more precise near-surface reference model. This detailed mapping is the main topic of this report.

The two tests of the ground based TEM system in Denmark in 2001 and 2002 are documented in the two reports "Undersøgelse af fejl ved transiente målinger udført med Geonics PROTEM47 måleinstrument, 2001" and "Test og sammenligning af Transient Elektromagnetiske instrumenter I Denmark, 2002".

The calibration procedure is found in the report "Vejledning I kalibrering af Geonics PROTEM47 måleinstrument, 2002", and guidelines for configuration setup and measuring scheme for standard 40x40 m ground based TEM-measurements in "Vejledning for udførelse af TEM sonderinger, 2002". All reports are in Danish and available online from the GFS website (www.gfs.au.dk).

4. NATIONAL TEM SITE REFERENCE MODEL

The rapid development of the SkyTEM system in recent years has made it possible to measure very early gates, thereby obtaining a high resolution of the near-surface geology. In 2011, GFS, has been involved in a number of surveys where the inversion result shows unrealistic very low resistivities in the upper ~5 m of the models. All cases (Sorø-Stenlille, Fyn and Næstved) are SkyTEM surveys where gates earlier than 12 μs have been used.

In order to clarify the reason behind the low resistivity in the upper meters, GFS has meticulously examined the data-processing of the Sorø-Stenlille survey, but no significant errors could be found in the SkyTEM-geometry, waveforms or filters. Furthermore, the height-processing has been carefully investigated, but again no errors were found. Finally, the actual inversion code (em1dinv) has been checked out, and the forward response has been compared with other EM codes, but no significant deviations were found.

GFS suggested a detailed mapping of the national test site to verify if the resistivity model used for calibrating the SkyTEM system is optimal for mapping the upper 15 m. When, more than 10 years ago, the model was determined, focus was not on the near-surface geology, but on the problem of ensuring that the ground based TEM systems all gave the same response and thereby the same resistivity model. Thus, the test site model does not take near-surface geological structures into account, since it is aimed at the deeper part of the geology. The model is then not optimal for calibrating the instruments for the early gates that have been used for the SkyTEM surveys in the last 1-2 years. For surveys completed more than 1-2 years ago, the first used gate was so relatively late (approximately 18 μs) that the near-surface geology could not be resolved due to lack of information from such layers. It is worth noting that with the current SkyTEM system and the addition of the coil-response inversion (see "Himmerland – Vurdering af SkyTEM metoden til sårbarhedskortlægning"), the first usable gate is at approximately 6 μs for the 300 m^2 SkyTEM system.

Preliminary investigations revealed that the 2001 test site model does not have the correct resistivity structure in the upper 15 m. As a consequence, it was decided to make a detailed ERT survey in a dense grid at the test site in order to attain the correct resistivity structure. The ERT measurements were supplemented with an EC-log to clarify any electrical anisotropy in the geological layers. The anisotropy corrected

resistivity structure from the ERT is then used to refine the test site model one last time.

4.1 ERT dataset

The ERT data were collected in the period 5-9. September, 2011. A total of 11 profiles were measured (Figure 3), with a profile length of 160 to 800 m. Ten of the profiles form a dense grid which covers the core of the test site. The ten short profiles have an electrode spacing of 2 m. A small electrode spacing of 2 m secures a high spatial solution and detailed description of the resistivity distribution, by which inhomogeneities are accurately described. The maximum depth of investigation is 15 – 20 m which safely covers the depth of interest. The distance of 15 m between adjacent profiles makes a 3D analysis reliable.

The long West-East orientated profile (800 m), which is in accordance with the SkyTEM profiles measured in connection with the SkyTEM/VTEM verification in 2009, was measured. The long profile, with an electrode spacing of 5 m, has a higher depth of investigation and a lower near-surface resolution compared to the short profiles with a 2 m electrode spacing.

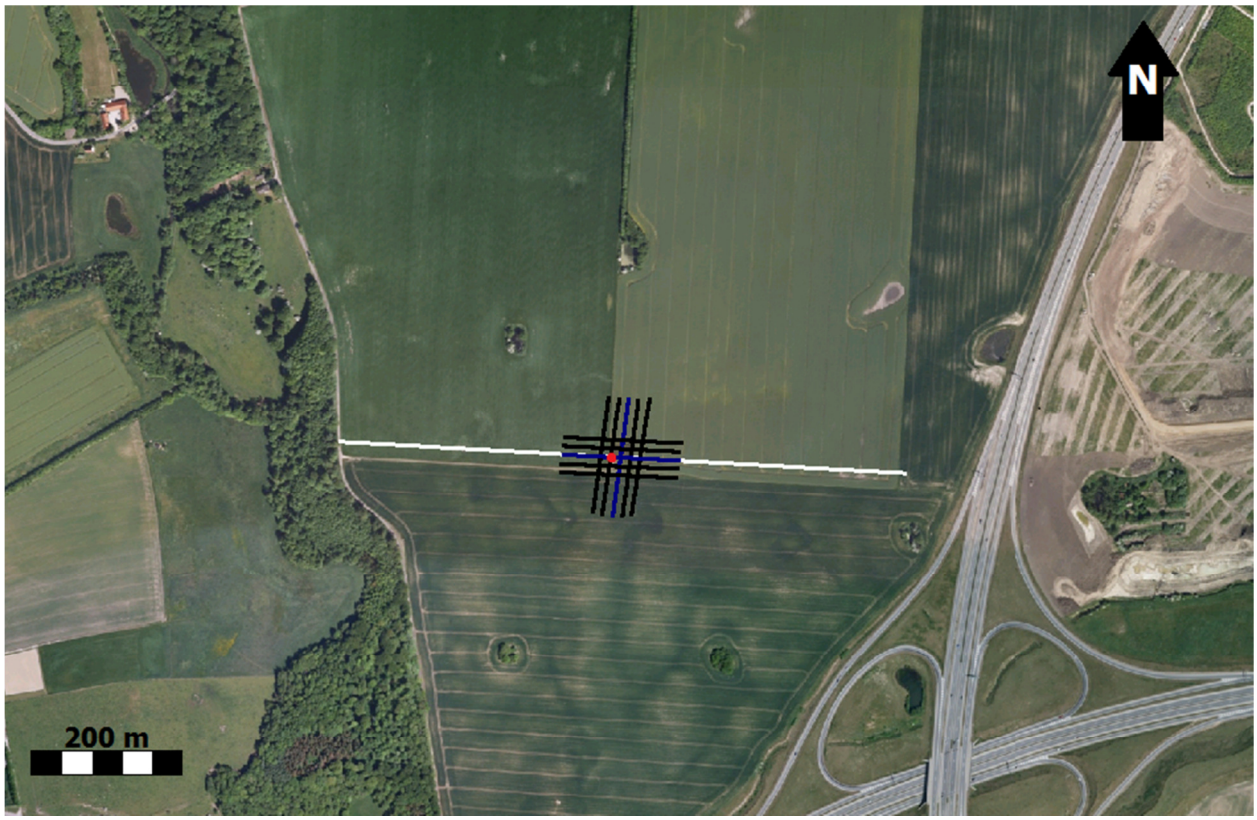

Figure 3. Detailed location map of the Danish National test site at Lyngby, Aarhus. The white line marks the position of the 800 m long profile with an electrode spacing of 5 m, and the black and blue lines are the 160 meter long profiles with an electrode spacing of 2 m. The inversion results of the two profiles shown with blue lines are shown in Figures Figure 4 and Figure 6. The EC-log is shown as a red circle. Aerial photo © COWI A/S.

Additionally, one EC-log was measured in order to quantify macro-anisotropy in the geological layers. In this context, it should be noted that the ERT measurements are sensitive to both the horizontal and the vertical resistivities, whereas the TEM measurements are sensitive to the horizontal resistivity only. This makes a direct comparison between TEM and ERT resistivities, on this level of accuracy, problematic if the anisotropy is not known. The anisotropy is calculated from the EC-log, as it measures the resistivity at a very fine scale of few cm. The EC-log position is shown in Figure 3 as a red circle.

4.2 Processing/ SCI inversion

The ERT data were processed in the Aarhus Workbench package following the guidelines presented by GFS in "Guide to processing and inversion of CVES data, 2009". In general the data quality for all pro-

files is very good, and less than 1% of the data points had to be removed in the processing.

The data were inverted with a 1D full non-linear damped least-squares inversion approach, the Spatial Constrained Inversion (SCI) concept by Viezolli et al., 2008. In general, a three-layer model is needed to fit the 160 m long profiles, whereas a five-layer layer model is needed for the 800 m long profile with a higher depth of investigation. As a consequence, all profiles were inverted with a five-layer model in the SCI-setup.

4.3 Inversion results

Figures Figure 4 and Figure 6 show the inversion results of two of the short profiles (160 m). The location of the profiles is shown in Figure 3. Their directions are close to the ones of the two profiles used for extending the national TEM site (Chapter 5). In general, the data fit is very good. Sounding curves and models for two soundings at the center of the two profiles attest that and are shown in Figures Figure 5 and Figure 7.

All profiles can be described with a three-layer model, where the first layer is 2 m thick and has a resistivity of around 30-40 Ωm. Beneath that layer is an 11 m thick layer with a resistivity of 40-60 Ωm. The topsoil layer of 2 m thickness is almost the plow layer of the field. As a consequence, it is slightly more conductive, as compared to the second layer in the sections, even though both layers constitute the till layer (see chapter 5.4). The boundary to the resistive sand and gravel layer is found in a depth of ~13 m.

Model parameters and UTM coordinates for the profiles are listed in Appendix 1.

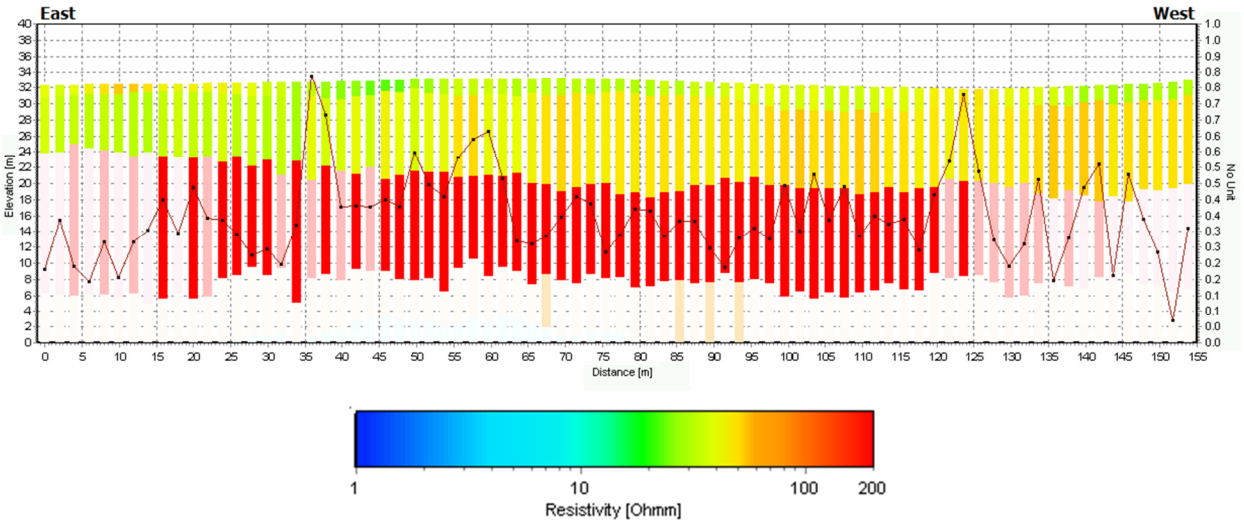

Figure 4. Resistivity section of the East-West profile. The location of the profile is shown in Figure 3. The profile crosses the South-North orientated profile in a profile distance of 80 m. The residual for the individual soundings is shown on top of the model section (legend at the right axis). The depth of investigation (DOI) is shown as faded bars. SCI inversion parameters: 5-layer model with a starting resistivity of 50 Ω.m, and loose lateral constraints of 1.5.

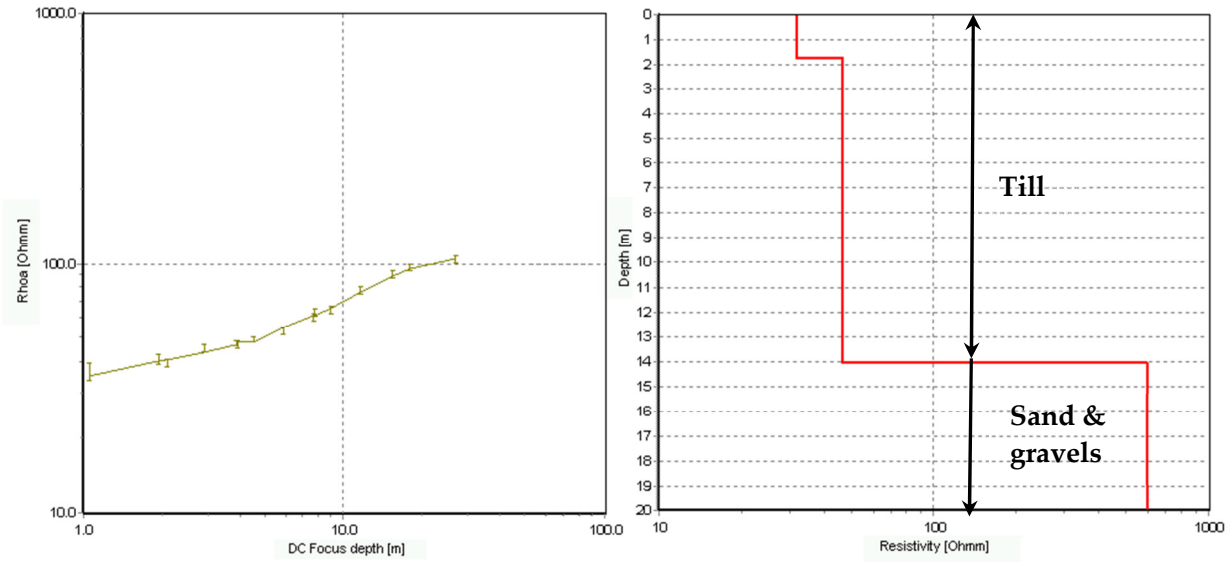

Figure 5. Left: Data fit for the sounding at the center of the West-East profile (Profile distance of 80 m). Right: Corresponding 1D model.

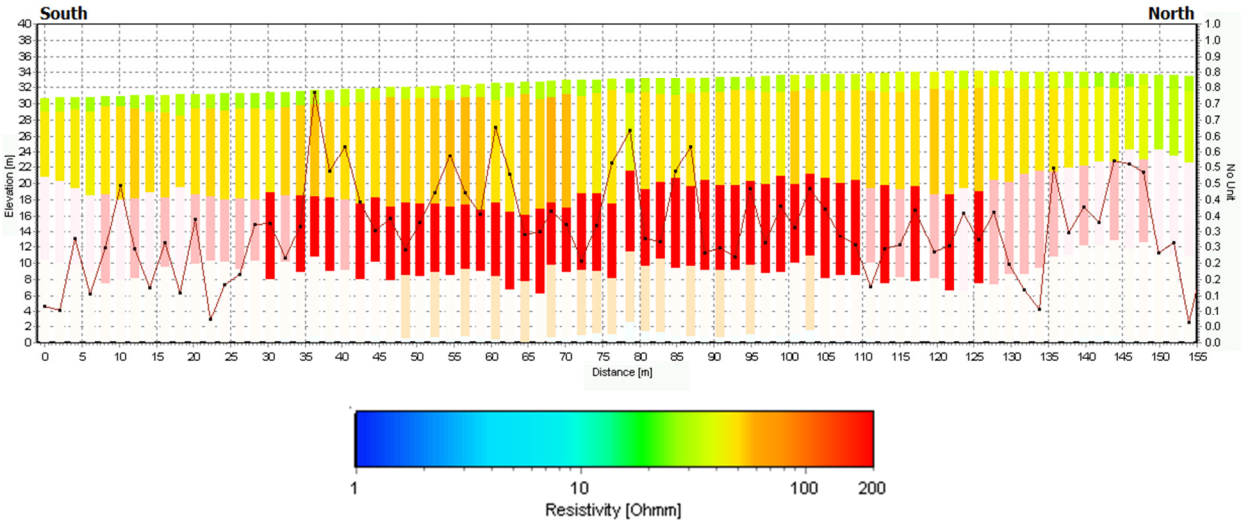

Figure 6. Resistivity section of the South-North profile. The location of the profile is shown in Figure 3. The profile crosses the West-East orientated profile in a profile distance of 80 m. The residual for the individual soundings is shown on top of the model section (legend at the right axis). The DOI is shown as faded bars. SCI inversion parameters: 5-layer model with a starting resistivity of 50 Ω.m, and loose lateral constraints of 1.5.

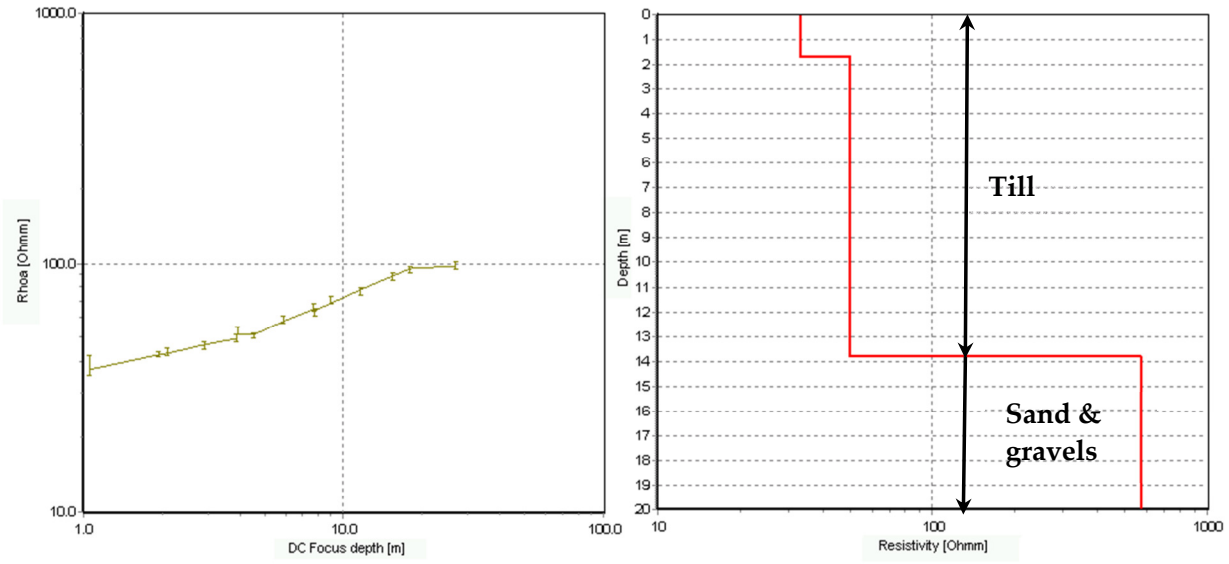

Figure 7. Left: Data fit for the sounding at the center of the South-North profile (Profile distance of 80 m). Right: Corresponding 1D model.

4.4 Refining the reference model in the upper 15 meters

In order to refine the reference model in the upper 15 m, a 60x60 m square was selected (red square in Figure 8). In this square, the data coverage is very high with only 15 m between the profiles and 2 meter electrode spacing, resulting in a total of 312 electrodes in the 3600 m^2 large grid. This ensures a very high resolution. Figure 8 also shows the top of the third layer of the 5-layer model issued from the SCI inversion, which is resistive and corresponds to sand and gravel. This map indicates a quite low spatial variability of the top of this layer, located between 12 and 15 m inside the square where spot calibration of SkyTEM systems is made. The refinement of the reference model only concerns the first two layers located above this interface.

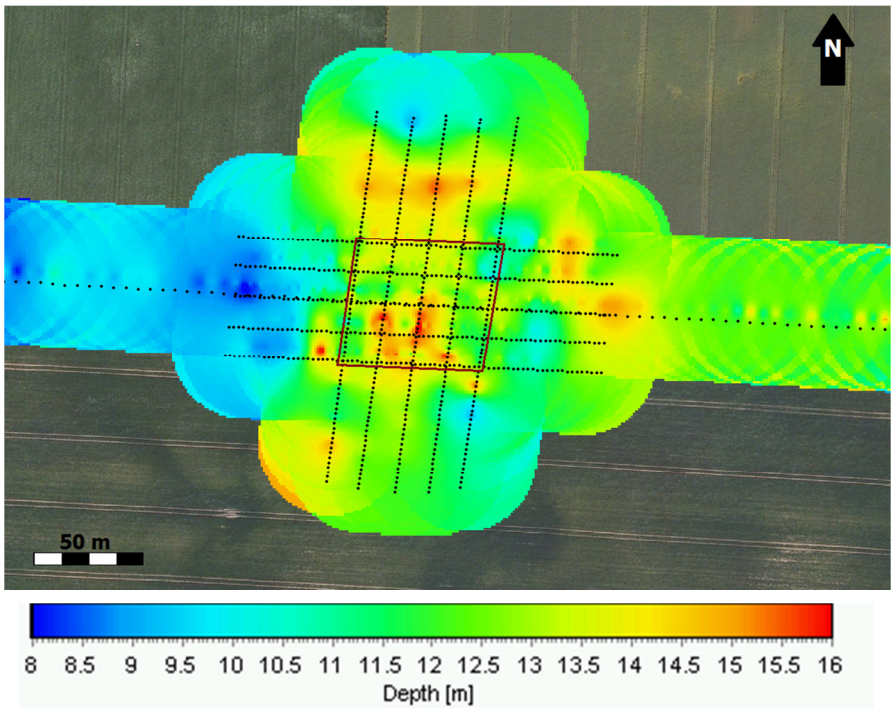

Figure 8. Depth to the boundary between the till layer with a resistivity of 33-47 Ωm and the sand/gravel layer with a resistivity above 100 Ωm. The red square marks the 60x60 m grid from which the mean thickness and the mean resistivity of the layers are calculated. Aerial photo © COWI A/S.

To show the spatial variability of the resistivity values of the two near-surface layers, a number of mean resistivity maps were created. The generated mean-resistivity maps have been gridded using the Kriging method, with a node spacing of 1 m and a search radius of 30 m, to obtain a regular grid of resistivities for each mean resistivity interval. The mean resistivity maps are shown in Figure 9 and are from a depth of 0-1 m, 1-2 m and 7-8 m (note that the resistivity color scale is linear and narrow so that small variations can be observed). As observed, the resistivity values are quite homogeneous for the different depth intervals. This confirms that the reference site can be approximated by a 1D model with a good precision.

From the 5-layer model of the SCI inversion we have proceeded to an average of the thicknesses of the first two layers which correspond to the till above the resistive layer of sand and gravel. The average resistivity in each layer was averaged by using the conductivity values since the TEM-method is most sensitive to differences in conductivity. The average thickness and resistivity values for layers one and two are shown in Table 7. We refer to the old reference model in Table 6 for comparison. The histograms of the properties of the first two layers are shown in These histograms show Gaussian-like distributions centered around the average values presented in Table 7. As seen in the mean-resistivity maps, the test site is quite homogeneous laterally, and only the top 13 m of the old reference model has been refined according to the ERT measurements. It results in the first 5 m of the reference model which are less conductive compared to the old reference model (compare Table 6 and Table 7). The depth to the bottom of the most resistive layer is kept at 32.6 m, and its thickness has been adjusted accordingly. For some ground TEM soundings made at the Lyngby site, it was necessary to add a deep and very conductive layer of 3 Ωm at a depth of about 265 m, to fit the last gates. Note that the resolution of this layer is uncertain, since it has an impact on the last few gates only.

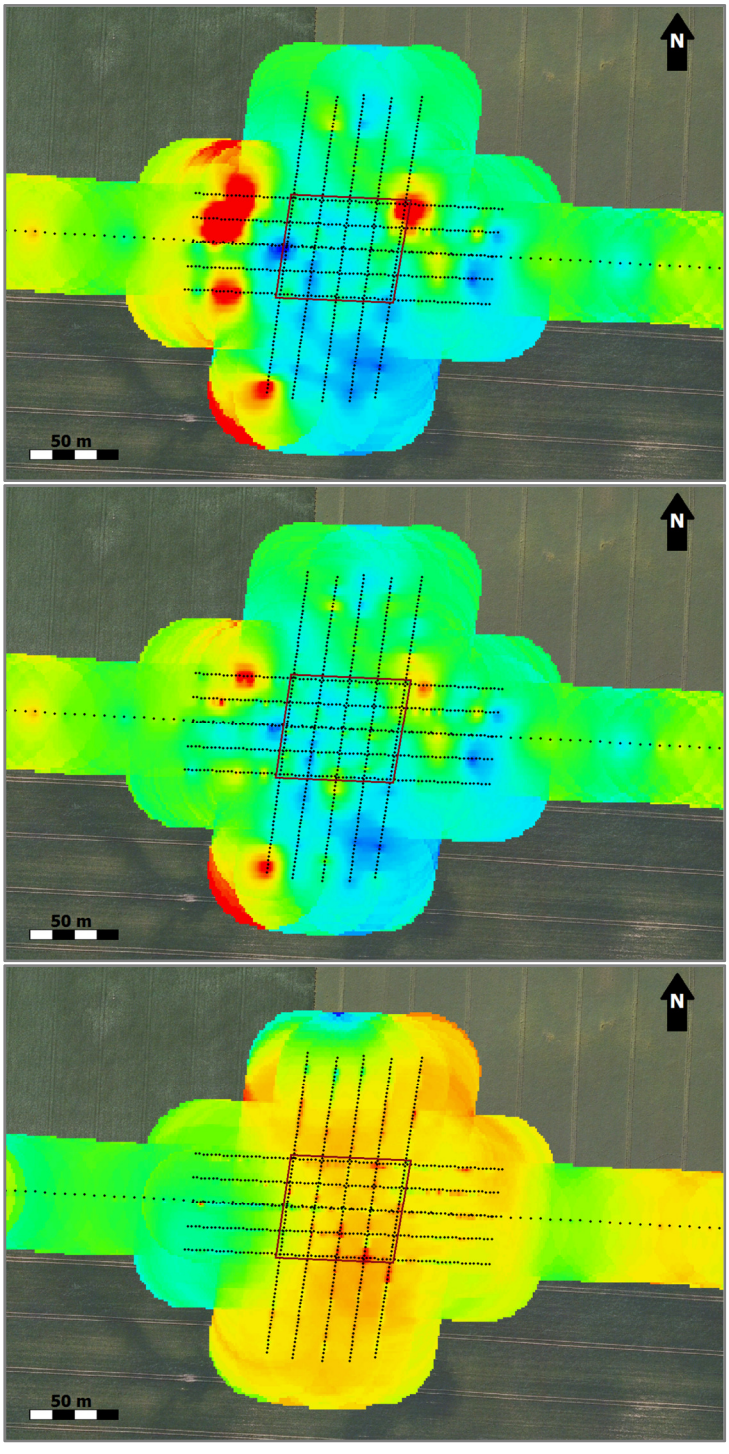

Depth
0-1 m

Depth
1-2 m

Depth
7-8 m

Figure 9. Mean-resistivity maps at different depths. Aerial photo © COWI A/S

	Resistivity	STD. Resistivity	Thickness	STD. Thickness	Depth	STD. Depth
Layer 1	15.4	9.17	3.5	Unresolved	3.5	Unresolved
Layer 2	155.2	8.49	29.1	1.74	32.6	1.15
Layer 3	9.8	1.23	23.0	1.19	55.5	1.17
Layer 4	2.4	1.03	61.1	1.08	116.7	1.06
Layer 5	270.6	Unresolved				

Table 6. Old reference model. Model parameters with model uncertainty (STD) stated as factors.

	Resistivity	STD. Resistivity	Thickness	STD. Thickness	Depth	STD. Depth
Layer 1	**33.8**	**1.11** ***(1.19)***	**2.1**	**2.32** ***(1.32)***	**2.1**	**2.32** ***(1.32)***
Layer 2	**47.7**	**1.09** ***(1.11)***	**11.0**	**1.21** ***(1.13)***	**13.1**	**1.13** ***(1.11)***
Layer 3	155.2	8.49	**19.5**	1.74	32.6	1.15
Layer 4	9.8	1.23	23.0	1.19	55.5	1.17
Layer 5	2.4	1.03	61.1	1.08	116.7	1.06
Layer 6	270.6	Unresolved	**148.3**	Unresolved	**265.0**	Unresolved
Layer 7	**3**	Unresolved				

Table 7. Refined reference model according to the interpretation of the ERT measurements. Model parameters with model uncertainty (STD) stated as factors. The changed values are highlighted in bold. The STD values in bold correspond to the model uncertainties estimated from the inversion of the DC soundings, whereas STDs in brackets are coming from the average estimation of the reference model, and so are linked to the spatial variability of the model parameters inside the square (red line in Figure 8).

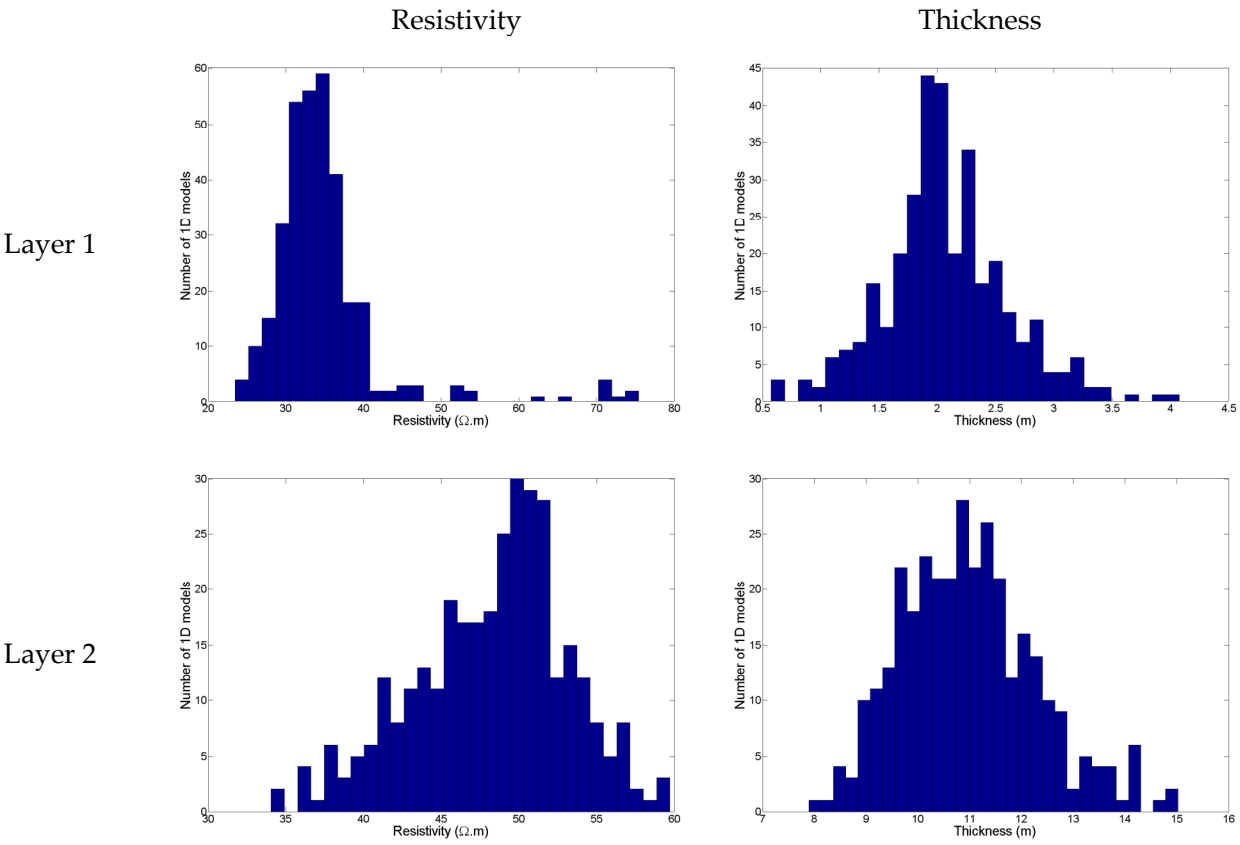

Figure 10. Histograms of the resistivity and thickness values of the first two top layers. The 1D models considered are located inside the red square shown in Figure 9 (from SCI inversion of ERT measurements). Mean values and standard deviation factors are summarized in Table 7.

4.5 Electrical Conductivity log

With electrical and electromagnetic methods a series of thin layers often have to be considered as one composite layer, which is macro-anisotropic if thin layers have different resistivities. To clarify any anisotropy in the upper 15 m, an EC-log was measured in the 60x60 grid, Figure 3. The EC-log was measured with a Geoprobe system and a SC400 probe. With this system, a standard Wenner configuration is used, with a distance of 1.5 cm between the electrodes. The small spacing between the electrodes guarantees a high vertical resolution and a detailed description of thin layers ~5 cm thick at least. The drill-stem is 3.8 cm in diameter and is hammered into the ground through the vibracore principle at a frequency of 33 Hz and a winch rating of 1.2 ton.

EC-log, which has been used for estimating the anisotropy at the test site, is shown in Figure 11. The resistivity values cannot be trusted, since there were several problems with calibrating the Geoprobe due to instrument errors, and hence the factor, by which the resistivities need to be shifted, could not be determined.

Even though the resistivity values cannot be compared directly with the reference model shown in Table 7, it is worth noting that the ratio between the two top layers in the EC-log (the layer boundaries are shown with black lines in Figure 11) and the resistivity ratio between the two top-layers in the ERT sounding at the same location as the EC-log are very close (Table 8). The anisotropy can also be determined whether the resistivity values are calibrated or not, since the same calibration factor would have been applied to the entire log of resistivity.

	EC-log	ERT
Ratio	23.1 Ωm / 30.7 Ωm = 0.75	33.8 Ωm / 47.7 Ωm = 0.71

Table 8. Ratio between the resistivity of the two top-layers for both the EC-log and ERT measurements.

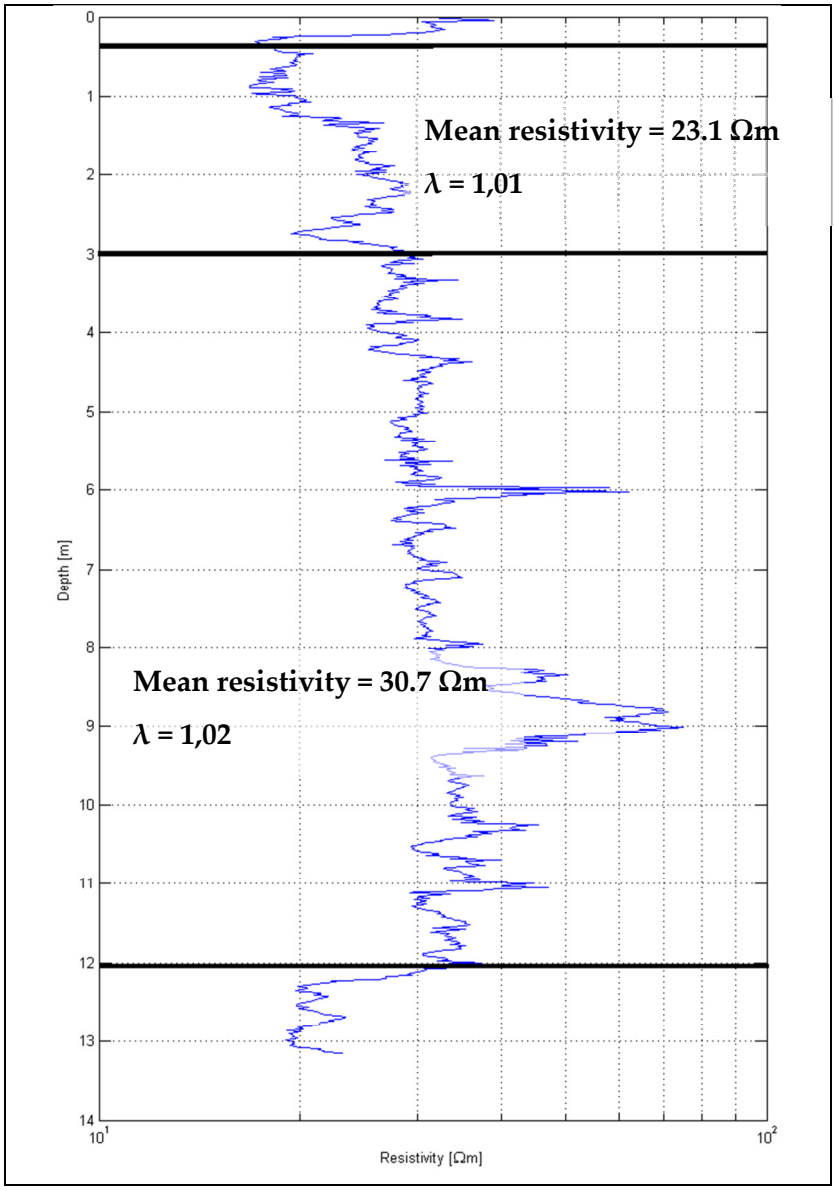

Figure 11. EC-log from the test site. The black lines mark the boundaries of the first two near-surface layers. The values from depth of 0-0.5 m, and below 12 m- have not been included in the calculation, because of measurement perturbations due to the priming of the drilling and to the reaching of the mechanically resistive 3rd layer of sand and gravel, respectively. ***Important****: values of resistivities are not calibrated.*

To determine the anisotropy in the two top-layers, the approach formulated by Christensen (2000) was used. With this approach the anisotropy coefficient (λ) can be found through the following formulas:

$$\lambda = \sqrt{\frac{\rho_V}{\rho_H}} = \sqrt{\frac{ST}{H^2}}, \quad (1)$$

Where T denotes the vertical resistance, S denotes the horizontal conductance and H denotes the total thickness of the sequence. The vertical and horizontal resistivities can be computed from:

$$\rho_v = \frac{T}{H}, \qquad \rho_H = \frac{H}{S} \quad (2)$$

T and S can be determined for a set of m layers with intrinsic resistivities ρ_i:

$$T = \sum_{i=1}^{m} \rho_i h_i \qquad S = \sum_{i=1}^{m} h_i/\rho_i \qquad H = \sum_{i=1}^{m} h_i, \quad (3)$$

For a sequence of m layers with resistivities ϱ_i and thicknesses h_i.

If it is assumed that the resistivity varies linearly in a semilogarhitmic plot between two measuring points, the resistivity between neighboring measuring points, z_a and z_b, can be calculated as:

$$\rho(z) = \rho_a \cdot exp\left[\ln\left(\frac{\rho_b}{\rho_a}\right)\frac{z - z_a}{z_b - z}\right], \; z_a \le z \le z_b \quad (4)$$

And the effective transverse resistance $T(z_a,z_b)$ can be found by:

$$T(z_a, z_b) = \int_{z_a}^{z_b} \rho(z)^{-1} dz = \frac{(\rho_b - \rho_a)(z_b - z_a)}{\ln \rho_b/\rho_a} \quad (5)$$

And the effective horizontal conductance $S(z_a,z_b)$ as:

$$S(z_a, z_b) = \int_{z_a}^{z_b} \rho(z)^{-1} dz = \frac{1}{\rho_a \rho_b} \frac{(\rho_b - \rho_a)(z_b - z_a)}{\ln \rho_b/\rho_a} \quad (6)$$

Once the results of formulas (5) and (6) have been summed inside the depth interval including the m layers (the sampling of the EC-log is one measurement every 1.5 cm), the vertical and horizontal resistivities as well as the coefficient of anisotropy can be calculated from equations (2) and (1), respectively.

Table 9 shows the calculated anisotropy coefficient λ for the two different layers. The anisotropy coefficient has been applied to the resistivity ρ_{DC} found in chapter 4.4 from the ERT measurements, in order to yield the anisotropy corrected resistivity, following the formula $\rho_H = \rho_{DC}/\lambda$, with ρ_{DC} defined as $\rho_{DC} = \sqrt{\rho_H \rho_V}$. As seen in Table 9, the anisotropy coefficient is very low, which means that the two top layers considered in the reference model can be considered to be macro-isotropic, so that the values of resistivities obtained from the ERT measurements can be used directly as "TEM" or horizontal resistivities for the calibration of TEM devices, here with a small correction factor of 1-2%.

	Layer 1	Layer 2
Anisotropy coefficient	1.01	1.02
Thickness	2.1 m	11.0 m
Resistivity	33.8 Ωm	47.7 Ωm
Anisotropy corrected resistivity	33.5 Ωm	46.8 Ωm

Table 9. Anisotropy coefficients and anisotropy corrected resistivities for the two top layers at the test site.

4.6 Final refined reference model

Table 10 summarizes the reference model for the national TEM test site at Lyngby, Aarhus.

	Resistivity	Thickness	Depth
Layer 1	33.5	2.1	2.1
Layer 2	46.8	11.0	13.1
Layer 3	155.2	19.6	32.6
Layer 4	9.8	23.0	55.5
Layer 5	2.4	61.1	116.7
Layer 6	270.6	148.3	265.0
Layer 7	3		

Table 10. Final refined reference model after anisotropy correction for the National TEM test site at Lyngby, Aarhus.

Figure 12 highlights the differences between the old and the new 1D reference models. Since previous investigations at the test site have not focused on the near surface, ERT measurements of 2011 were designed to give a better description of the upper 15 m, but with a lower depth of investigation. From these measurements the till and the top of the sandy layer have been updated. Some ground TEM soundings with very late gates and a large depth of investigation have shown effects of a very conductive and deep layer attributed to chalk saturated with relic salt water. Since this layer has an impact only in the few last gates of the High-Moment, its parameters (resistivity and depth) are badly resolved. Its adding to the reference model helps to have a slightly better fit at the last gates. The forward modeling of the two reference models in Figure 13 shows the differences in the data curve, with a higher apparent resistivity at the first gates of the SLM curves.

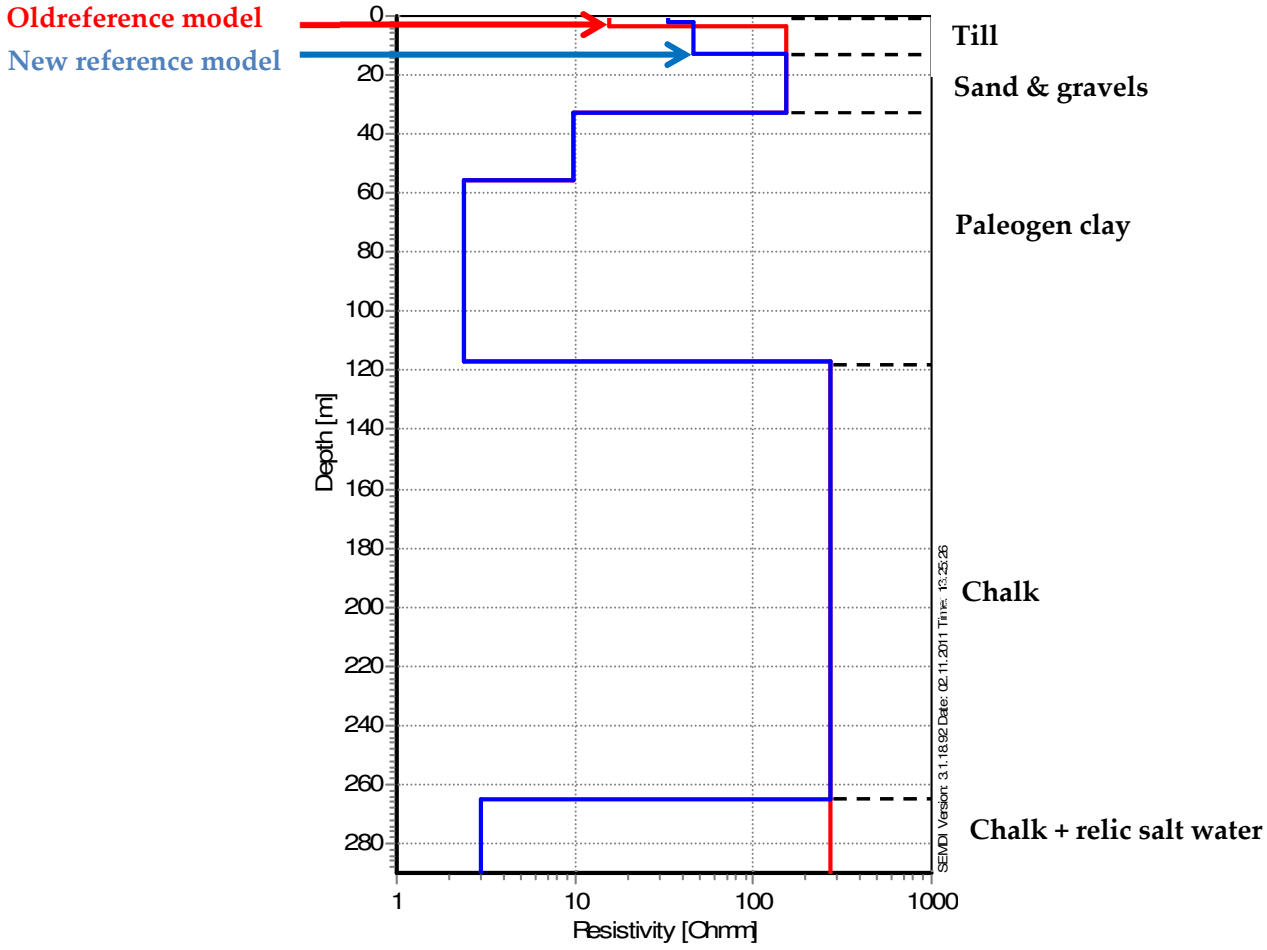

Figure 12. The old and the new refined reference models at the national TEM test site at Lyngby.

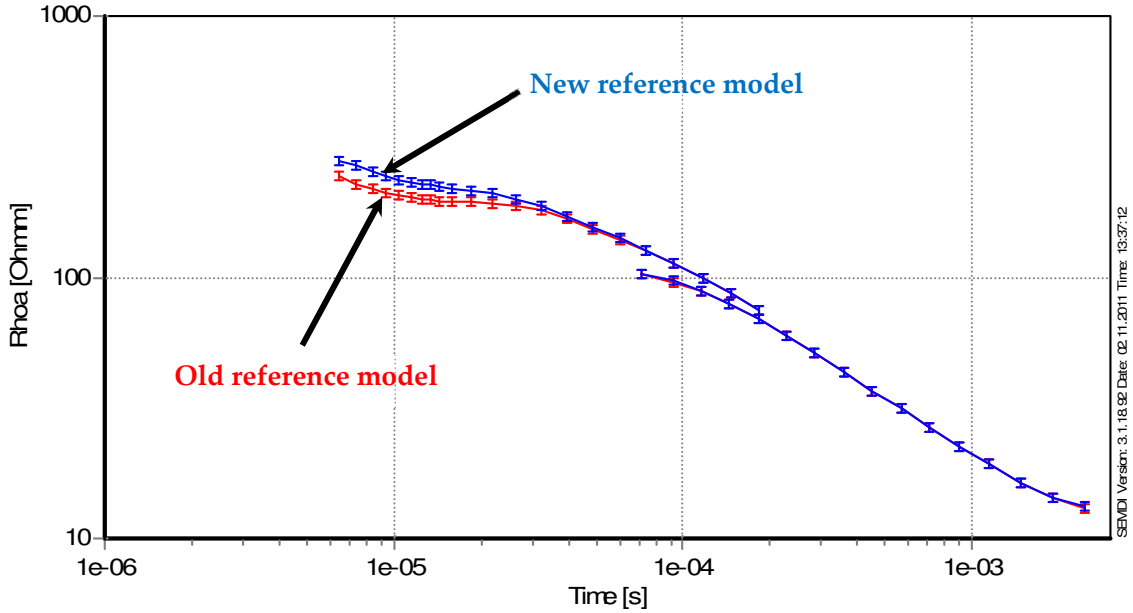

Figure 13. Forward modeling of the old (red curve) and new (blue curve) reference models with a SkyTEM setup at 30 m and error bars set at 3 %. The HM curve is almost unchanged contrary to the first gates of the SLM.

5. EXTENSION OF THE NATIONAL TEM SITE

In 2009, the test site was extended from being a point location to consist of two crossing lines, approximately one kilometer long (Figure 14). The two lines consist of reference models for every 40 m, which makes calibration, validation and tests possible for airborne TEM system under survey conditions. Further, some airborne TEM systems like VTEM cannot make hovering measurements, which makes point calibration impossible. The lines thus opened the test site for any airborne TEM system, and not only SkyTEM.

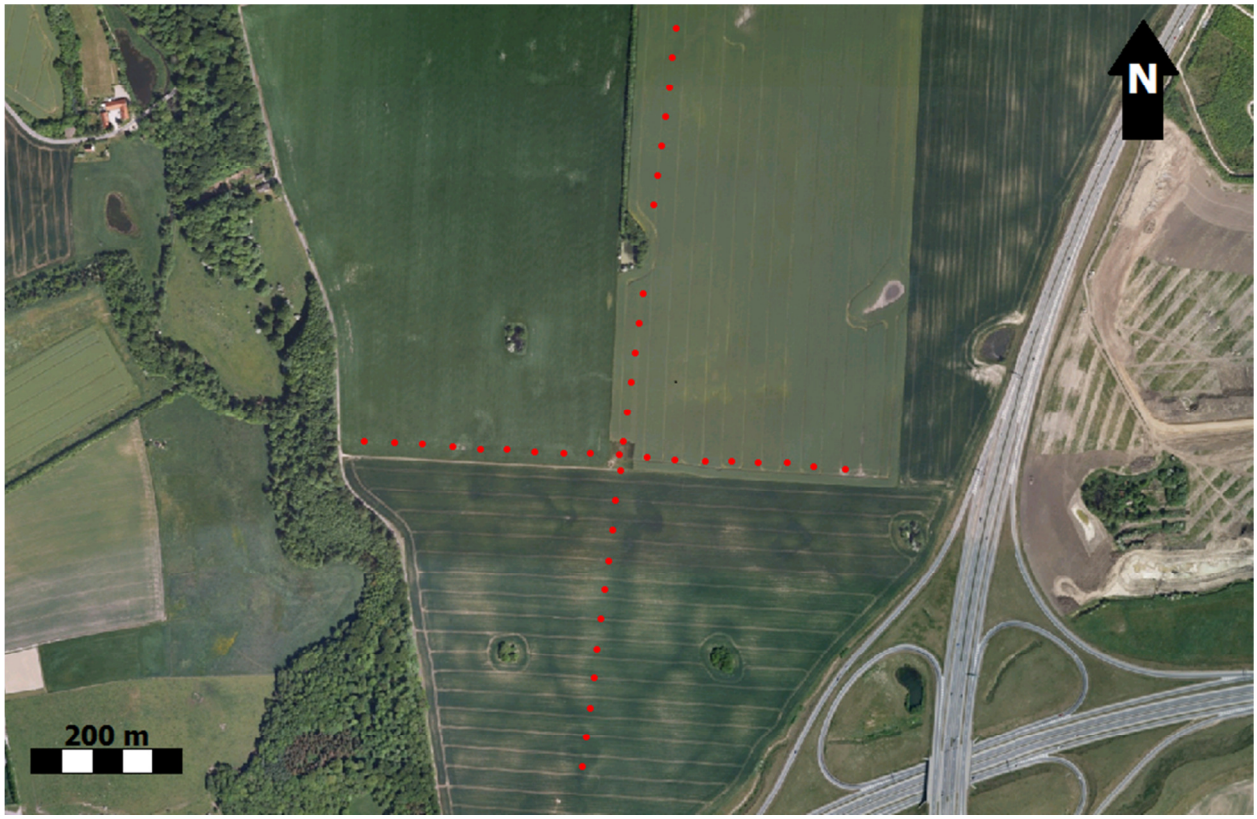

Figure 14. Extension of the national TEM site. Red dots show the positions of the ground based TEM soundings forming a 700 m long West-East orientated profile and an 1100 m South-North orientated profile. Aerial photo © COWI A/S.

The test site extension was carried out with a pre-calibrated ground-based TEM system, WalkTEM/TEM40, sharing the technological framework of the SkyTEM system.

5.1 WalkTEM/TEM40 setup

The TEM soundings were carried out in a central loop configuration with a 40 x 40 m transmitter loop using a low moment (SLM) and a high moment (HM) to record the full sounding curve. The soundings were placed edge to edge with 40 m spacing as red dots shows on in Figure 14. The WalkTEM/TEM40 system specification is listed in Table 11.

	Low Moment setup	High Moment setup
Transmitter loop	40 x 40 m^2	40 x 40 m^2
Current	1 A	8 A
Transmitter moment	1600 Am^2	12800 Am^2
Time gate (Beginning of ramp time)	8.1 μs to ~ 0.72 ms	0.12 ms to ~ 12 ms
Receiver coils effective area	105 m^2	4200 m^2
Low pass filters	300 kHz, 450 kHz	300 kHz, 450 kHz
Waveform SLM	ramp-on 125 μs	ramp-on 700 μs
	ramp-off 3.0 μs	ramp-off 5.5 μs
Calibration; time shift, factor	-3.1 μs, 0.97	-3.1 μs, 1.02

Table 11. The WalkTEM/TEM40 system specifications.

Compared to the Geonics ProTEM47 system, the WalkTEM/TEM40 transmitter moment is twice as large, which, combined with a better receiver coil for the high moment, has resulted in high-quality data to approximate 12 ms for the calibration lines compared to ~7 ms for the original test site sounding performed in 2001.

5.2 Calibration of WalkTEM/TEM40

The WalkTEM/TEM40 system was pre-calibrated at the original test site with the standard calibration procedure. Figure 15 shows plots with the forward response from the reference model for the WalkTEM/TEM40 setup, and the measured WalkTEM/TEM40 reponse after applying calibration constants for both the high and the low moments.

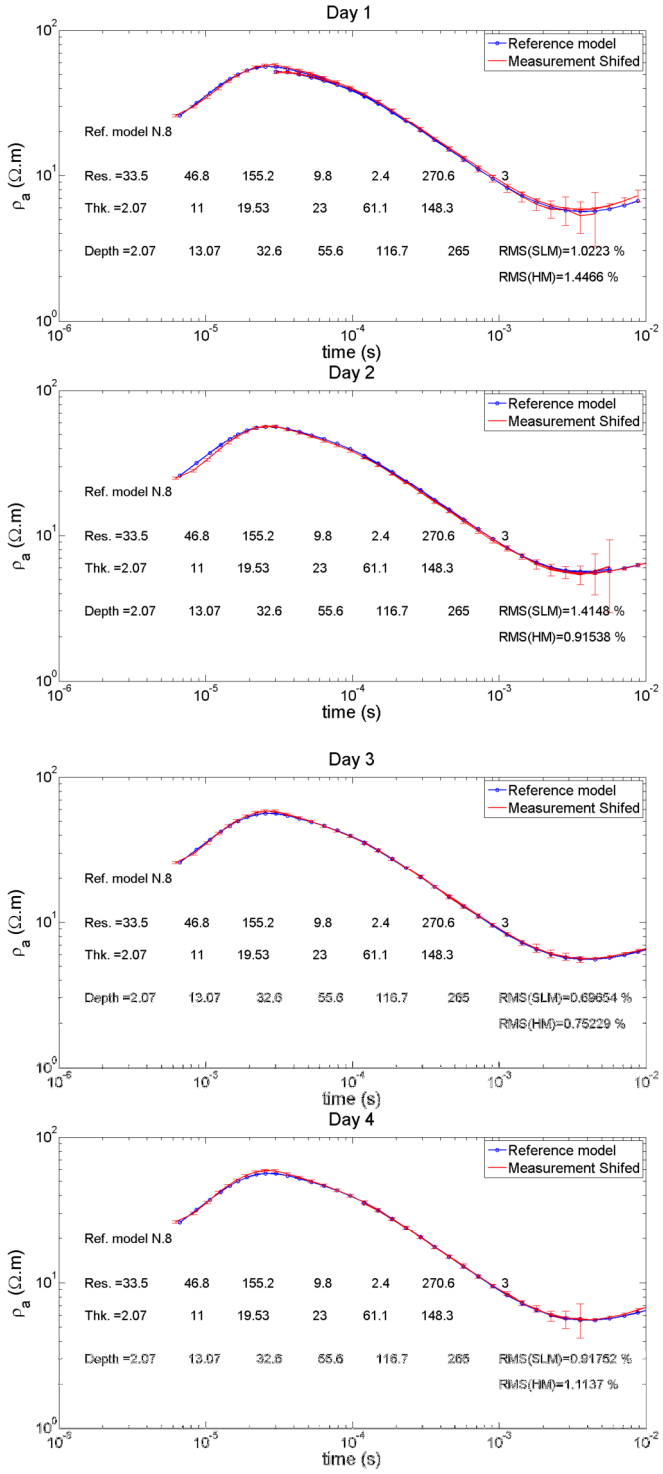

*Figure 15. Data fit for the refined reference model and the WalkTEM/*TEM40 *setup for measurements performed on four different days. Error bars are the measured data, the blue line is the forward response from the reference model. The transition between the SLM and HM curves is continuous.*

For this calibration, measurements made on four different days are considered. The purpose of using these four days instead of one only is to show the absence of drift in the instrumentation .

Some of the soundings resolve a deep and conductive 3 Ωm layer at a depth of about 265 m. This layer has no impact on the estimated time shift of a few μs, but had been added to the reference model which is previously summarized in Table 10.

Curves fit between the updated reference model and the calibration measurements are displayed in Figure 15. The comparison between the old and new reference shifts is summarized in Table 12. The factor shifts do not change with the updated reference model, and the difference lies in the time shift, which is **-1.1 μs** for both the Low-Moment and the High Moment. Note that this difference in time shift has almost no impact on the data acquired with the HM, since the first gate for this moment is generally later than 40 μs.

Moment	Difference of time shift	New/Old factor shift
SLM	-1.1 μs	1.0
HM	-1.1 μs	1.0

Table 12. Difference and ratio between the old and the new calibration parameters for the WalkTEM/TEM40 setup.

5.3 Processing/LCI inversion

The standard data processing scheme using the SiTEM program was applied to the WalkTEM/TEM40 data. It includes manual inspection of all sounding curves and exclusion of strongly noise- affected late-time data points. Data have been assigned at a uniform standard deviation of 3 % (in db/dt), plus the standard deviation calculated from the stacking of the data.

Data were then inverted with a least-squares inversion approach, modeling the full system response and using the laterally constrained inversion (LCI) concept by Auken et al. (2005).

The two profiles are inverted in separate LCI-chains (Figures Figure 16 and Figure 17). A six-layer model is needed to fit the data in general. However, looking at the soundings individually, not all soundings have information of the last layer (layer six). The sixth low-resistive layer is saltwater saturated chalk and is known to be present throughout the test site area. Therefore, the six-layer LCI-setup was chosen for the two test lines.

The lateral constraints applied in the LCI setup are very loose, a factor of 1.7 for resistivities and +/- 12 m variation for the layer boundaries. For layer six, tighter lateral constraints were applied.

5.4 Inversion results

In Figures Figure 16 and Figure 17, the inversion results of the two profiles are presented. In general, we obtained a very good data fit for both sections. The normalized data fit for the individual soundings are listed in Appendix 2.

The topsoil layer with a resistivity of 34-50 Ωm is a 13 m thick till layer, which caps a 20 m thick resistive sand and gravel layer. Below the sand and gravel are two conductive clay layers with a thickness of 20 and 60 m, respectively. At the elevation of -80 m is a thick chalk layer which is present in almost all of Denmark. At the elevation of approximately -230 m the chalk is saturated with residual saltwater, and hence the resistivity drops to ~3 Ωm.

Model parameters and UTM-locations for the two sections are listed in Appendix 2. An extended xyz-file including the model parameter analyses, processed data-files, etc. are available for download from the national **ge**ophysical **r**elational **da**tabase, GERDA, at www.gerda.geus.dk.

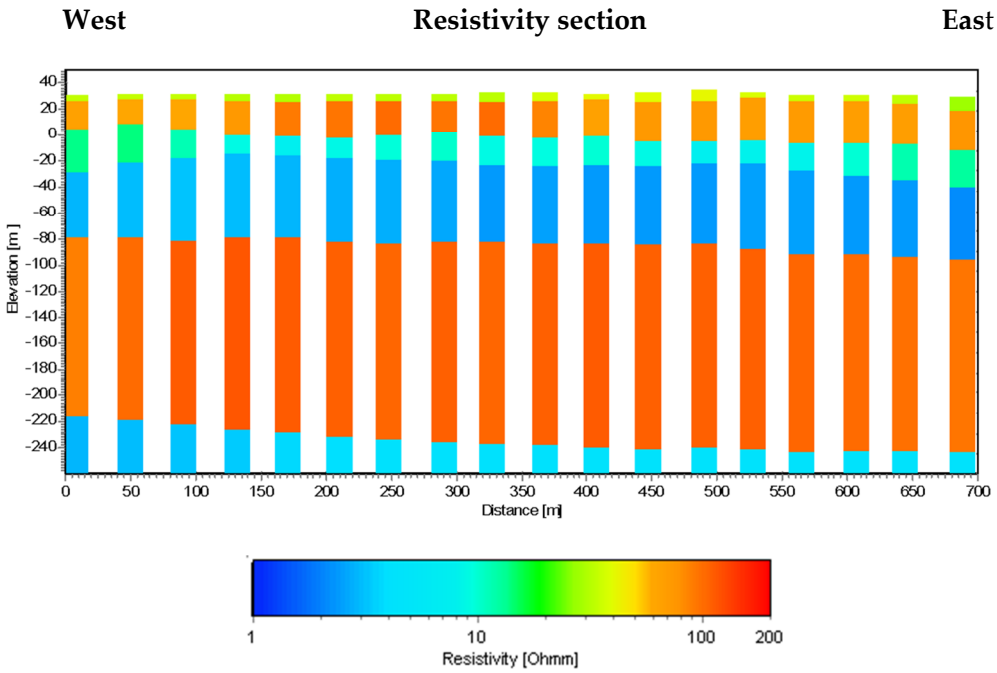

Figure 16. Resistivity section of the West-East profile (WalkTEM/TEM40). The location of the profile is shown on Figure 14. The profile crosses the South-North orientated profile in a profile distance of 360 m.

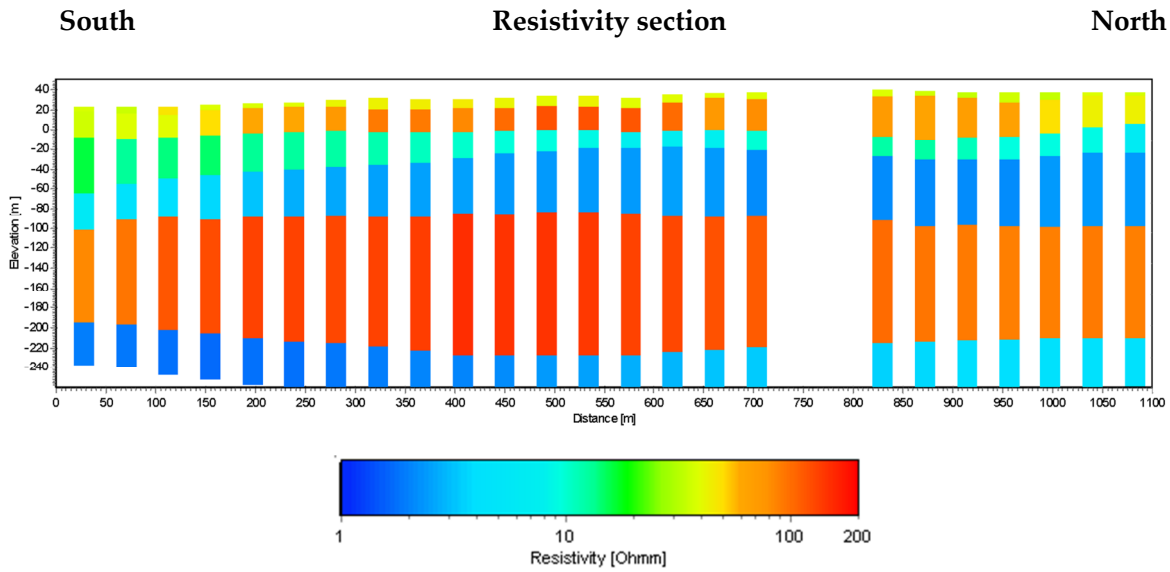

Figure 17. Resistivity section of the South-North profile (WalkTEM/TEM40). The location of the profile is shown on Figure 14. The profile crosses the West-East orientated profile in a profile distance of 450 m.

6. SORØ SURVEY: REFINEMENT OF THE NEAR-SURFACE

The previous update of the model of the Lyngby reference site (Chapter 4) leads us to estimate new calibration factors which will induce some changes in the upper 15 m. Since the resistivity of the top layer was increased in the latest update, these changes will result in the disappearance of the first very conductive layer (around 30 Ωm) obtained in several SkyTEM surveys where early times have been used. The change of the first 15 m tends to be smaller when the actual resistivity of the near-surface decreases, since a good response of near-surface conductive layers can be observed from "late" gates starting at 10 μs.

In this section, the refined reference model is applied to the Sorø survey made in June 2009. Some characteristics of the SkyTEM setup can be found in Table 13. For more details, please refer to the report of the survey (in Danish).

Flight altitude	25-35 m
Speed	45 km/h
Area of the transmitter loop	314 m²
Number of turns SLM/HM	1 / 2
Amp. of SLM/HM	8 A / 93 A
Turn-off of SLM/HM	~4 μs / ~27 μs

Table 13. Characteristics of the SkyTEM setup for the Sorø survey.

6.1 Calibration

For the Sorø survey, the measurements at the Lyngby reference site were done at seven different heights: 0.2 m, 5 m, 10 m, 15 m, 20 m, 25 m, and 30 m.

The calibration procedure is now done by means of an objective fitting routine programmed in Matlab instead of a visual fitting. The script needs only the data files (*.tem) of the measurements at the Lyngby site as inputs. Then the misfit between the measurements and the forward modeling of the reference site is reduced by the intrinsic optimization function of Matlab called *fmincon*. This function solves non-linear problems by least-squares misfit, and with the combination (in the present case) of the SQP (Sequential Quadratic Programming), Quasi-Newton and line search algorithms. With this script, a unique couple of time

and factor shifts are determined for each moment in such a way that apparent resistivity curves match the reference model for all heights.

Curves fit between the old or the new refined reference model and the calibration measurements are displayed in Figure 18 for low heights from 0.2 m to 15 m, and in Figure 19 for heights closer to the operation altitude, from 20 m to 30m. Except for heights of 5 m and 25 m, where the standard deviation was originally larger, the RMS is globally between 1 and 2 % for both old and new reference models. However, the calibration with the new refined reference model leads to new time shifts which are summarized with shifts estimated with the old reference model in Table 14.

Moment	Time shift		Factor shift	
Reference model	Old[2]	New	Old	New
SLM	-1.42 µs	-2.51 µs	0.93	0.93
HM	-2.12 µs	-3.22 µs	0.97	0.97

Table 14. Time and factor shifts estimated for the Sorø SkyTEM setup with the old and the new reference models.

Moment	**Difference of time shift (New-Old)**	Ratio of factor shift (New/Old)
SLM	**-1.09 µs**	1.0
HM	**-1.10 µs**	1.0

Table 15. Difference and ratio between the old and the new calibration parameters for the Sorø SkyTEM setup.

[2] The time shifts estimated here for the old reference models differ slightly from those originally set in the geometry file (-1.3 µs for the SLM, and -2.5 µs for the HM). This small difference is due to the fact that the methods used for the calibration differ, since the new calibration procedure uses a Matlab script as described before. Since the purpose here was to estimate the difference due to the update of the reference model, it has been necessary to use the same calibration method for both old and new reference models to make a good comparison. For a slightly better precision, people who deal with Sorø data should directly change the time shifts in the geometry file with the new ones estimated for the refined reference model, instead of adding the difference of time shift.

The comparison between the old and the new reference shifts is summarized in Table 15. As can be observed, the factor shifts does not change with the updated reference model, and the difference lies in the time shift, which is -1.09 μs for the Low-Moment and -1.10 μs for the High Moment, i.e. very close to the value of -1.1 μs found for the WalkTEM/TEM40 system (see Table 12). Note that this difference in time shift has a much smaller impact on the HM for which the first gate lies between 30 μs and 40 μs.

Old reference model **New reference model**

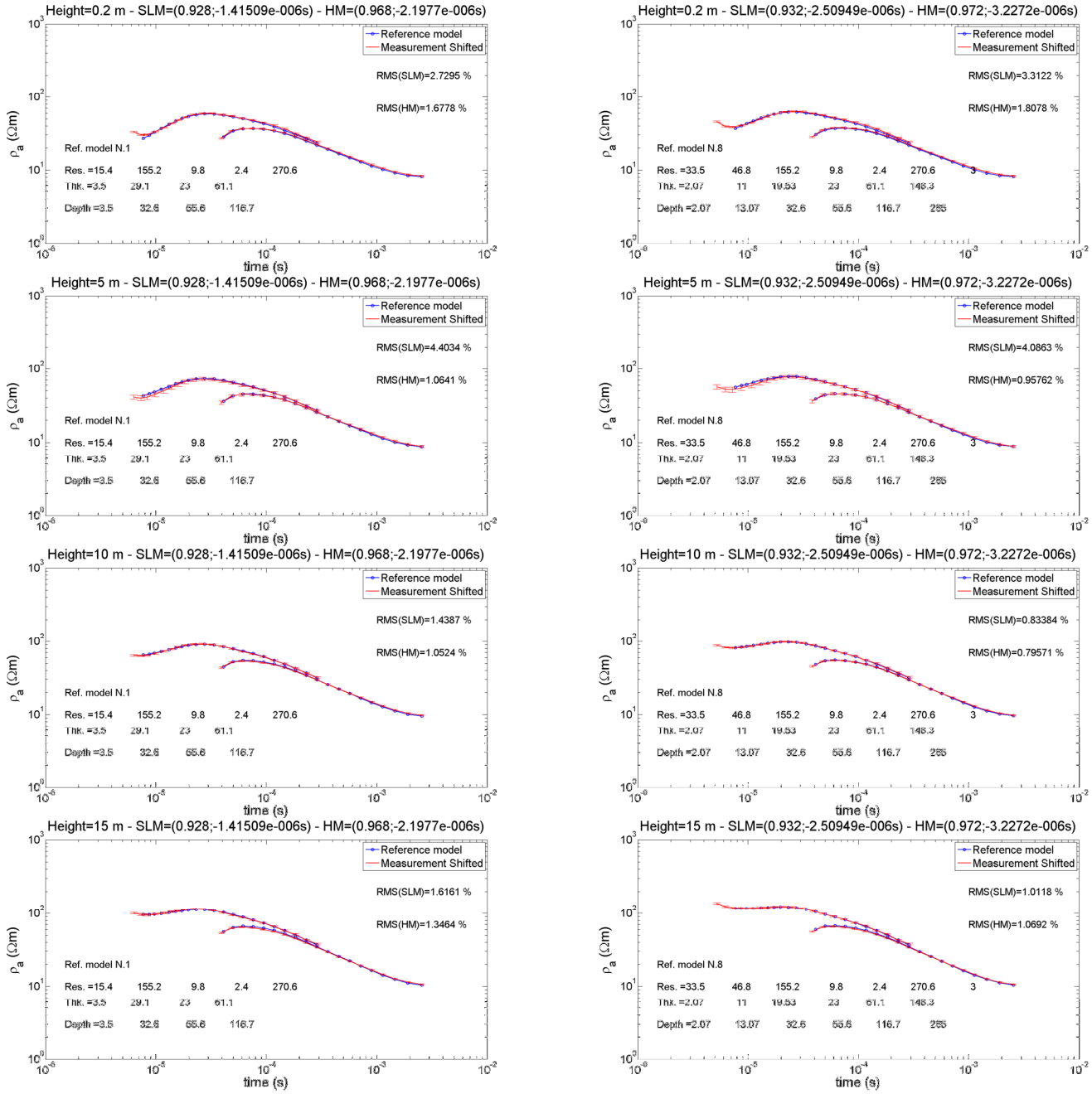

Figure 18. Curves fit of the Sorø SkyTEM setup with the old (left column) and the new (right column) reference models at the heights of 0.2 m, 5 m, 10 m, and 15m (from the top to the bottom).

Old reference model **New reference model**

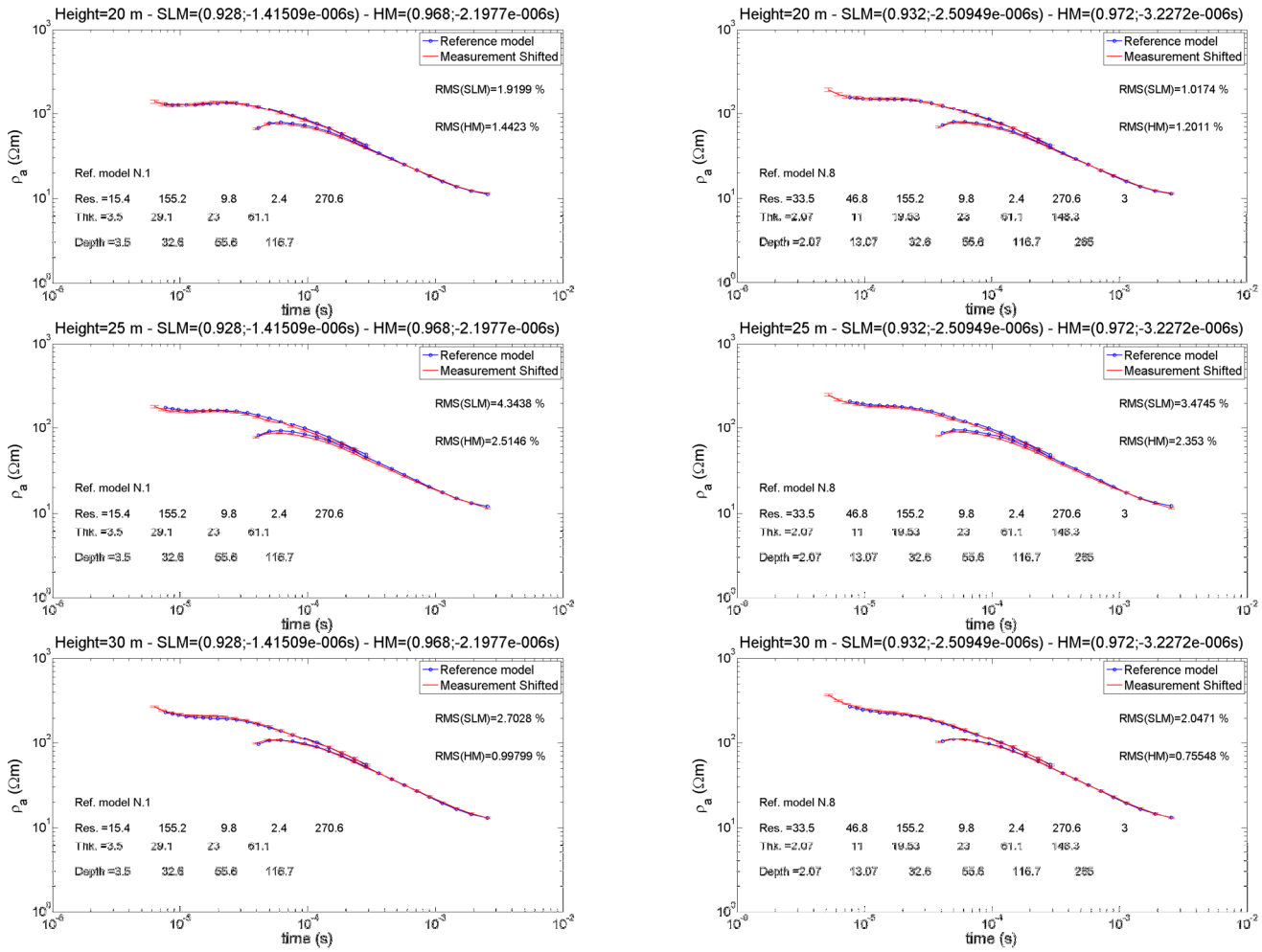

Figure 19. Curves fit of the Sorø SkyTEM with the old (left column) and the new (right column) reference models at the heights of 20 m, 25 m and 30 m (from the top to the bottom).

6.2 Application of the refined shifts to the Sorø data

The interpretation of the Sorø data with the new calibration is compared to the one with the calibration based on the old reference model, and also to ERT measurements made in the survey area. Results from LCI and SCI are compared with a focus on the resistivity changes of the first 15 m due to the new calibration. A discussion is also undertaken about the effect of inversion parameters such as the starting model and the first gate used.

Note: all figures with different starting models have been kept in the new version of June 2012 in order to preserve the numbering of the figures. However, almost no difference is now observed in the inversion results between starting models of 50 Ωm and of 100 Ωm.

Differences in inversion results between the old and the new calibrations

ERT measurements are available from the Sorø area and will be used here for comparison with the SkyTEM survey. The 1D laterally constrained inversion results have been used for ERT data instead of the 2D inversion results, so that straightforward comparison can be made with the SkyTEM results. Two profiles are chosen so that a flight line is located almost just above an ERT profile, thus limiting differences due to spatial changes in the geology and interpolation of the inversion results (the second profile is further presented page 49).

The inversion parameters are set according to the new parameters used for the update of the Søro survey report (GFS, 2012). The first low moment gate used was gate 6 at 8.72 μs, and then at 6.21 μs with the new time shift. Table 16 summarizes the center times of the two very early gates 5 and 6, in function of the reference model considered. As detailed in the table, we use notations 6_{old} and 6_{new} below, which refer to the gate shifted with the old time shift and with the new time shift, respectively.

Gate number	Without calibration	With calibration based on the old reference model	With calibration based on the new reference model
5	7.72 μs	6.30 μs (5_{old})	5.21 μs (5_{new})
6	8.72 μs	7.30 μs (6_{old})	6.21 μs (6_{new})

Table 16. Center times of the very early gates used for the Sorø data. The center times are shifted according to the time shifts estimated for the old and the new reference models, which can be found in Table 14.

The result for the first profile is displayed in Figure 20. The top section is the ERT result, the middle section is the SkyTEM result with the old time shift, and the bottom section is the SkyTEM result with the new time shift. As can be observed, the new shift results in a more resistive top layer almost all along the section, particularly between the positions 250 m and 650 m, and also between 1100 m and 1250 m. In the ERT section, this top resistive layer is everywhere, including the positions between 1300 m and 1700 m (top section in Figure 20) where the layer is very thin, around 3 m. It is expected that the thin resistive top layer will be very poorly resolved with airborne TEM measurements in this part of the section, especially with the very conductive lens located near the surface which gives a strong response, even in the very early gates. As observed in the bottom section of Figure 20 with the new reference model, the thin resistive layer even does not exist in the SkyTEM results. A Top Of Investigation, like the Depth Of Investigation (DOI) concept, should be investigated in order to give an idea of whether the information about the near surface is poor or not.

Figure 20 and Figure 21 correspond to a starting model of 50 Ωm and of 100 Ωm, respectively. Contrary to the first version of the report, no difference in the inversion results can be observed with the new coil response by setting a more resistive starting model, even in more conductive areas where information about a resistive and thin first top layer is very poor. These previous small differences could have been induced by the older and less accurate coil response used before. In this updated version of the report, it gives us more confidence on the stability of the inversion process regarding a homogeneous starting model with a different average resistivity (despite this one is still critical for surveys where high resistivity changes are encountered between saline and non saline areas).

Comments about the differences observed between the ERT and the SkyTEM profiles can be found in the next section page 45.

The results in Figures *Figure 20* and *Figure 21* show also that the application of the new time shift gives changes only in the first 15 m, and no modification in the deeper structures. Figures *Figure 20* and *Figure 21* are taken from LCI inversion tests made with the first gate 6 (see center time in Table 16). Further tests have shown that the consideration of the gate 5 also has an impact on the resistivity of the first 15 m (see next section page 45).

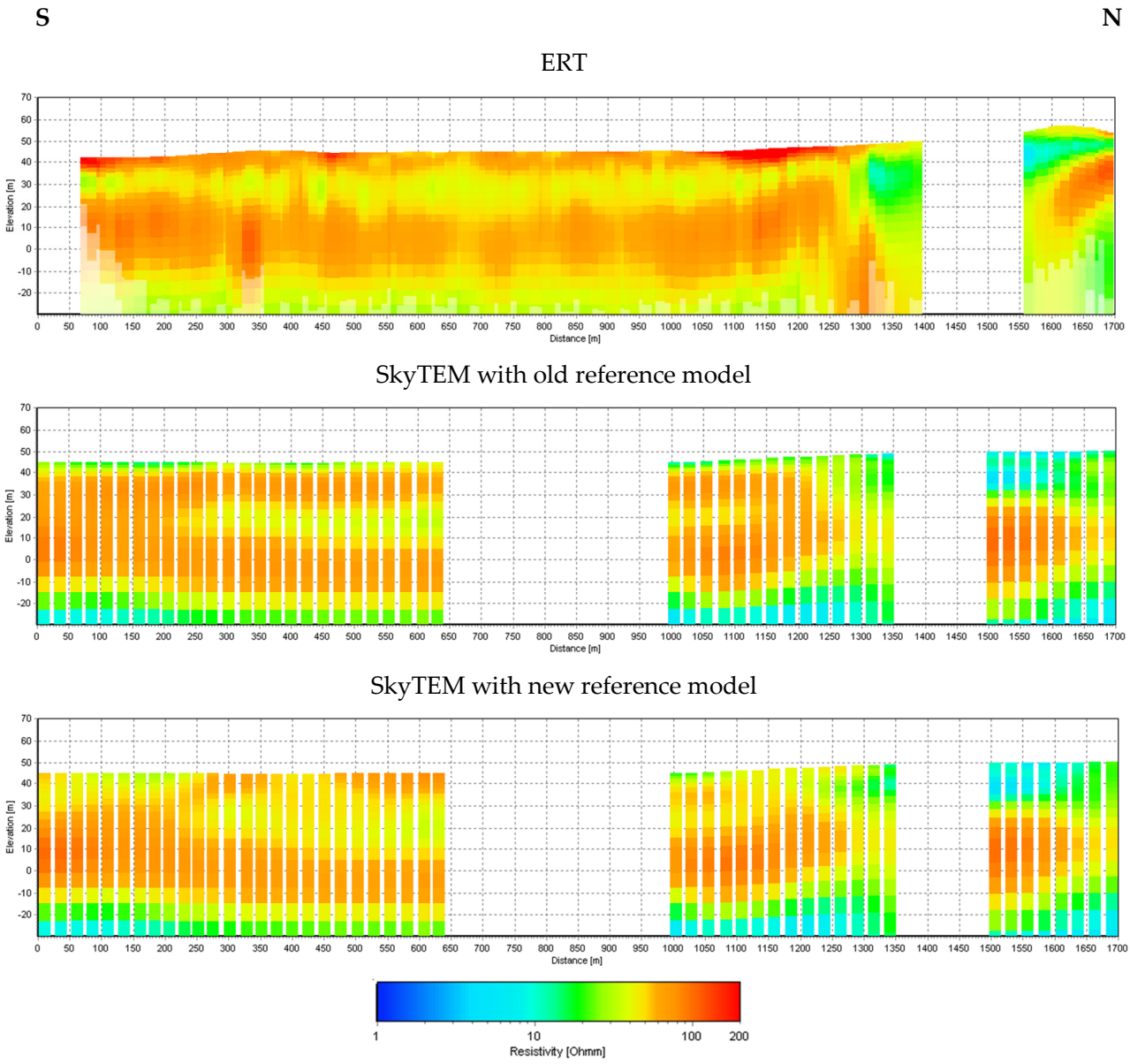

*Figure 20. Profile 1 - LCI smooth bias inversion on Sorø data. Top: ERT data. Middle: SkyTEM data with the old shift. Bottom: SkyTEM data with the new shift. The inversion parameters are: vertical constraint = 2, lat. const.=1.35, starting model of **50 Ωm**, and first gate 6. Note: kept in version of May 2012 for compatibility in the figures' numbering, but no difference is now observed when compared to a starting model of 100 Ωm.*

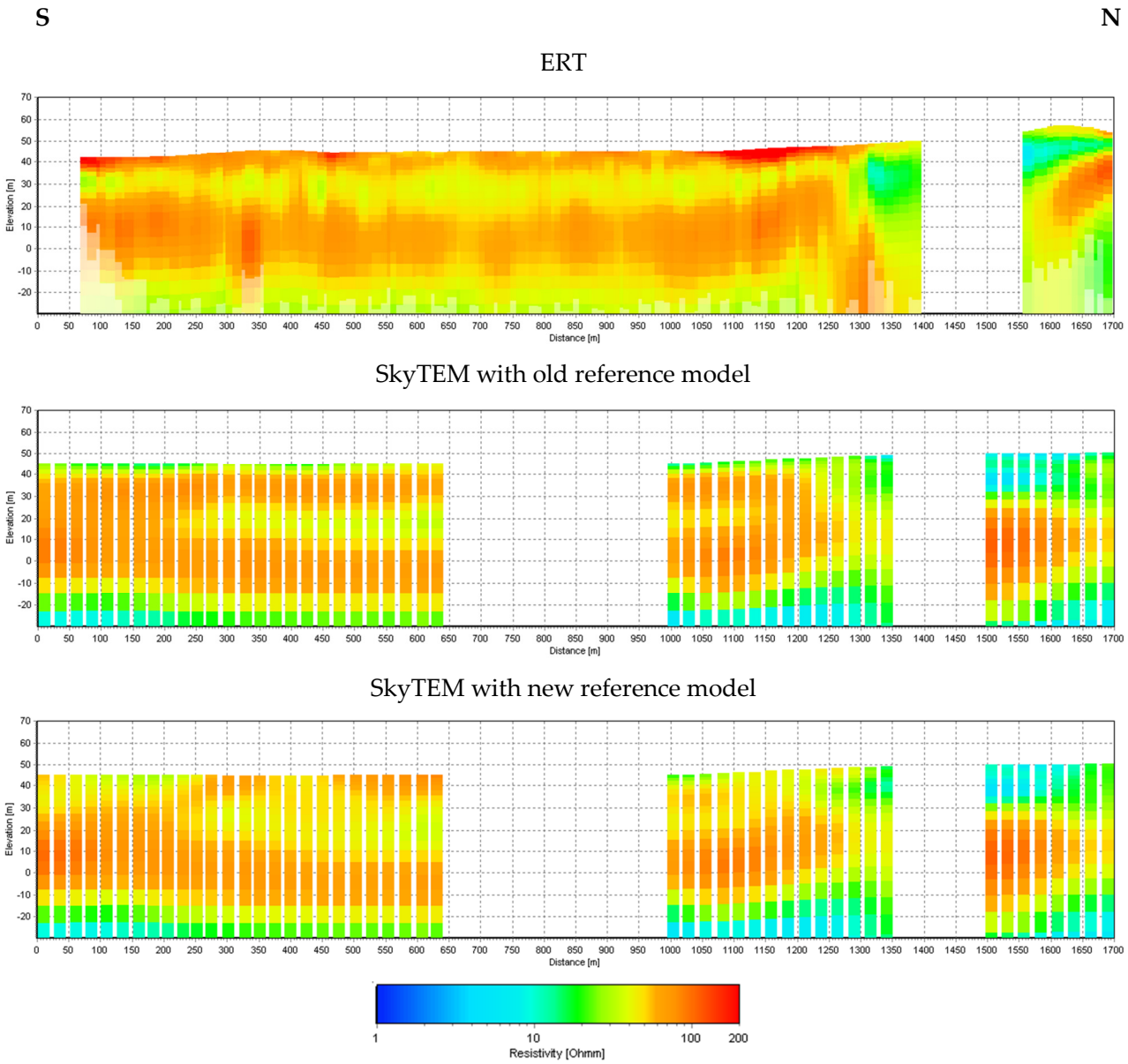

*Figure 21. Profile 1 - LCI smooth bias inversion on Sorø data. Top: ERT data. Middle: SkyTEM data with the old shift. Bottom: SkyTEM data with the new shift. The inversion parameters are: vertical constraint = 2, lat. const.=1.35, starting model of **100 Ωm**, and first gate 6. Note: kept in version of May 2012 for compatibility in the figures' numbering, but no difference is now observed when compared to a starting model of 50 Ωm.*

The effect of the very early gates

In previous LCI tests the first gate considered for the Low-Moment was gate 6 (see center time in Table 16). The effect of considering the supplementary gate 5 (see center time in Table 16) is shown in Figure 22 for a starting model of 50 Ωm. The top resistive layer appears a little bit more resistive and closer to the ERT values with the supplementary gate 5, especially between positions 250 m and 650 m. This effect is observed more clearly in Figure 24 with a better color contrast. As mentioned for Figure 20 and Figure 21 there is no difference with a more resistive starting model of 100 Ωm (Figure 23).

Globally the data residual is slightly higher with gate 5 (Figure 24). However, the data residual still has a good value, generally below 0.5 (thus largely below the standard deviation of the data). Sounding curves in Figure 25 show that the data fit is good at the earliest gates, if gate 6 (left plot of Figure 25) or gate 5 (right plot of Figure 25) is considered as the first gate.

Contrary to the first version of the report, the conductive second layer is not much more conductive and contrasted compared to the ERT section (*Figure 22* and *Figure 23*). The thickness of the first resistive top layer is also closer to the one shown by the ERT. This improvement shows the importance of a very accurate description of the coil response when dealing with very early gates. Despite this better match, there are still some parts of the profile which appear more conductive close to the surface in the SkyTEM sections. This could be explained by the different sensitivities of the two geophysical methods, by time variation of the near-surface conditions, and by lateral near-surface variability despite the distance of less than 100 m between the two datasets.

S **N**

ERT

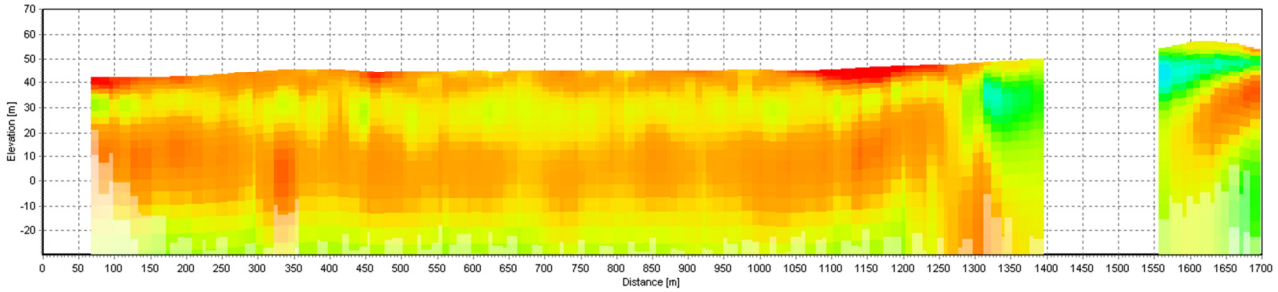

SkyTEM with new reference model and first gate 6_{new}

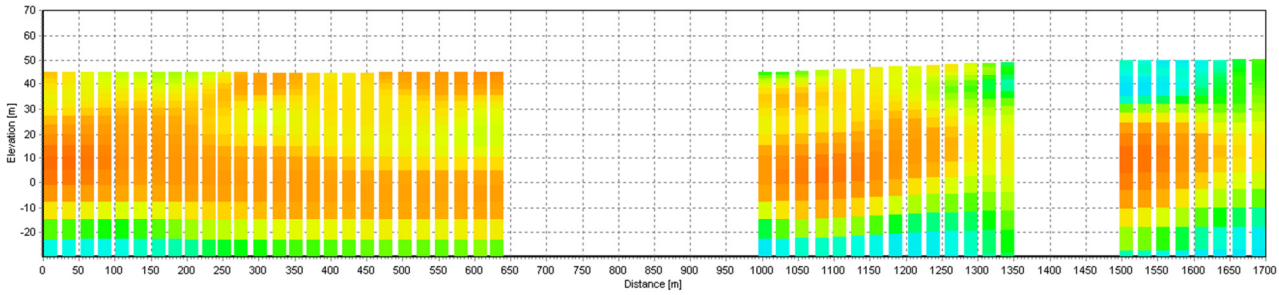

SkyTEM with new reference model and first gate 5_{new}

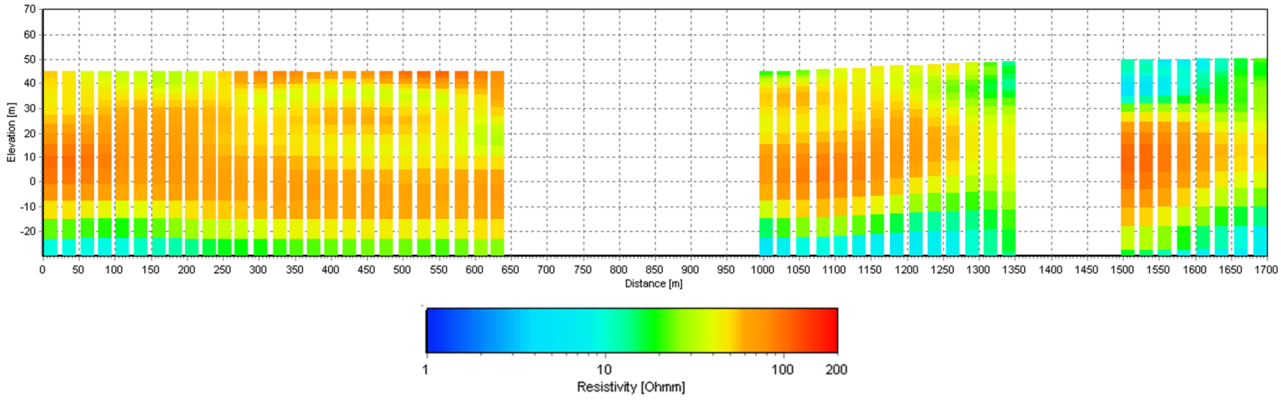

Figure 22. Profile 1 - LCI smooth bias inversion on Sorø data with the new time shift. Top: ERT data. Middle: SkyTEM data with the first gate 6_{new}. Bottom: SkyTEM data with the first gate 5_{new}. The inversion parameters are: vertical constraint = 2, lat. const.=1.35, starting model of ***50 Ωm****. Note: kept in version of May 2012 for compatibility in the figures' numbering, but no difference is now observed when compared to a starting model of 100 Ωm.*

S **N**

ERT

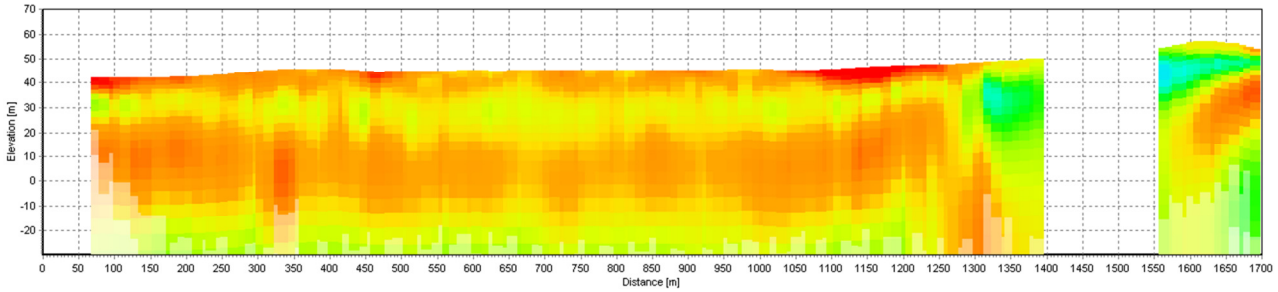

SkyTEM with new reference model and first gate 6_{new}

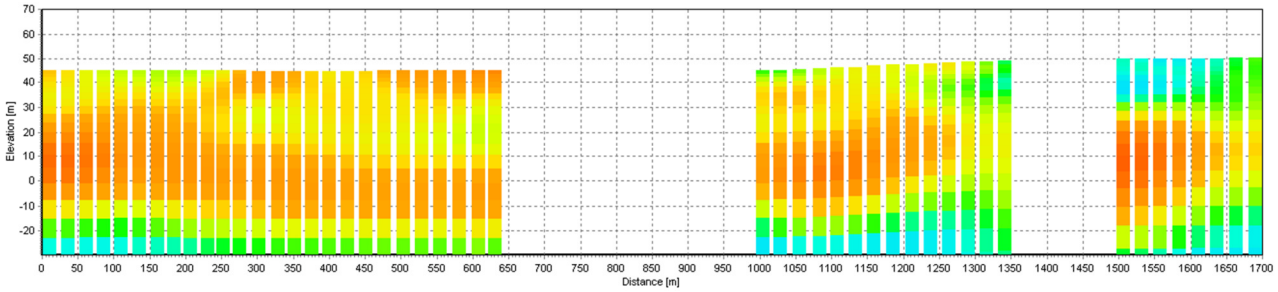

SkyTEM with new reference model and first gate 5_{new}

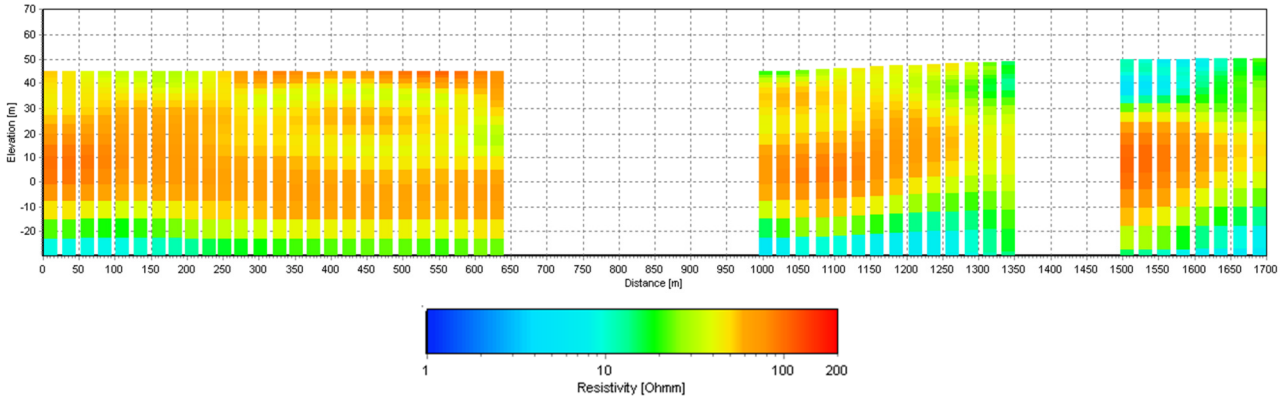

*Figure 23. Profile 1 - LCI smooth bias inversion on Sorø data with the new time shift. Top: ERT data. Middle: SkyTEM data with the first gate 6_{new}. Bottom: SkyTEM data with the first gate 5_{new}. The inversion parameters are: vertical constraint = 2, lat. const.=1.35, starting model of **100 Ωm**. Note: kept in version of May 2012 for compatibility in the figures' numbering, but no difference is now observed when compared to a starting model of 50 Ωm.*

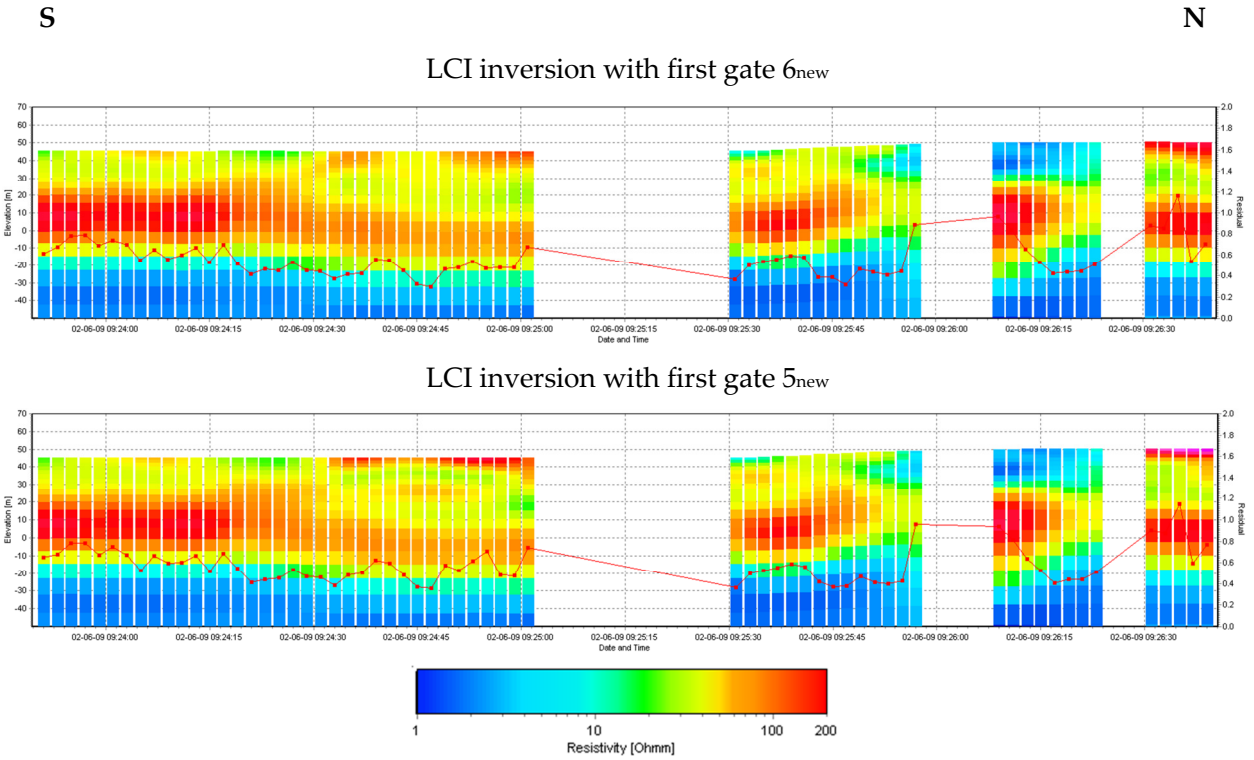

Figure 24. Profile 1 (SkyTEM results)– Top: data residual with first gate 6new. Bottom: data residual with first gate 5new.

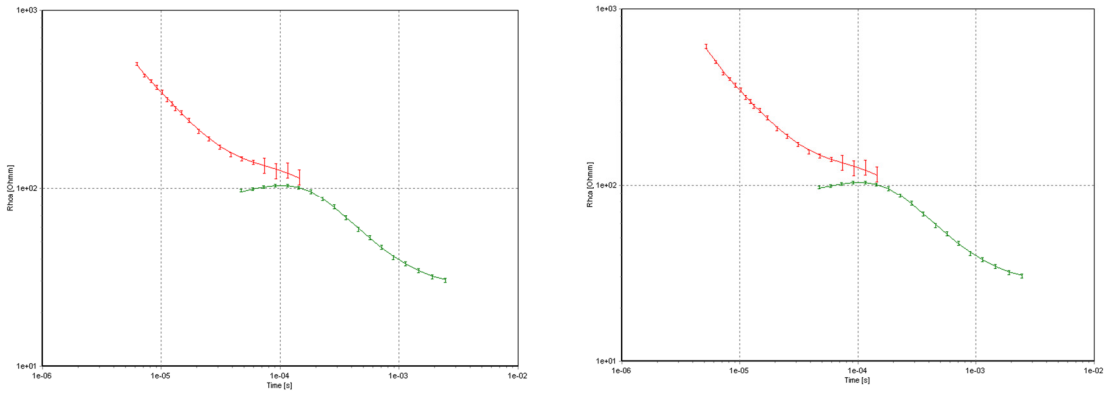

Figure 25. Profile 1 – Sounding curves (SkyTEM results) – Left: data fit with first gate 6new. Right: data fit with first gate 5new.

Other comparisons from SCI inversions

Figure 26 shows the second profile where ERT and SkyTEM results are compared. All inversion results are from SCI inversions, (also ERT was inverted using SCI). It is observed that the first 5 m becomes more resistive with the new time shift, and that the new results are then more consistent with the ERT profile where the first 5 m are also resistive. The second and more conductive layer appears only vaguely in the ERT profile. This small resistivity contrast is not expected to be well resolved with transient AEM data. Contrary to the first version of the report where this second layer appears more conductive and more contrasted in the SkyTEM section, the resistivity values are now in the same range as the ERT ones. As for the first profile there is still a small part of the profile where the first meters appear more conductive compared to the ERT. However, the overall top resistivity is clearly in better accordance with ERT measurements when considering the new time shift.

Figures *Figure 27* and *Figure 28* show comparison of the SkyTEM results with a borehole, with the old and the new shift, respectively. The first top layer (glacial sand) is globally more resistive, and the application of the new time shift results in an increase of the resistivity (Figure 28). Despite a shift of 2 m of the elevation of the borehole compared to digital elevation model used for SkyTEM soundings, the thickness of the resistive first layer is very similar to the one observed for the glacial sand in the borehole when the new time shift is considered in Figure 28. The boundaries of the glacial clayey till between the two sandy layers almost match the interfaces found with SkyTEM if the borehole is shifted 2 m upper (the bottom one appears less sharper in SkyTEM section). The transitions between these layers are probably not sharp, and moreover the SkyTEM inversion is a smooth one for which boundaries are not expected to be defined so precisely.

Figure 29 shows the mean horizontal resistivity at the depth of 0-5m, for the old and the new reference model. To compare with the SCI inversion of ERT data, the mean resistivity from the inversion of this data set has been left as colored points, so they can be superimposed to the mean resistivity maps created from the SkyTEM results. As can be observed, the near-surface resistivity becomes much higher and much closer to the ERT values with the new reference model (bottom map in *Figure 29*). It is even more clearly seen that SkyTEM resistivity decreases where ERT resistivity is lower (orange color in the South-East part of the bottom map in *Figure 29*) and reaches high values where ERT resistivity is higher (red color in the North-West part of the bottom map in *Figure 29*). So, with the new reference model, we observe coherence between ERT and SkyTEM results.

Figure 30 shows the mean horizontal resistivity at the depth of 5-10 m, for the old and the new reference model. As for sections in Figures *Figure 20* to *Figure 23* the medium resistivity obtained for the less resistive second layer is more coherent compared to ERT values at the same depth when considering the new time shift. Other mean resistivity maps can be found in Appendix 3. Deeper maps show that the differences between the old and the new time shifts become less and less important with depth down to 20 m. Below this depth almost no difference is observed, which indicates that the supplementary time shift of -1.1 μs has an impact only on the first 20 m. Regarding differences in resistivity levels between ERT and SkyTEM, resistivity values are expected to be badly resolved in resistive areas with TEM methods mainly sensitive to conductive layers.

The data residuals displayed on maps of Figure 31, for the old and new time shift, show that the data residual remains stable and generally below 0.5 or very close to 1. This data fit is much better compared to the first version of the report where the use of the old coil response induced a less good fit mainly above forest areas where the flight altitude and the importance of the coil response compared to the earth response are higher.

N **S**

ERT

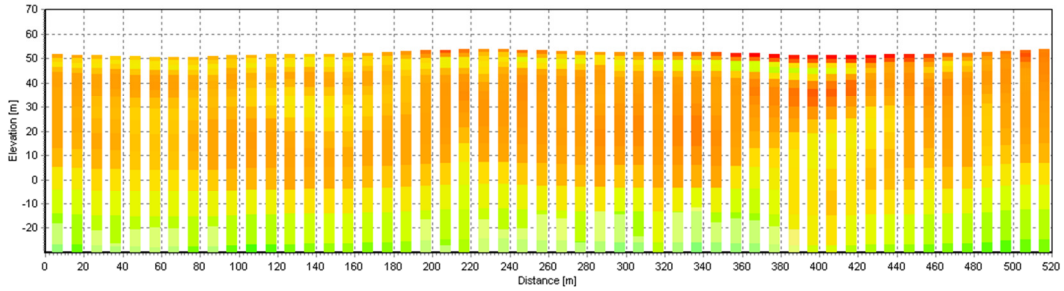

SkyTEM data with old reference model

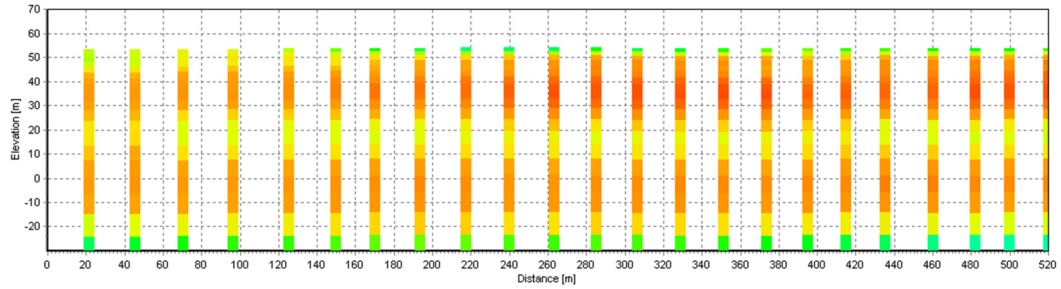

SkyTEM data with new reference model

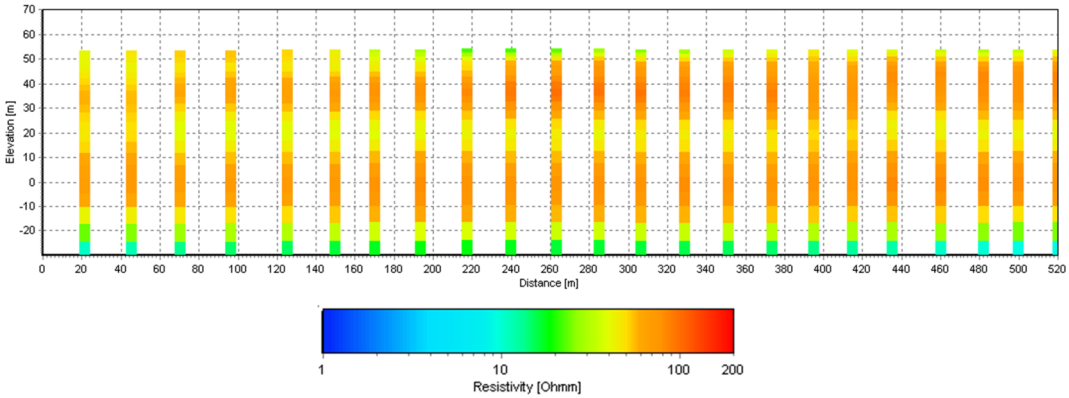

Figure 26. Profile 2 - SCI smooth coil-response inversion of Sorø SkyTEM data. Top: ERT result (smooth SCI). Middle: SkyTEM section with the old time shift. Bottom: SkyTEM section with the new time shift. Inversion parameters: vertical constraint = 2, lat. const.=1.35, starting model of 100 Ωm, and first gate 5.

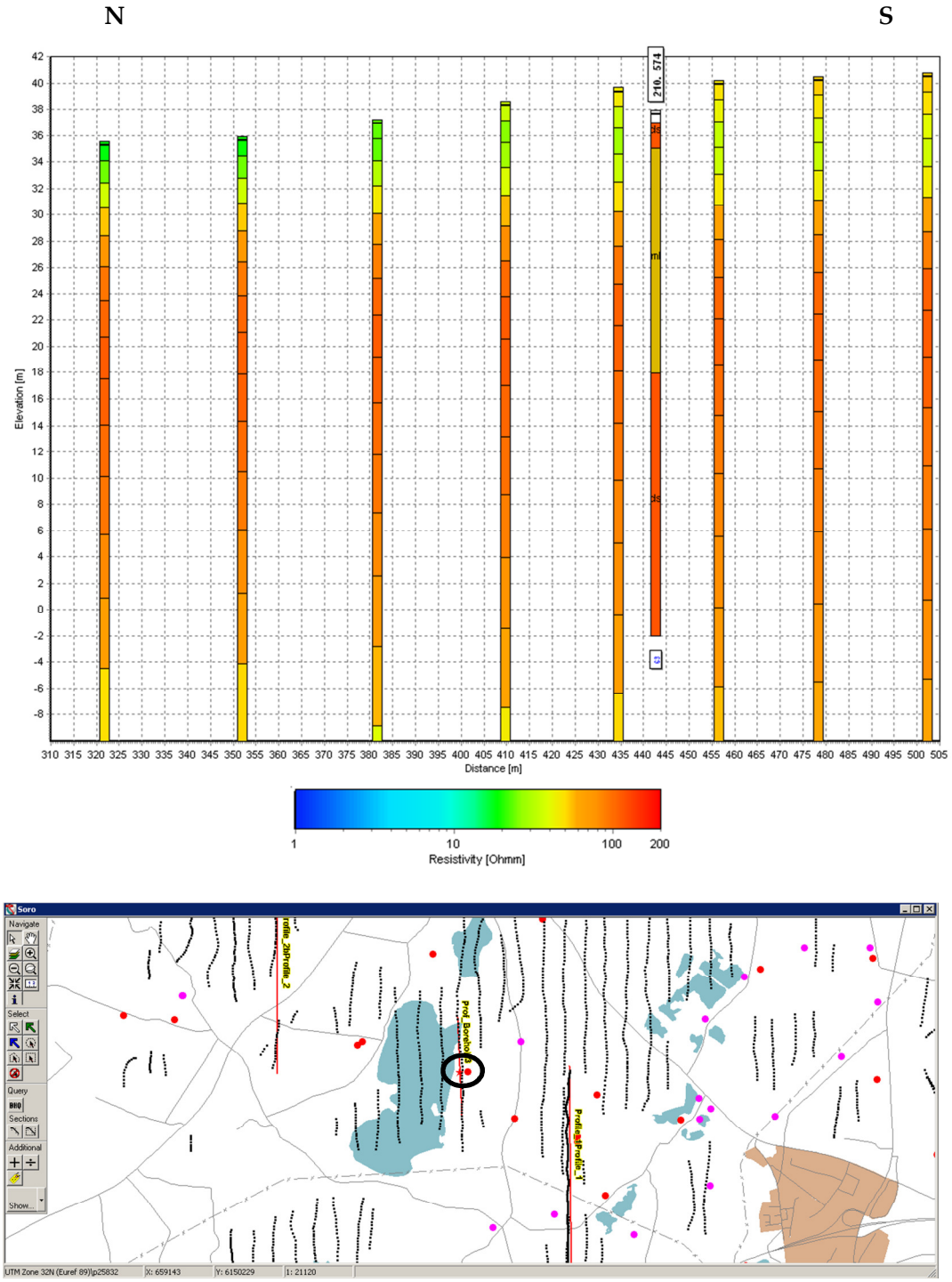

*Figure 27. Borehole - SCI smooth bias inversion on Sorø SkyTEM. data with the **old time shift** Inversion param.: vert. constraint = 2, lat. const.=1.35, starting model of 100 Ωm, and first gate 5*$_{old}$*.The borehole and the neighboring SkyTEM soundings are located inside the dark circle on the map.*

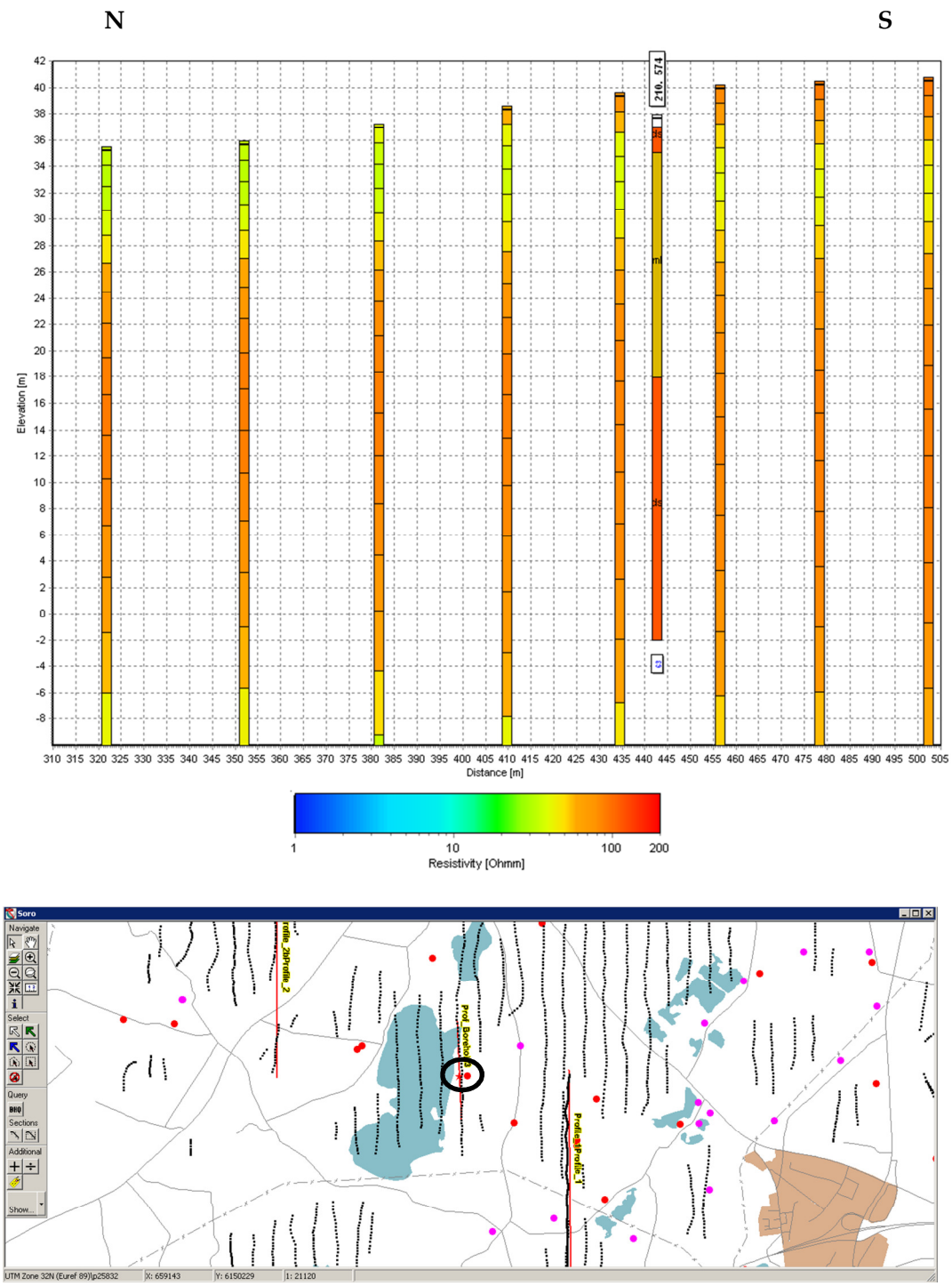

*Figure 28. Borehole - SCI smooth bias inversion on Sorø SkyTEM data with the **new time shift**. Inversion param.: vert. constraint = 2, lat. const.=1.35, starting model of 100 Ωm, and first gate 5*$_{new}$*.The borehole and the neighboring SkyTEM soundings are located inside the dark circle on the map.*

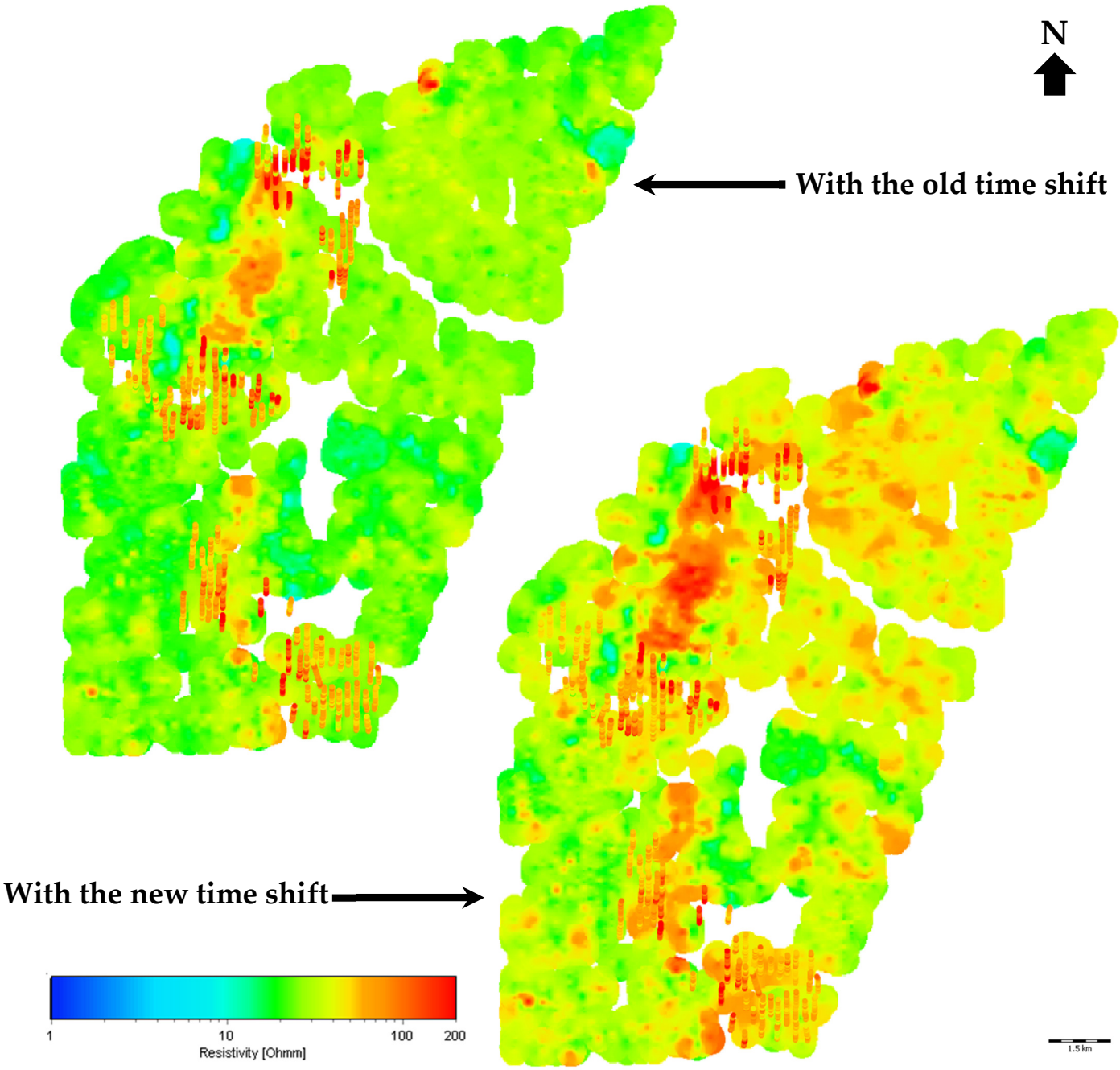

Figure 29. Mean resistivity map for depth 0-5 m - SCI smooth bias inversion on Sorø SkyTEM data with the old and the new time shifts. Inversion parameters: vertical constraint = 2, lat. const.=1.35, starting model of 100 Ωm, and first gate 5$_{old}$. The colored points correspond to the mean resistivity obtain from a SCI smooth inversion of ERT data.

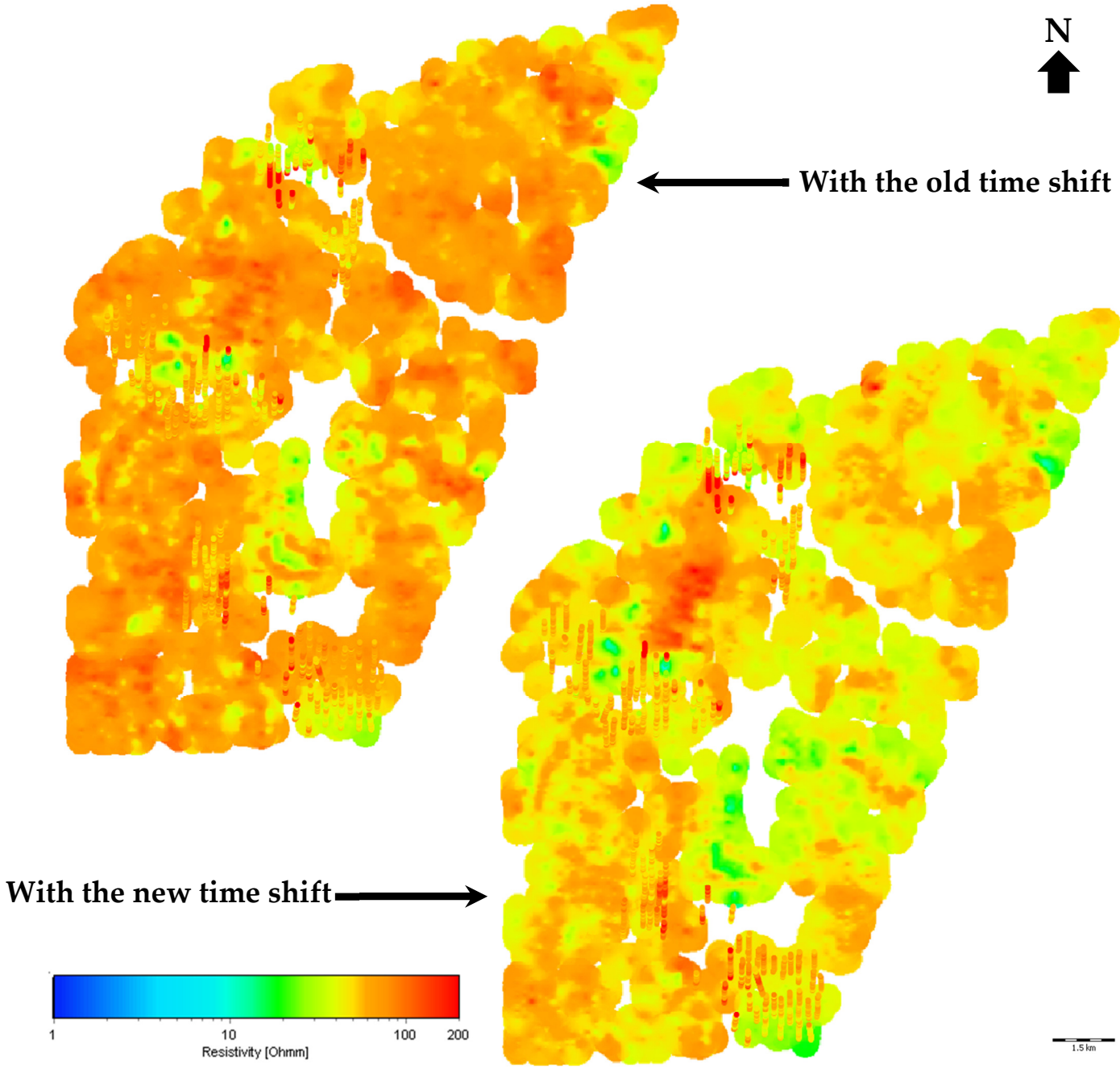

Figure 30. Mean resistivity map for depth 5-10 m - SCI smooth bias inversion on Sorø SkyTEM data with the old and the new time shifts. Inversion parameters: vertical constraint = 2, lat. const.=1.35, starting model of 100 Ωm, and first gate 5. The colored points correspond to the mean resistivity obtain from a SCI smooth inversion of ERT data.

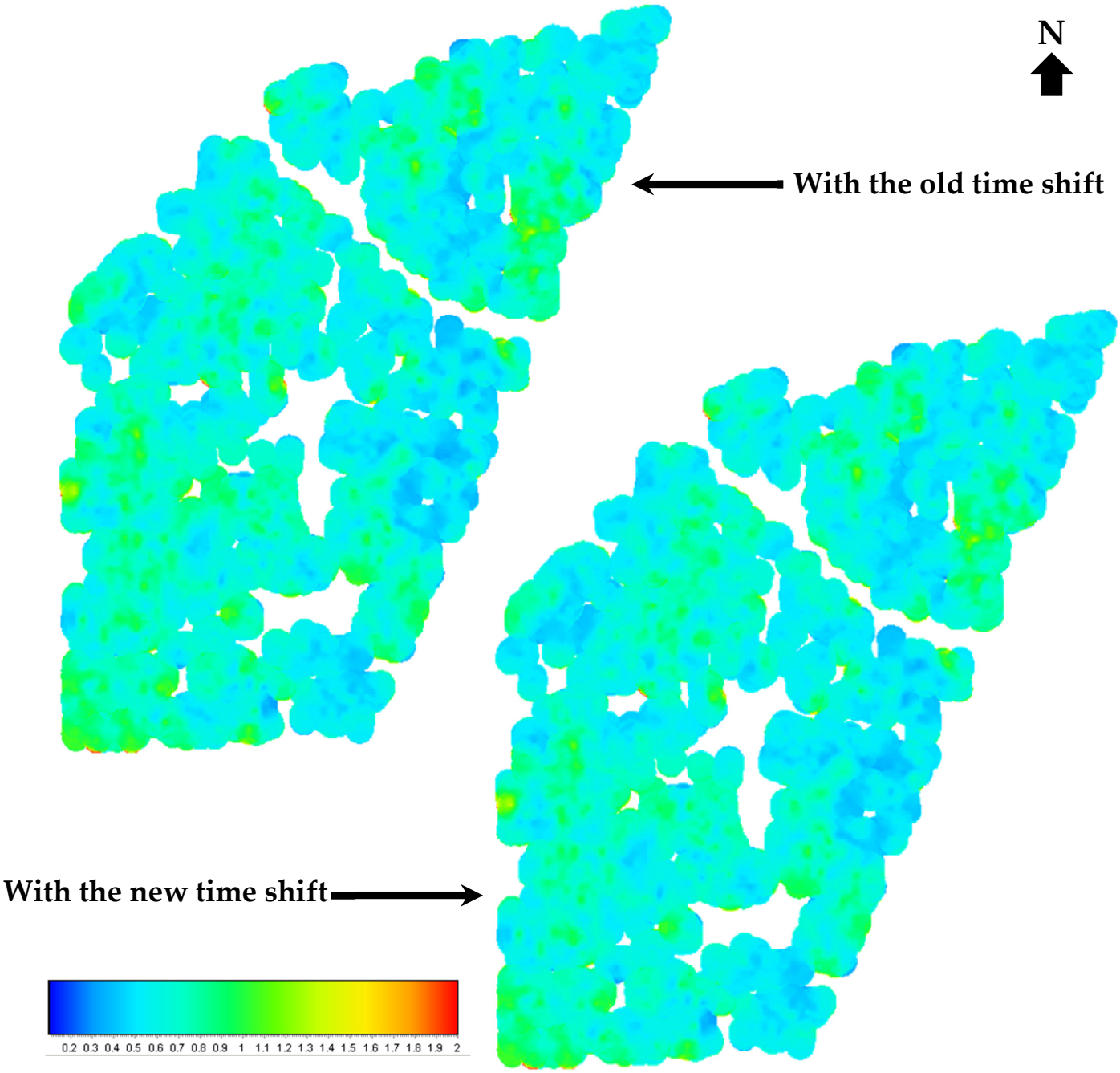

Figure 31. Data residual - SCI smooth bias inversion on Sorø SkyTEM data with the old and the time shifts. Inversion parameters: vertical constraint = 2, lat. const.=1.35, starting model of 100 Ωm, and first gate 5.

6.3 Conclusions and suggestions

Below we summarize conclusions and suggestions made for the Sorø-Stenlille survey:

1. The estimated difference in the time shift for the calibration of the used SkyTEM system is about the same as for that estimated for the WalkTEM/TEM40 instrument, between -1.1 and -1.0 μs. This indicates that the correction of the time shift is partly independent of the characteristics of the TEM system and that a similar correction could be applied to other TEM devices previously calibrated at the Lyngby reference site.
2. The new time shift from the refined reference model makes it possible to get a more resistive top layer than previously. This is also much more coherent with ERT measurements.
3. Application of the new time shift does not lead to observable changes in the geological structures below the depth of 20 m. Regarding differences in resistivity levels between ERT and SkyTEM, resistivity values are expected to be badly resolved in resistive areas with TEM methods mainly sensitive to conductive layers.
4. It has been shown that the adding of a supplementary very early gate (close to 6-7 μs) actually provides more details in the upper 20 m and improves the vertical resolution where conductivity is not too high.
5. Top Of Investigation should be investigated to give better insight into the reliability of the layer parameters estimated after the inversion. It is expected that the parameters of a first top resistive layer are less well defined as long as the conductivity of the second layer increases and/or the thickness of the resistive layer decreases.

7. CALIBRATION OF OTHER SKYTEM SYSTEMS

The following tables summarize the additional time shift needed to upgrade the calibration from the old reference model to the new and refined reference model. The same Matlab calibration script has been applied to other SkyTEM systems with different loop sizes (see description of the script in section 6.1), one very large which is aimed for deep soundings, and one very small designed for near-surface exploration.

7.1 Large SkyTEM loop of 494 m²

Table 17 summarizes some of the characteristics of the SkyTEM system used for the Tønder survey (September 2008). The Matlab calibration script has been applied on the data acquired at Lyngby prior to the survey. The difference observed between the calibration with the old and the new reference model is summarized in Table 18.

Flight altitude	30-40 m
Speed	45 km/h
Area of the transmitter loop	494 m²
Number of turns SLM/HM	1 / 4
Amp. of SLM/HM	11 A / 95 A
Turn-off of SLM/HM	~5 µs / ~55 µs

Table 17. Characteristics of the SkyTEM loop of 494m².

Moment	**Difference of time shift (New-Old)**	Ratio of factor shift (New/Old)
SLM	**-1.13 µs**	1.0
HM	**-1.25 µs**	1.0

Table 18. Difference and ratio between the old and the new calibration parameters for the SkyTEM loop of 494m² (Tønder survey, September 2008).

7.2 Small SkyTEM loop of 132 m²

Table 19 summarizes some of the characteristics of the SkyTEM system used for the survey of the NiCA project (June 2011). The Matlab calibration script has been applied on the data acquired at Lyngby prior to the survey. The difference observed between the calibration with the old and the new reference model is summarized in Table 20.

Flight altitude	25-35 m
Speed	100 km/h
Area of the transmitter loop	132 m²
Number of turns SLM/HM	1 / 1
Amp. of SLM/HM	7.5 A / 56 A
Turn-off of SLM/HM	~4 µs / ~12 µs

Table 19. Characteristics of the SkyTEM loop of 132 m² (NiCA project, June 2011)..

Moment	**Difference of time shift (New-Old)**	Ratio of factor shift (New/Old)
SLM	**-1.12 µs**	1.0
HM	**-1.18 µs**	1.0

Table 20. Difference and ratio between the old and the new calibration parameters for the SkyTEM loop of 132 m² (NiCA project, June 2011).

7.3 Summary of the calibration of TEM systems

Tables Table 21 to Table 24 summarize the difference obtained in the shift parameters for all TEM systems presented in this report due to the calibration of the systems with the new refined reference model, compared to the calibration with the old reference model. There is no difference in the factor shift, and the difference in the time shift can be resumed to **-1.1 µs** for both Low and High moments, and more importantly for every TEM system. This difference of time shift has been confirmed by the analysis of synthetic data curves of old and new reference model that have to be shifted by the same time in order to match (Figure 32), confirming that the difference of time is due to the refinement of the reference model and independent of

the TEM system. Note that the difference of time shift for the High Moment (still very close to -1.1 μs) has slightly more important variations because of the lack of precision for this moment whose first gate is around 30-40 μs. Moreover, the application of this additional time shift will have almost no impact on this moment contrary to the Low Moment.

Moment	**Difference of time shift**	Ratio of factor shift
SLM	**-1.1 μs**	1.0
HM	**-1.1 μs**	1.0

Table 21. Difference and ratio between the old and the new calibration parameters for the WalkTEM/TEM40 setup (40m by 40m loop).

Moment	**Difference of time shift**	Ratio of factor shift
SLM	**-1.12 μs**	1.0
HM	**-1.18 μs**	1.0

Table 22. Difference and ratio between the old and the new calibration parameters for the SkyTEM loop of 132 m² (NiCA project, June 2011).

Moment	**Difference of time shift**	Ratio of factor shift
SLM	**-1.09 μs**	1.0
HM	**-1.10 μs**	1.0

Table 23. Difference and ratio between the old and the new calibration parameters for the SkyTEM loop of 314 m² (Sorø survey, May 2009).

Moment	**Difference of time shift**	Ratio of factor shift
SLM	**-1.13 μs**	1.0
HM	**-1.25 μs**	1.0

Table 24. Difference and ratio between the old and the new calibration parameters for the SkyTEM loop of 494 m² (Tønder survey, September 2008).

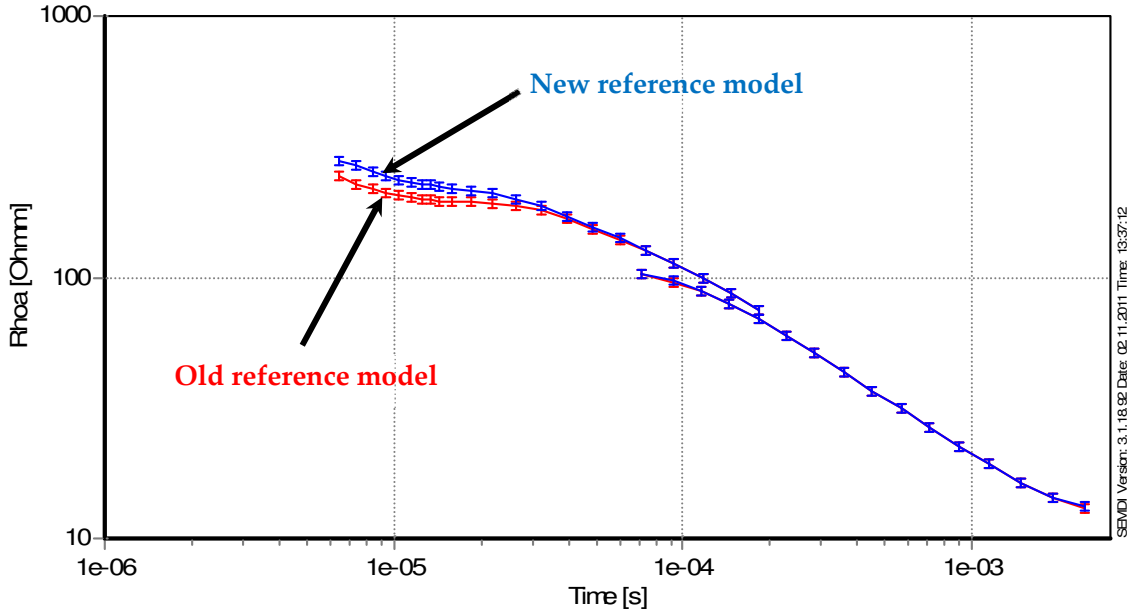

Figure 32. Forward modeling of the old (red curve) and new (blue curve) reference models with a SkyTEM setup at 30 m and error bars set at 3 %. The HM curve is almost unchanged contrary to the first gates of the SLM. The forward response of the old reference model has to be shifted with -1.1 µs to match the one of the new refined reference model.

8. CONLUSION

The following summarizes the main conclusions:

1) The refinement of the test site model in the upper 15 m showed higher resistivities in the first 13 m of the reference model, as compared to the old reference model. Furthermore, the refinement showed:
   - that the anisotropy coefficient in the upper 13 m of the test site model is close to 1.0. This means that the obtained ERT measurements at the test site correspond directly to the formation resistivity of the ground, and can be compared directly to the horizontal resistivity as measured with the TEM method.
   - that, as seen on the mean-resistivity maps, the test site is homogeneous, which means that the lateral variations are small.

   The facts that there is almost no anisotropy and that the site is homogeneous mean that the test site is very suitable for a one-dimensional model, and hence for calibration of ground based and airborne TEM systems.

2) The fact that the reference model has been changed in the upper part of the model does not influence the deeper part of the model (below 15 m), and consequently the deeper layers are still mapped correctly. The refined reference that has to be used for future calibrations is summarized in *Table 25*.

	Resistivity	Thickness	Depth
Layer 1	33.5	2.1	2.1
Layer 2	46.8	11.0	13.1
Layer 3	155.2	19.6	32.6
Layer 4	9.8	23.0	55.5
Layer 5	2.4	61.1	116.7
Layer 6	270.6	148.3	265.0
Layer 7	3		

Table 25. Refined reference model for the National TEM test site at Lyngby, Aarhus.

3) The refinement of the reference model means that an additional time shift of **-1.1 μs** has to be added to the old time shifts specified in the geometry files used for the Aarhus Workbench, including the time of the front gate always modeled for the High-Moment. This additional time shift is independent of the TEM system, has to be applied to both SLM and HM moments, and the factor shift does not need to be changed (see Table 26).

Moment	**Difference of time shift**	Ratio of factor shift
SSLM	**-1.1 μs**	1.0
HM	**-1.1 μs**	1.0

Table 26. Difference and ratio between the old and the new calibration parameters for all TEM systems.

4) The two TEM lines forming the extension of the test site has been updated with the relevant shift, and should be used as reference models for any airborne TEM system, opening the test site for validation and tests for airborne TEM systems under survey conditions.
5) The new time shift was applied to the Sorø-Stenlille survey (Chapter 6), resulting in a much better correspondence with the ERT measurements in the area. It implies changes in the upper 15 m with no change of the deeper geology, and the resistivity of the first 5 m is now larger that 30 Ω.m, generally above 70 Ω.m, except for a few areas where the top layer can be conductive. This is verified by ERT measurements made in the survey area.
6) The Sorø-Stenlille survey also revealed that in order to resolve the near-surface it is crucial to have the coil-response to obtain very early gates at 6-7 μs. Otherwise, thin resistive layers in the near-surface are difficult to map correctly.

9. REFERENCES

Auken, E., A. V. Christiansen, B. H. Jacobsen, N. Foged, and K. I. Sørensen, 2005, Piecewise 1D Laterally Constrained Inversion of resistivity data. Geophysical Prospecting, **53**, p. 497-506.

Christensen, N. B., 2000, Difficulties in determining electrical anisotropy in subsurface investigations. Geophysical Prospecting, **48**, p. 1-19.

GFS, 2001, Undersøgelse af fejl ved transistente malinger udført med Geonics PROTEM 47 måleinstrumentet, www.gfs.au.dk.

GFS, 2002, Test og sammenligning af transient elektromagnetiske instrumenter i Danmark – TEM Test 2002, www.gfs.au.dk.

GFS, 2002, Vejledning i kalibrering af Geonics PROTEM 47 måleinstrument, www.gfs.au.dk.

GFS, 2002, Vejledning for udførelse af TEM sonderinger, 2002, ww.gfs.geo.au.dk.

GFS, 2008, Spatially Constrained Inversion of SkyTEM data, concept and examples, www.gfs.au.dk.

GFS, 2009, Guide to processing and inversion of CVES data, www.gfs.au.dk.

GFS, 2011, Himmerland vurdering af SkyTEM metoden til sårbarhedskortægning, www.gfs.au.dk.

GFS, 2012, SkyTEM kortlægning Sorø-Stenlille, www.gfs.au.dk.

A. Viezzoli, A. V. Christiansen, E. Auken, and K. I. Sørensen. Quasi-3D modeling of airborne TEM data by Spatially Constrained Inversion. *Geophysics* 73 (3):F105-F113, 2008.

APPENDIX 1

Model parameters for South-North ERT profile

XUTM	YUTM	ELEV	NLAYER	DATFIT	RHO1	RHO2	RHO3	THK1	THK2	THK3
564432	6224398	30.7	3	0.1178	33.5	46.5	425.9	1.70	8.19	10.4
564432	6224400	30.7	3	0.1056	32.9	45.7	426.6	1.69	8.73	10.2
564432	6224402	30.8	3	0.3275	31.9	46.8	423.4	1.56	9.85	9.57
564433	6224404	30.8	3	0.1559	29.3	44.1	428.3	1.77	10.5	9.62
564433	6224406	30.9	3	0.2967	29.7	48.0	438.5	1.28	10.9	11.1
564433	6224408	30.9	3	0.4942	27.7	51.0	436.9	1.29	11.6	9.99
564433	6224410	31.0	3	0.2932	29.7	53.0	438.2	1.64	11.1	10.0
564434	6224412	31.0	3	0.1741	30.2	50.4	443.5	1.99	10.1	10.9
564434	6224414	31.0	3	0.3127	34.4	51.0	435.5	2.23	10.5	8.82
564434	6224416	31.1	3	0.1575	31.3	48.6	445.0	2.58	8.99	10.7
564435	6224418	31.1	3	0.3881	31.6	49.4	439.2	1.72	10.8	8.64
564435	6224420	31.2	3	0.7426	30.8	51.8	440.4	1.85	10.9	8.09
564435	6224422	31.2	3	0.1822	28.4	49.3	446.6	2.13	11.0	7.92
564435	6224424	31.2	3	0.2150	29.6	47.8	458.4	1.89	11.2	8.84
564436	6224426	31.3	3	0.3732	29.3	48.7	460.1	1.89	11.4	7.73
564436	6224428	31.4	3	0.3775	29.0	46.0	490.3	2.10	10.3	10.8
564436	6224430	31.4	3	0.2662	30.3	52.3	486.6	1.88	11.0	8.38
564436	6224432	31.5	3	0.3674	28.3	52.8	515.7	1.74	11.2	9.67
564437	6224434	31.6	3	0.7863	34.2	55.4	523.7	1.75	11.5	7.50
564437	6224436	31.7	3	0.5372	33.1	52.1	556.6	1.49	11.9	9.24
564437	6224438	31.7	3	0.6179	33.6	50.5	572.6	2.18	11.5	8.96
564438	6224440	31.8	3	0.4431	34.8	51.3	598.3	1.66	12.6	9.57
564438	6224442	31.9	3	0.3542	35.6	50.5	597.0	1.52	12.1	8.13
564438	6224444	32.0	3	0.3933	33.6	54.5	633.9	1.19	13.7	9.17
564438	6224446	32.0	3	0.2905	33.5	51.8	636.5	1.46	13.0	9.03
564439	6224448	32.1	3	0.3796	37.1	52.3	636.1	1.46	13.0	9.13
564439	6224450	32.2	3	0.4701	34.2	53.4	631.0	1.47	13.1	8.66
564439	6224452	32.2	3	0.5899	34.3	56.2	634.7	1.80	13.3	8.62
564439	6224454	32.3	3	0.4725	34.5	55.9	628.1	1.53	13.4	8.09
564440	6224456	32.4	3	0.4047	35.3	55.1	626.4	1.61	14.1	7.70
564440	6224458	32.5	3	0.6772	31.4	49.8	622.3	2.07	12.8	9.13
564440	6224460	32.5	3	0.5277	32.7	48.9	639.5	1.82	14.2	9.70
564440	6224462	32.6	3	0.3406	31.9	54.3	636.7	1.52	14.9	8.41
564441	6224464	32.7	3	0.3507	31.5	53.0	648.1	2.22	13.6	10.6
564441	6224465	32.8	3	0.4157	31.4	58.4	614.9	2.06	13.1	7.85
564441	6224467	32.8	3	0.3731	32.1	56.2	608.9	1.72	14.1	8.09
564442	6224469	32.9	3	0.2564	30.5	50.0	587.9	2.06	12.1	9.55
564442	6224471	33.0	3	0.3702	30.5	46.7	583.7	1.73	12.5	9.72
564442	6224473	33.0	3	0.5635	34.4	50.1	589.1	1.37	14.1	9.39
564442	6224476	33.1	3	0.6688	28.0	41.5	558.6	1.78	9.69	10.1
564443	6224478	33.1	3	0.3254	33.2	49.9	574.8	1.67	12.1	9.65
564443	6224480	33.2	3	0.3164	33.2	49.3	557.4	1.98	11.0	9.69
564443	6224482	33.2	3	0.5367	30.2	47.1	549.4	2.24	10.3	11.3
564443	6224484	33.3	3	0.6173	36.7	50.3	531.5	1.94	11.7	9.97
564444	6224486	33.3	3	0.2814	31.2	46.3	533.4	1.94	10.9	11.2
564444	6224488	33.4	3	0.2987	30.4	50.1	530.4	1.96	11.7	10.5
564444	6224490	33.4	3	0.2692	30.2	48.8	532.4	1.73	11.9	10.6
564444	6224492	33.5	3	0.4834	32.1	47.4	528.5	1.83	11.4	10.4
564445	6224494	33.6	3	0.3131	32.2	47.1	529.8	2.18	11.5	11.1
564445	6224496	33.6	3	0.4319	31.9	44.9	527.8	2.21	10.4	12.0
564445	6224498	33.7	3	0.3626	37.2	53.2	511.6	2.08	11.6	9.92
564446	6224500	33.7	3	0.4852	34.4	51.3	506.2	1.97	10.6	10.2
564446	6224502	33.8	3	0.4202	34.4	48.3	533.4	2.28	10.8	12.5
564446	6224504	33.8	3	0.3360	36.2	50.4	528.3	2.27	11.5	11.5
564446	6224506	33.8	3	0.3060	35.0	48.7	535.8	2.26	11.2	11.8
564447	6224508	33.9	3	0.1787	39.7	53.0	517.4	2.31	12.1	9.46
564447	6224510	33.9	3	0.2938	37.3	48.2	542.6	2.51	11.7	12.2
564447	6224512	34.0	3	0.3063	38.6	50.7	532.1	2.65	12.1	10.9
564448	6224514	34.0	3	0.4189	38.0	50.2	533.6	2.43	12.0	11.8
564448	6224516	34.1	3	0.2849	40.8	53.3	519.1	2.35	13.1	10.4
564448	6224518	34.2	3	0.3047	39.5	51.7	517.4	2.45	13.0	12.1
564448	6224520	34.2	3	0.4082	35.5	49.8	504.4	2.42	12.4	12.7
564449	6224522	34.2	3	0.3228	42.4	53.1	483.7	2.26	12.9	11.5
564449	6224524	34.1	3	0.4121	36.6	48.2	476.8	2.14	11.6	12.9
564449	6224526	34.1	3	0.2473	41.0	50.9	454.5	2.24	11.7	11.5
564449	6224528	34.1	3	0.1669	37.7	47.3	447.4	2.36	10.5	12.5
564450	6224530	34.1	3	0.1081	37.6	47.6	433.7	2.32	10.2	12.2
564450	6224532	34.1	3	0.5469	38.4	47.9	414.0	2.30	10.3	10.6
564450	6224534	34.0	3	0.3477	32.7	46.0	408.3	2.12	9.98	10.9
564451	6224536	34.0	3	0.4267	33.9	45.1	395.1	2.08	9.81	9.99
564451	6224538	33.9	3	0.3810	29.2	42.6	395.3	1.96	9.29	10.5
564451	6224540	33.9	3	0.5696	29.0	43.6	388.6	1.94	9.30	9.83
564451	6224542	33.8	3	0.5616	26.9	41.4	404.1	1.78	7.73	12.6
564452	6224544	33.8	3	0.5356	35.4	40.7	394.2	1.51	9.34	10.3
564452	6224546	33.7	3	0.2821	31.9	32.9	412.6	1.61	7.76	13.1
564452	6224548	33.6	3	0.3137	30.7	34.0	413.6	1.78	8.29	12.5
564452	6224550	33.5	3	0.6358	31.5	36.9	411.1	2.02	8.90	11.6
564453	6224552	33.4	3	0.2746	30.0	35.4	405.1	2.60	9.42	9.99

UTM-coordinate system: WGS84 zone 32N
ELEV: surface elevation
DATFIT: Normalized data residual
RHO# : Resistivity of layer #
THK# : Thickness of layer #

Model parameters for West-East ERT profile

XUTM	YUTM	ELEV	NLAYER	DATFIT	RHO1	RHO2	RHO2	THK1	THK2	THK3
564367	6224478	32.3	3	0.2307	39.7	36.8	516.8	1.62	6.95	17.5
564369	6224478	32.3	3	0.3856	36.4	34.8	511.4	1.49	6.84	17.9
564371	6224478	32.3	3	0.2400	39.4	33.9	511.5	1.31	6.09	19.0
564373	6224478	32.3	3	0.1927	43.3	33.3	505.7	1.21	6.75	18.3
564375	6224478	32.4	3	0.3159	50.0	33.5	501.6	1.20	7.02	18.0
564377	6224478	32.4	3	0.2050	53.9	33.2	505.9	1.24	7.25	18.1
564379	6224478	32.4	3	0.3169	53.6	33.2	502.9	1.02	7.91	17.2
564380	6224478	32.4	3	0.3543	49.9	30.7	527.7	1.31	7.48	18.9
564382	6224478	32.4	3	0.4489	43.5	34.7	517.1	1.00	8.09	17.8
564384	6224478	32.4	3	0.3463	41.5	35.5	513.8	1.22	8.18	17.1
564386	6224477	32.5	3	0.4864	44.0	34.8	524.6	1.36	8.25	17.6
564388	6224477	32.5	3	0.3915	41.9	33.1	536.9	1.03	7.98	17.6
564390	6224477	32.5	3	0.3850	43.1	37.0	516.9	1.41	8.39	14.6
564392	6224477	32.5	3	0.3415	40.2	33.3	524.3	1.34	7.82	14.9
564394	6224477	32.6	3	0.2756	36.2	31.1	558.8	1.75	7.91	14.4
564398	6224477	32.6	3	0.2469	35.7	34.3	570.1	1.83	9.72	11.7
564400	6224477	32.7	3	0.3707	28.6	29.4	657.0	1.96	7.94	17.6
564402	6224477	32.7	3	0.8397	33.9	40.1	627.6	1.74	10.5	12.2
564404	6224477	32.7	3	0.7161	27.0	37.7	642.4	2.10	8.50	13.4
564406	6224476	32.7	3	0.4267	25.7	37.3	685.0	2.29	8.93	13.6
564408	6224476	32.8	3	0.4317	26.3	41.0	682.6	1.94	9.71	11.8
564410	6224476	32.8	3	0.4271	23.8	36.4	707.3	1.79	9.01	12.9
564412	6224476	32.9	3	0.4479	23.4	44.2	707.5	1.42	10.9	11.4
564414	6224476	33.0	3	0.4279	23.6	39.9	728.1	1.59	10.2	13.0
564416	6224476	33.0	3	0.5988	28.6	37.7	732.9	1.14	10.4	13.6
564418	6224476	33.0	3	0.4959	27.2	40.8	714.9	1.72	9.93	13.2
564420	6224476	33.0	3	0.4588	32.5	41.2	723.7	1.90	9.75	14.9
564422	6224476	33.0	3	0.5833	36.1	48.8	663.4	2.18	10.1	11.3
564424	6224476	33.1	3	0.6407	33.5	50.8	633.7	2.07	10.0	10.4
564426	6224475	33.1	3	0.6635	35.1	40.9	663.8	1.92	10.0	12.6
564428	6224475	33.1	3	0.5158	34.0	41.2	644.1	1.96	10.2	11.3
564430	6224475	33.1	3	0.3194	31.0	39.1	650.7	2.15	9.62	12.2
564432	6224475	33.1	3	0.3101	32.5	43.7	666.2	1.88	11.1	12.6
564434	6224475	33.1	3	0.3368	32.0	49.1	633.6	2.11	11.0	11.2
564436	6224475	33.1	3	0.3965	33.4	51.6	623.0	2.03	12.0	11.2
564438	6224475	33.1	3	0.4597	32.9	49.1	607.5	1.84	11.7	12.0
564440	6224475	33.1	3	0.4368	31.4	46.8	588.0	1.93	11.2	11.2
564442	6224475	33.1	3	0.2864	31.6	45.3	592.0	1.62	11.3	11.9
564444	6224475	33.0	3	0.3375	30.9	47.9	587.1	1.44	12.9	10.3
564446	6224474	32.9	3	0.4221	31.8	46.4	598.1	1.72	12.3	11.9
564448	6224474	32.9	3	0.4135	31.5	47.6	585.6	1.94	12.6	11.1
564450	6224474	32.8	3	0.3355	35.7	49.1	551.1	1.83	12.0	11.1
564452	6224474	32.7	3	0.3828	31.6	48.9	531.4	1.69	12.0	11.1
564454	6224474	32.7	3	0.3823	36.3	46.2	528.6	1.81	11.0	12.2
564456	6224474	32.6	3	0.2967	35.6	45.4	523.4	1.88	10.9	12.1
564458	6224474	32.5	3	0.2386	37.3	45.6	514.5	1.81	10.0	11.8
564460	6224474	32.5	3	0.3283	39.4	46.4	523.2	2.08	10.2	12.5
564462	6224474	32.4	3	0.3611	38.8	46.5	517.6	2.51	9.11	12.8
564464	6224474	32.4	3	0.3257	39.8	51.1	503.6	2.76	9.81	12.3
564466	6224473	32.3	3	0.4952	38.8	50.9	508.2	3.19	9.34	13.9
564468	6224473	32.3	3	0.3508	36.9	54.4	496.6	3.06	9.82	12.8
564470	6224473	32.2	3	0.5295	39.7	50.5	503.9	3.17	9.65	13.8
564472	6224473	32.2	3	0.3871	36.2	52.8	498.7	3.05	9.71	13.1
564474	6224473	32.2	3	0.4919	37.6	49.4	506.6	3.27	9.53	13.7
564476	6224473	32.1	3	0.3361	35.9	53.5	502.4	2.87	10.5	12.3
564478	6224473	32.1	3	0.3984	37.3	51.9	506.4	3.16	9.99	12.3
564480	6224473	32.0	3	0.3721	39.2	48.4	499.7	2.68	9.90	11.9
564482	6224473	32.0	3	0.3890	38.0	49.5	518.9	2.93	10.2	12.0
564484	6224473	31.9	3	0.2906	41.3	44.8	525.5	2.69	9.86	12.8
564486	6224472	31.9	3	0.4668	44.5	47.9	500.8	2.49	9.90	10.7
564488	6224472	31.8	3	0.5689	44.1	43.6	497.3	2.25	9.09	12.3
564490	6224472	31.8	3	0.7789	48.0	45.6	487.0	1.90	9.62	11.8
564492	6224472	31.8	3	0.5391	47.2	45.9	472.6	1.95	9.51	11.8
564494	6224472	31.8	3	0.3238	43.0	46.1	473.2	2.16	9.64	12.3
564496	6224472	31.9	3	0.2396	41.3	47.5	478.4	2.33	10.0	13.7
564498	6224472	31.9	3	0.3098	39.0	45.2	468.1	2.63	9.33	13.9
564500	6224472	32.0	3	0.5141	38.7	51.7	446.1	2.27	10.9	11.3
564502	6224472	32.0	3	0.1971	37.9	53.9	435.3	2.25	11.7	10.0
564504	6224472	32.1	3	0.3290	34.7	52.2	439.8	2.52	10.5	12.0
564506	6224471	32.2	3	0.4868	28.4	53.4	436.1	1.98	11.6	11.6
564508	6224471	32.2	3	0.5608	32.5	54.3	423.5	1.79	12.7	9.50
564510	6224471	32.3	3	0.2109	29.6	46.4	424.0	2.39	11.5	10.6
564512	6224471	32.4	3	0.5285	30.5	50.3	416.8	2.18	12.4	9.14
564514	6224471	32.4	3	0.3886	29.4	50.5	427.8	2.00	11.1	11.8
564515	6224471	32.5	3	0.2860	31.6	47.8	430.9	2.16	11.1	11.9
564517	6224471	32.7	3	0.6953	28.5	48.9	440.5	2.10	11.1	12.9
564519	6224471	32.8	3	0.3608	30.8	50.3	440.8	1.78	11.1	13.0

UTM-coordinate system: WGS84 zone 32N
ELEV: surface elevation
DATFIT: Normalized data residual
RHO# : Resistivity of layer #
THK# : Thickness of layer #

APPENDIX 2

Model parameters for the two test lines used for the extension of the national TEM test site.

South-North profile

XUTM	YUTM	ELEV	NLAYER	RHO1	THK1	RHO2	THK2	RHO3	THK3	RHO4	THK4	RHO5	THK5	RHO6
564387	6224037	22.5	6	37.5	4.6	36.1	25.1	16.2	56.6	6.1	37.7	83.7	92.5	2.0
564392	6224079	22.7	6	35.2	6.2	38.8	25.5	12.9	46.6	4.4	36.3	95.6	104.2	1.9
564397	6224121	22.9	6	47.9	8.3	39.6	22.9	13.9	41.8	3.8	38.6	116.4	114.1	1.7
564403	6224163	24.6	6	38.8	4.9	49.8	25.2	14.7	40.8	3.6	45.3	124.8	114.5	1.7
564408	6224205	25.7	6	38.1	4.1	59.4	25.0	13.1	39.4	3.1	46.1	130.5	121.5	1.7
564413	6224247	27.3	6	39.7	4.1	62.5	25.4	12.7	38.3	2.8	48.5	131.0	124.5	1.8
564419	6224288	30.0	6	42.4	7.1	74.3	23.9	12.4	37.2	2.6	49.5	130.3	127.5	1.9
564424	6224330	31.4	6	43.5	10.6	91.8	23.1	11.8	34.0	2.5	52.5	131.9	129.3	2.0
564429	6224372	31.0	6	44.4	10.9	92.2	22.6	11.0	31.0	2.5	55.7	137.5	133.6	2.0
564434	6224414	31.1	6	45.4	9.4	83.8	24.1	10.3	26.5	2.5	56.3	149.1	141.6	2.1
564440	6224456	32.4	6	42.3	10.3	103.2	23.5	9.6	23.8	2.3	60.5	145.6	141.2	2.2
564445	6224498	33.7	6	40.5	9.9	119.3	23.9	9.4	22.6	2.4	61.2	145.6	142.8	2.3
564450	6224539	34.0	6	42.9	11.3	119.1	22.0	8.8	20.3	2.3	63.4	142.4	143.8	2.5
564456	6224581	32.3	6	39.3	10.5	118.2	23.3	7.8	17.7	2.3	65.6	134.6	142.9	2.7
564461	6224623	35.0	6	39.7	7.6	103.0	28.1	7.2	17.3	2.4	70.1	127.5	136.0	2.9
564466	6224665	36.1	6	39.8	3.8	73.3	32.1	8.0	19.2	2.3	69.8	120.4	132.8	3.1
564472	6224707	37.2	6	38.8	6.1	80.4	31.5	9.9	20.8	2.2	66.5	111.9	131.0	3.3
564488	6224832	39.4	6	38.7	6.9	71.1	39.5	12.3	20.2	2.1	65.9	103.1	121.5	3.6
564493	6224874	38.2	6	36.2	3.5	63.8	44.3	12.3	20.2	2.2	68.0	96.8	116.1	3.7
564498	6224916	37.5	6	34.0	6.0	68.2	39.5	11.0	22.4	2.2	66.9	92.6	115.5	3.9
564504	6224958	37.6	6	35.9	9.9	65.5	34.3	9.4	23.2	2.2	68.3	89.2	113.1	4.0
564509	6224999	37.5	6	34.4	8.2	49.8	33.1	9.4	23.7	2.3	71.7	89.0	111.3	4.0
564514	6225041	37.5	6	38.6	3.0	43.8	32.0	9.0	26.4	2.4	74.3	91.0	111.8	4.1
564520	6225083	37.5	6	37.2	2.8	43.7	28.9	6.4	29.0	2.4	74.8	90.2	111.6	4.1

West-East profile

XUTM	YUTM	ELEV	NLAYER	RHO1	THK1	RHO2	THK2	RHO3	THK3	RHO4	THK4	RHO5	THK5	RHO6
564079	6224497	31.2	6	33.7	4.5	65.7	21.9	13.7	33.2	2.9	51.0	90.7	136.1	2.9
564121	6224495	31.5	6	34.4	4.1	61.7	18.7	14.0	29.9	3.0	57.7	101.0	139.6	3.0
564161	6224493	31.7	6	34.4	4.2	61.3	23.3	11.4	21.6	3.2	63.4	111.5	141.4	3.2
564203	6224490	31.8	6	31.9	5.3	74.5	26.0	8.9	15.5	3.0	63.6	115.5	147.2	3.4
564242	6224486	31.9	6	31.4	5.7	93.9	27.4	7.9	14.3	2.9	63.3	113.5	150.0	3.7
564281	6224486	32.0	6	33.3	5.3	96.8	28.1	8.8	16.4	2.8	64.0	108.4	149.3	3.9
564319	6224482	32.1	6	32.6	5.0	101.4	26.8	9.6	19.3	2.7	64.8	106.9	149.5	4.0
564361	6224480	32.3	6	32.9	5.1	94.4	25.0	10.2	22.4	2.6	62.6	107.3	152.5	4.1
564398	6224480	32.7	6	32.8	6.7	101.7	26.5	9.0	22.4	2.4	59.9	105.7	153.8	4.2
564439	6224478	33.2	6	37.5	6.9	87.5	28.3	9.3	22.0	2.5	59.0	107.2	155.0	4.2
564478	6224476	32.2	6	40.5	4.2	66.0	29.0	10.0	22.0	2.4	59.9	110.8	157.3	4.2
564518	6224472	32.7	6	39.6	6.7	74.5	30.7	8.9	19.2	2.4	60.3	110.4	156.8	4.2
564560	6224469	34.7	6	41.2	8.1	74.0	31.8	7.9	16.9	2.4	61.6	110.0	156.0	4.3
564598	6224469	33.6	6	38.3	4.8	69.2	32.9	8.3	18.2	2.5	65.7	107.3	152.7	4.3
564635	6224468	31.1	6	35.6	4.8	72.0	32.6	8.4	21.3	2.5	64.4	104.4	151.0	4.3
564677	6224467	31.3	6	36.3	4.5	69.3	33.1	9.9	24.8	2.4	61.2	101.7	150.1	4.3
564714	6224462	30.9	6	33.5	6.2	68.8	32.2	11.7	27.3	2.3	58.7	98.5	148.7	4.3
564758	6224459	29.6	6	28.0	10.1	76.0	31.3	12.7	28.1	2.2	56.6	96.2	146.8	4.3

UTM-coordinate system: WGS84 zone 32N
ELEV: surface elevation
RHO# : Resistivity of layer #
THK# : Thickness of layer #

Extended xyz-files including the model parameter analyses are available from GFS' website (www.gfs.au.dk). The inversion results, raw and processed data are available for download from the national **ge**ophysical **r**elational **da**tabase, GERDA, at www.gerda.geus.dk.

APPENDIX 3

Mean resistivity maps of the Sorø survey in function of depth.

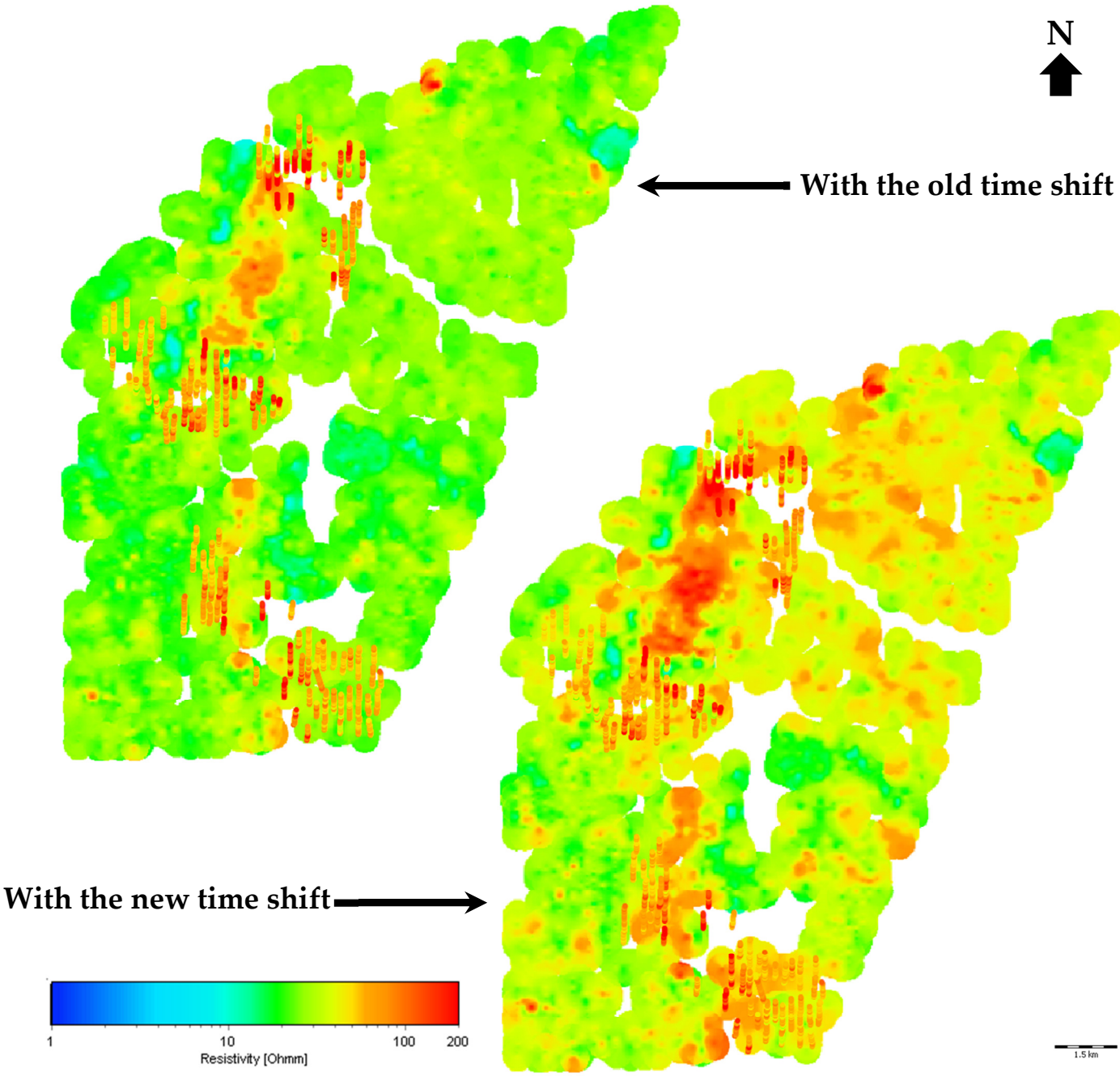

Figure 33. Mean resistivity map for depth 0-5 m - SCI smooth bias inversion on Sorø SkyTEM data with the old and the new time shifts. Inversion parameters: vertical constraint = 2, lat. const.=1.35, starting model of 100 Ωm, and first gate 5$_{old}$. The colored points correspond to the mean resistivity obtain from a SCI smooth inversion of ERT data.

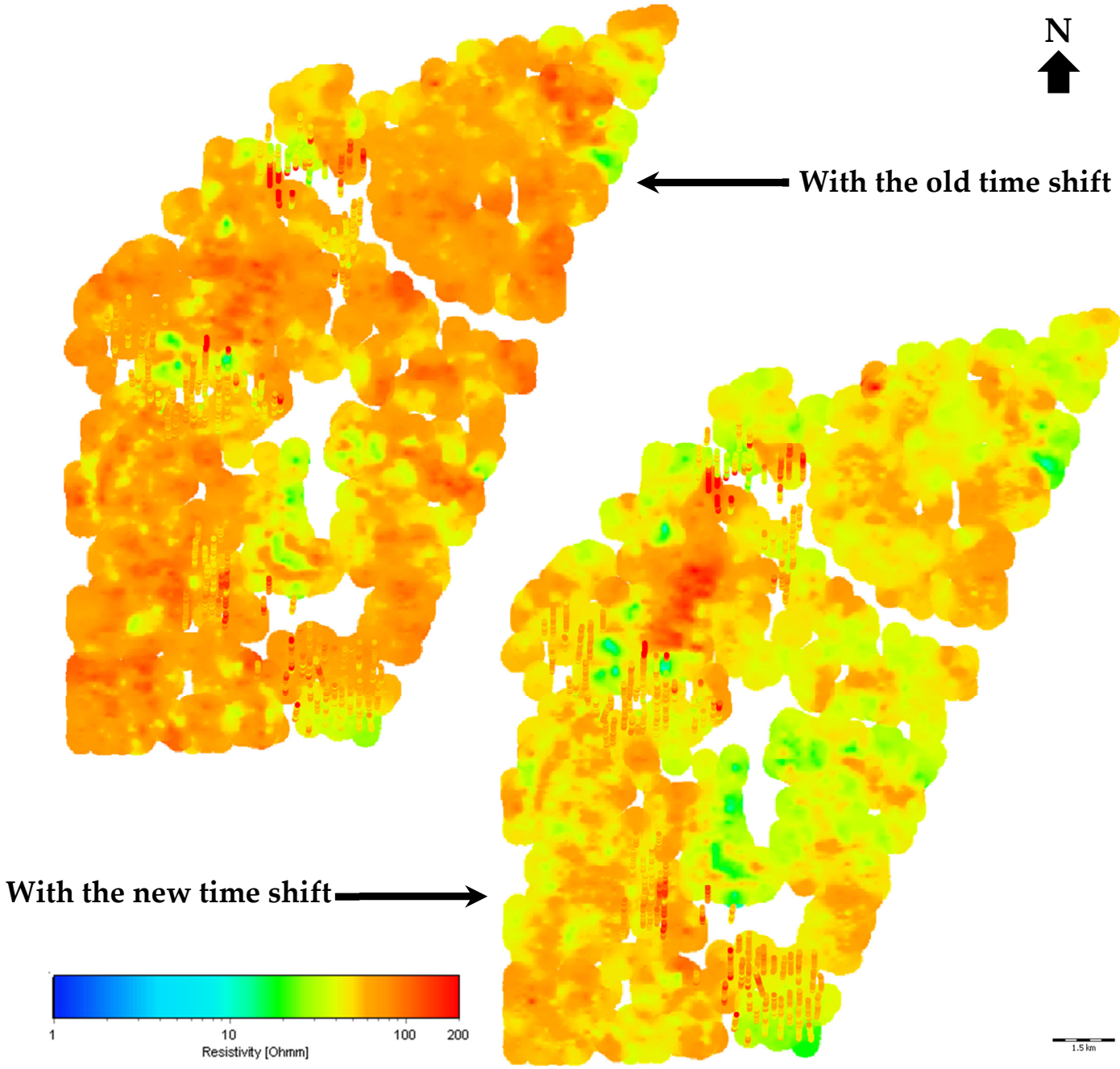

Figure 34. Mean resistivity map for depth 5-10 m - SCI smooth bias inversion on Sorø SkyTEM data with the old and the new time shifts. Inversion parameters: vertical constraint = 2, lat. const.=1.35, starting model of 100 Ωm, and first gate 5. The colored points correspond to the mean resistivity obtain from a SCI smooth inversion of ERT data.

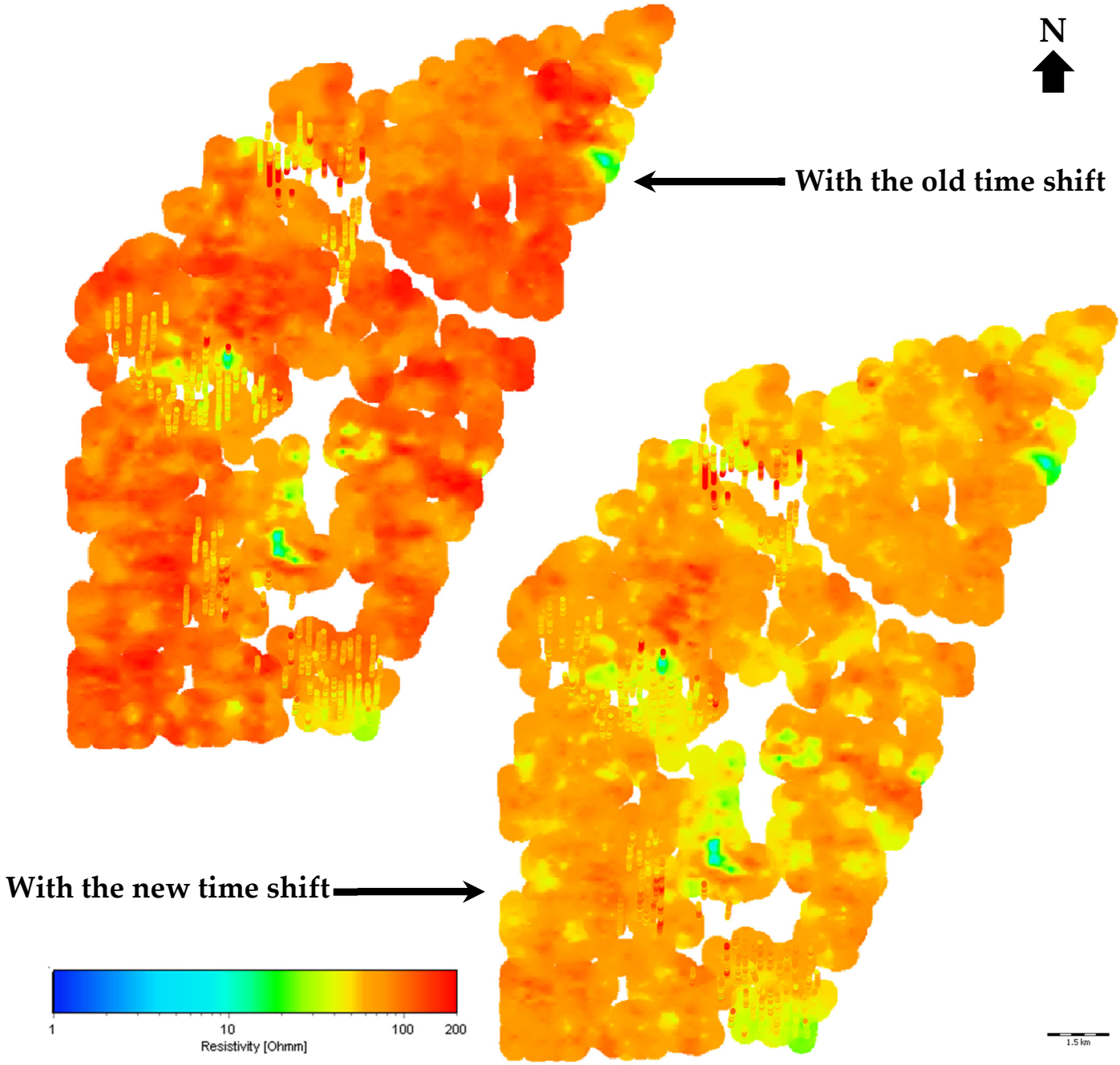

Figure 35. Mean resistivity map for depth 10-15 m - SCI smooth bias inversion on Sorø SkyTEM data with the old and the new time shifts. Inversion parameters: vertical constraint = 2, lat. const.=1.35, starting model of 100 Ωm, and first gate 5. The colored points correspond to the mean resistivity obtain from a SCI smooth inversion of ERT data.

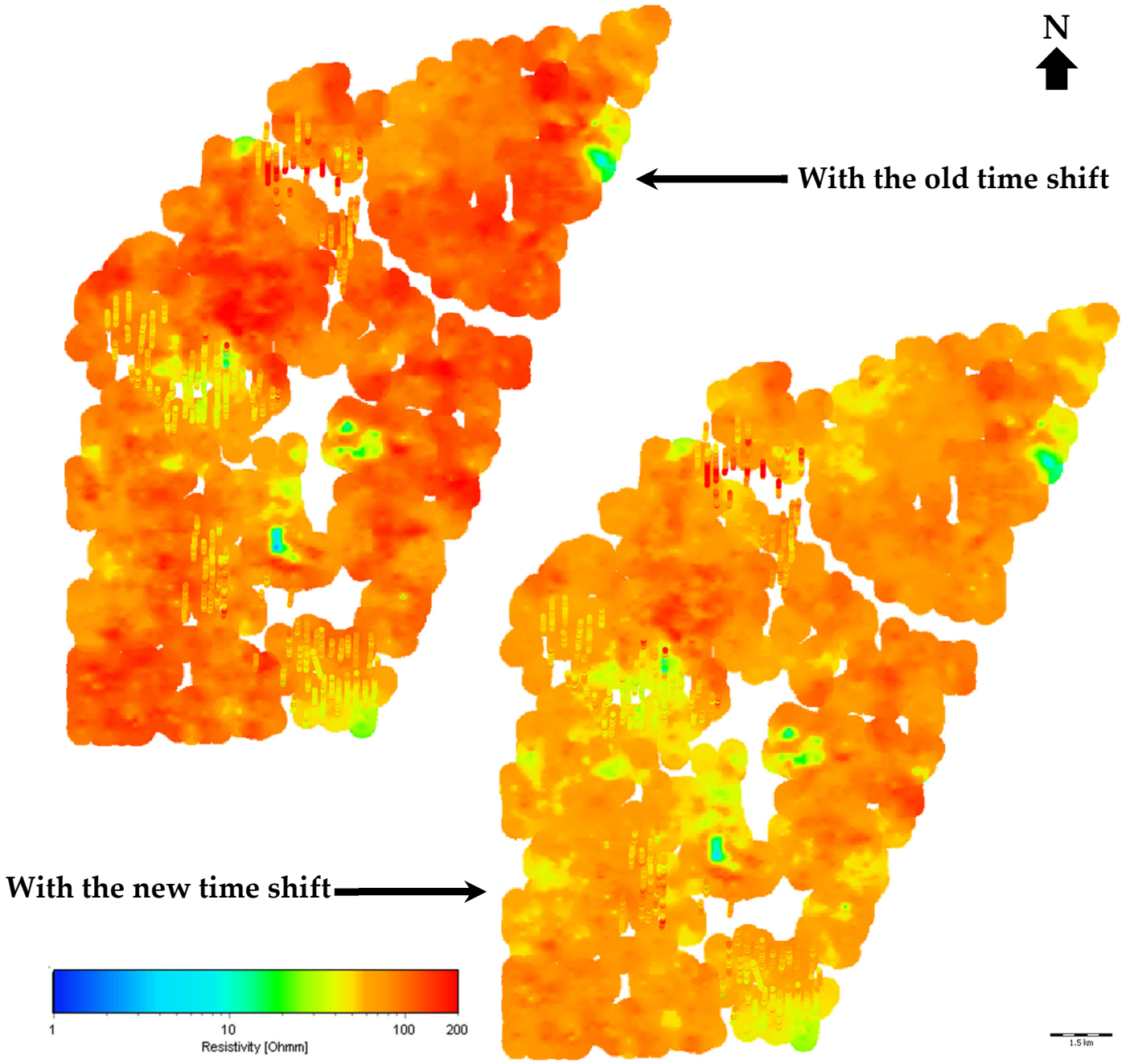

Figure 36. Mean resistivity map for depth 15-20 m - SCI smooth bias inversion on Sorø SkyTEM data with the old and the new time shifts. Inversion parameters: vertical constraint = 2, lat. const.=1.35, starting model of 100 Ωm, and first gate 5. The colored points correspond to the mean resistivity obtain from a SCI smooth inversion of ERT data.

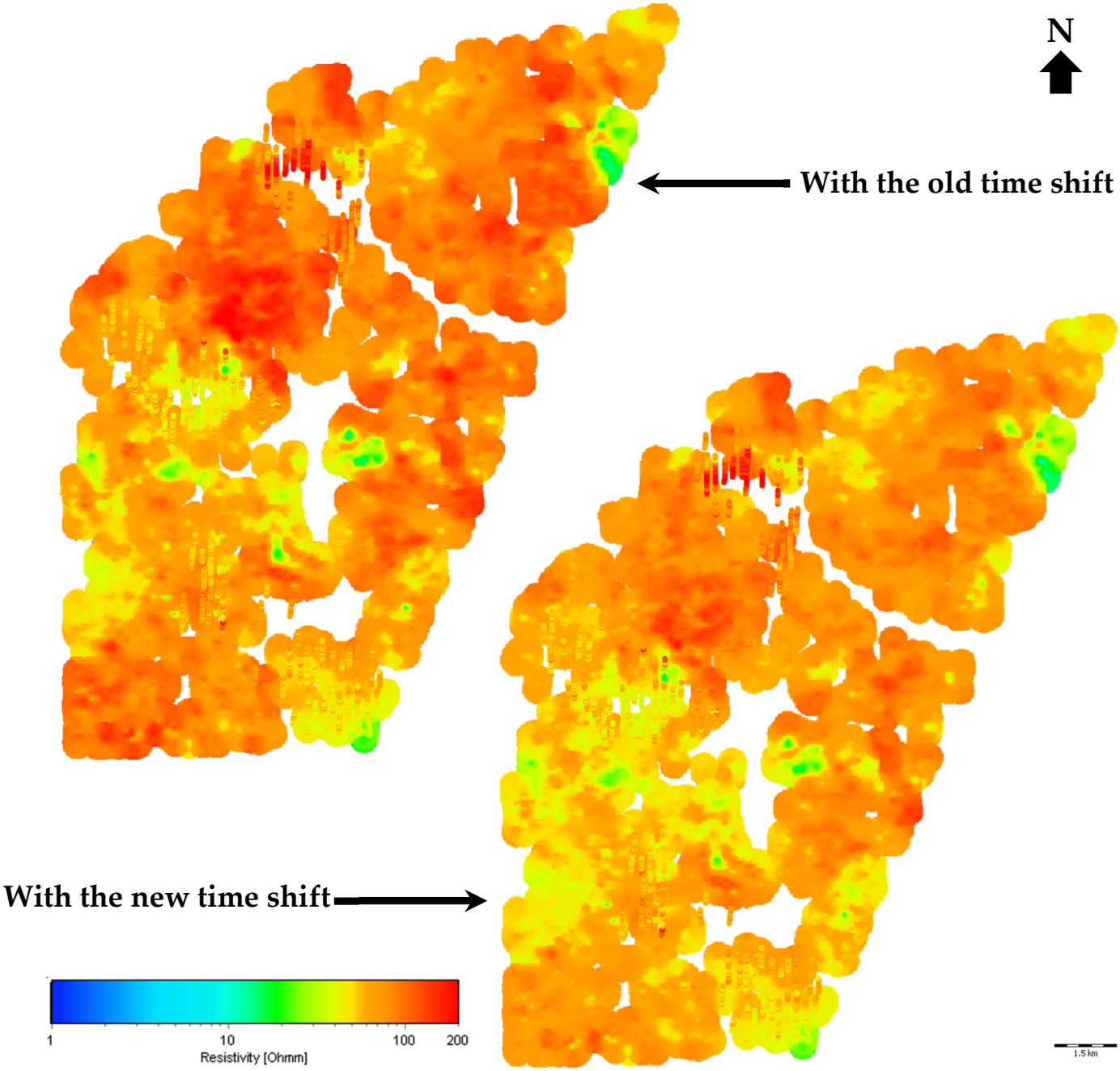

Figure 37. Mean resistivity map for depth 20-25 m - SCI smooth bias inversion on Sorø SkyTEM data with the old and the new time shifts. Inversion parameters: vertical constraint = 2, lat. const.=1.35, starting model of 100 Ωm, and first gate 5. The colored points correspond to the mean resistivity obtain from a SCI smooth inversion of ERT data.

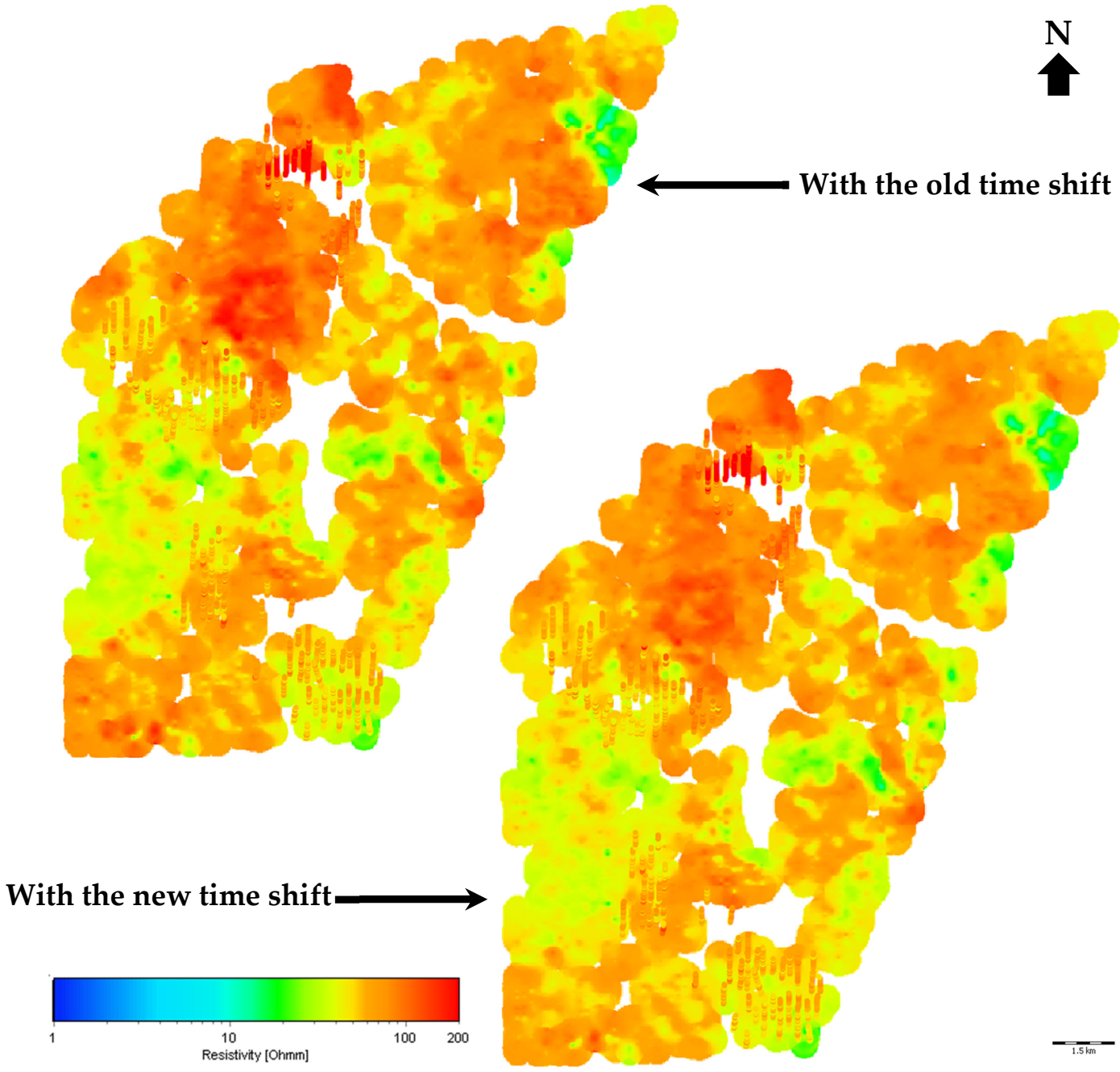

Figure 38. Mean resistivity map for depth 25-30 m - SCI smooth bias inversion on Sorø SkyTEM data with the old and the new time shifts. Inversion parameters: vertical constraint = 2, lat. const.=1.35, starting model of 100 Ωm, and first gate 5. The colored points correspond to the mean resistivity obtain from a SCI smooth inversion of ERT data.

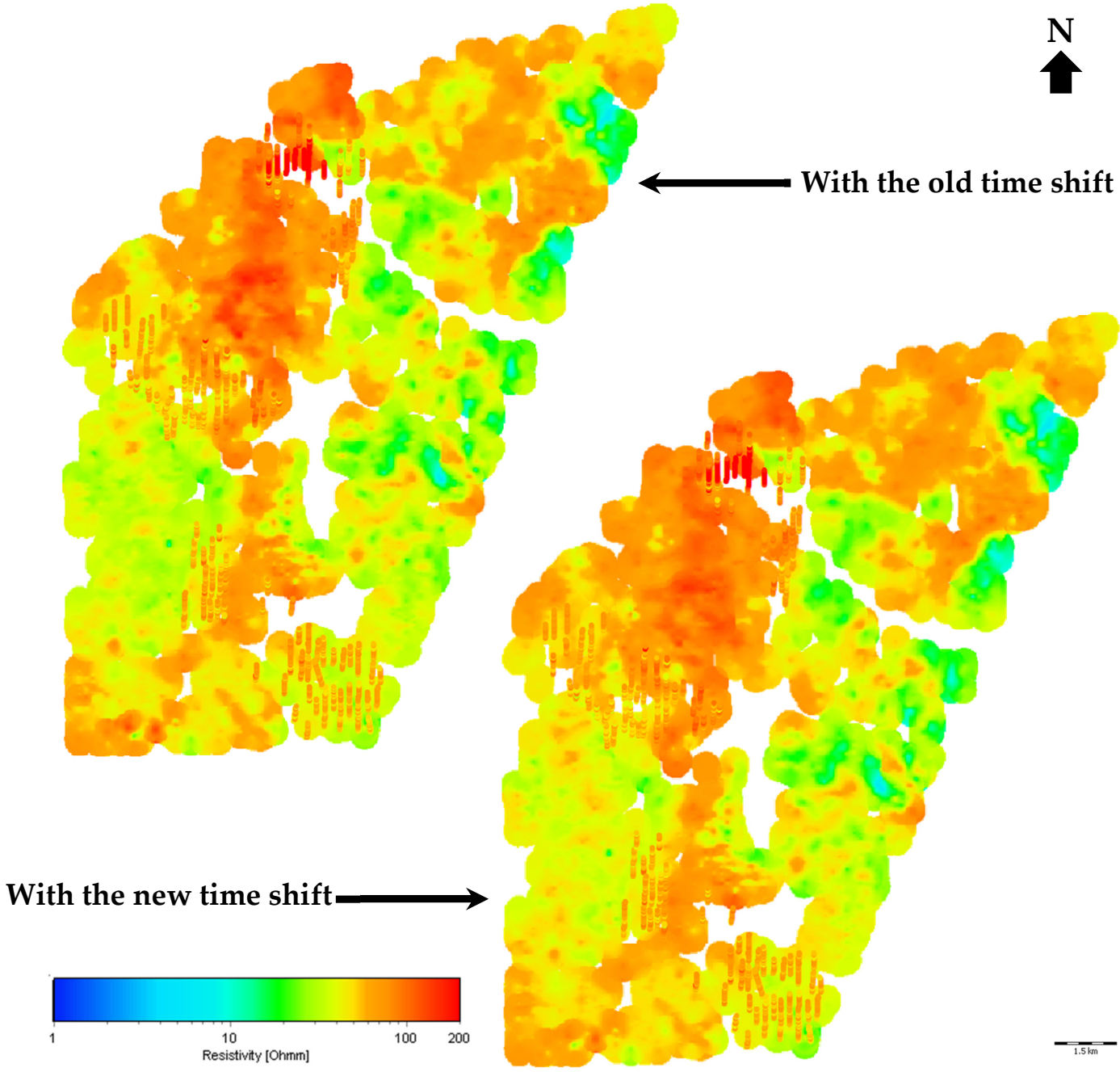

Figure 39. Mean resistivity map for depth 30-35 m - SCI smooth bias inversion on Sorø SkyTEM data with the old and the new time shifts. Inversion parameters: vertical constraint = 2, lat. const.=1.35, starting model of 100 Ωm, and first gate 5. The colored points correspond to the mean resistivity obtain from a SCI smooth inversion of ERT data.

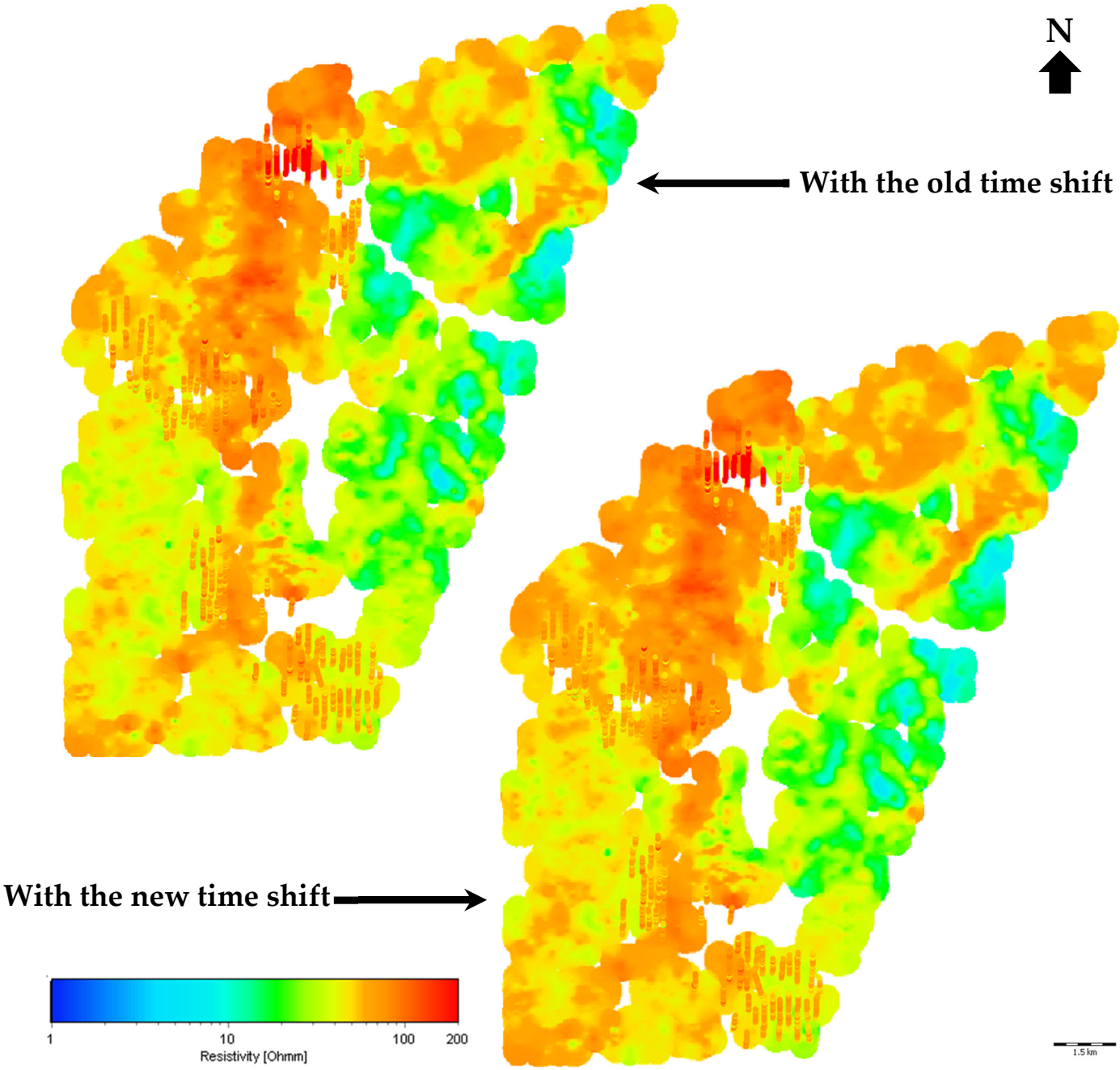

Figure 40. Mean resistivity map for depth 35-40 m - SCI smooth bias inversion on Sorø SkyTEM data with the old and the new time shifts. Inversion parameters: vertical constraint = 2, lat. const.=1.35, starting model of 100 Ωm, and first gate 5. The colored points correspond to the mean resistivity obtain from a SCI smooth inversion of ERT data.

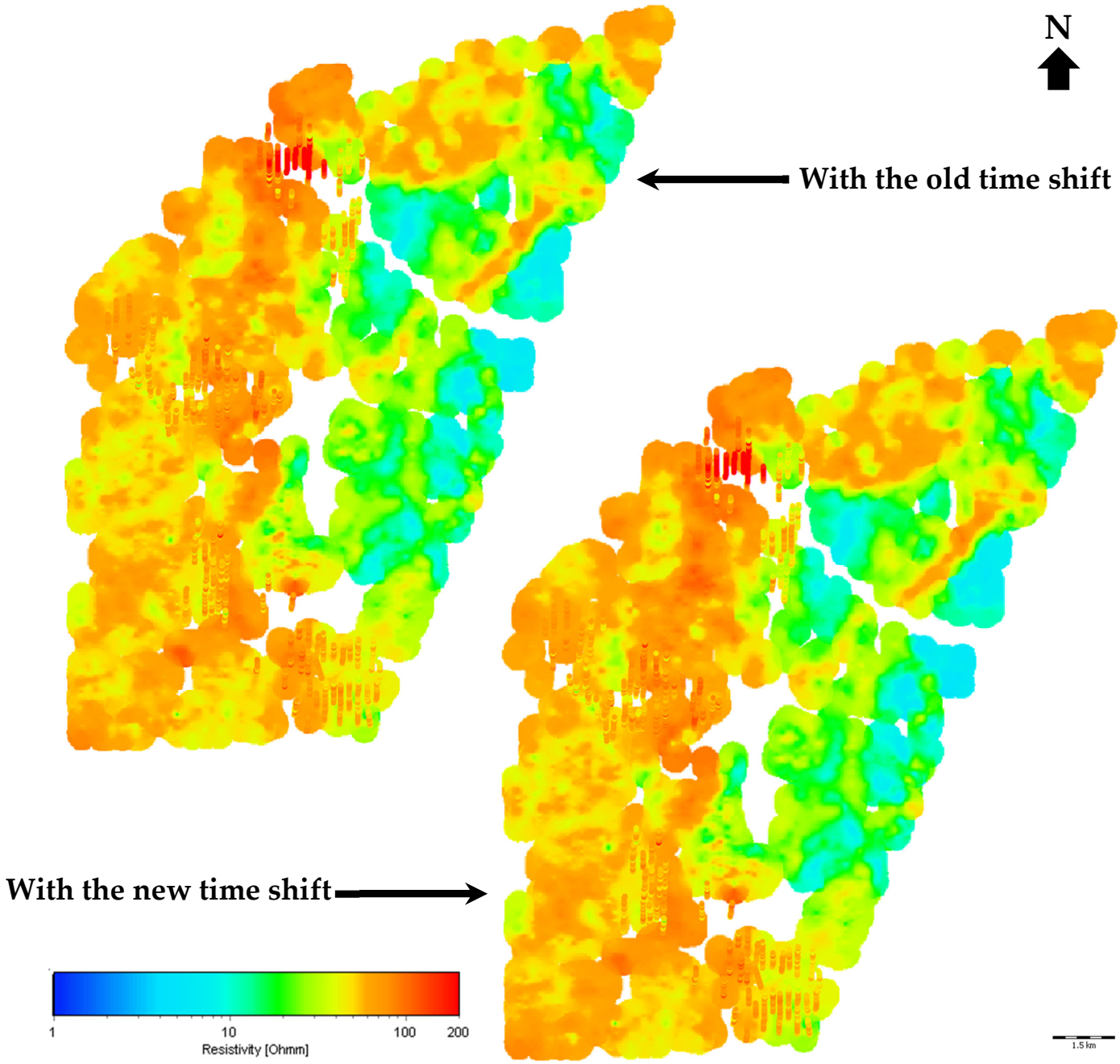

Figure 41. Mean resistivity map for depth 40-45 m - SCI smooth bias inversion on Sorø SkyTEM data with the old and the new time shifts. Inversion parameters: vertical constraint = 2, lat. const.=1.35, starting model of 100 Ωm, and first gate 5. The colored points correspond to the mean resistivity obtain from a SCI smooth inversion of ERT data.

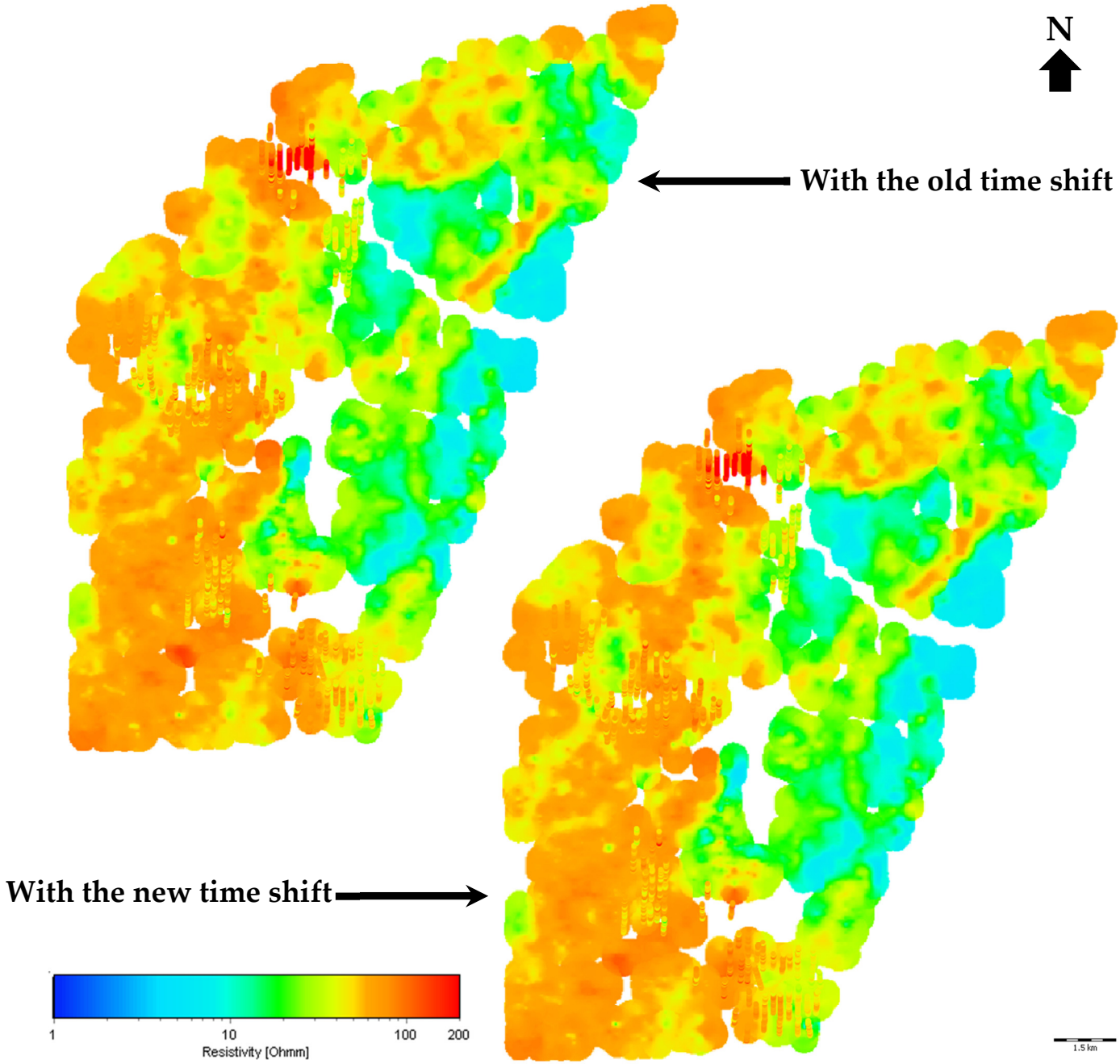

Figure 42. Mean resistivity map for depth 45-50 m - SCI smooth bias inversion on Sorø SkyTEM data with the old and the new time shifts. Inversion parameters: vertical constraint = 2, lat. const.=1.35, starting model of 100 Ωm, and first gate 5. The colored points correspond to the mean resistivity obtain from a SCI smooth inversion of ERT data.

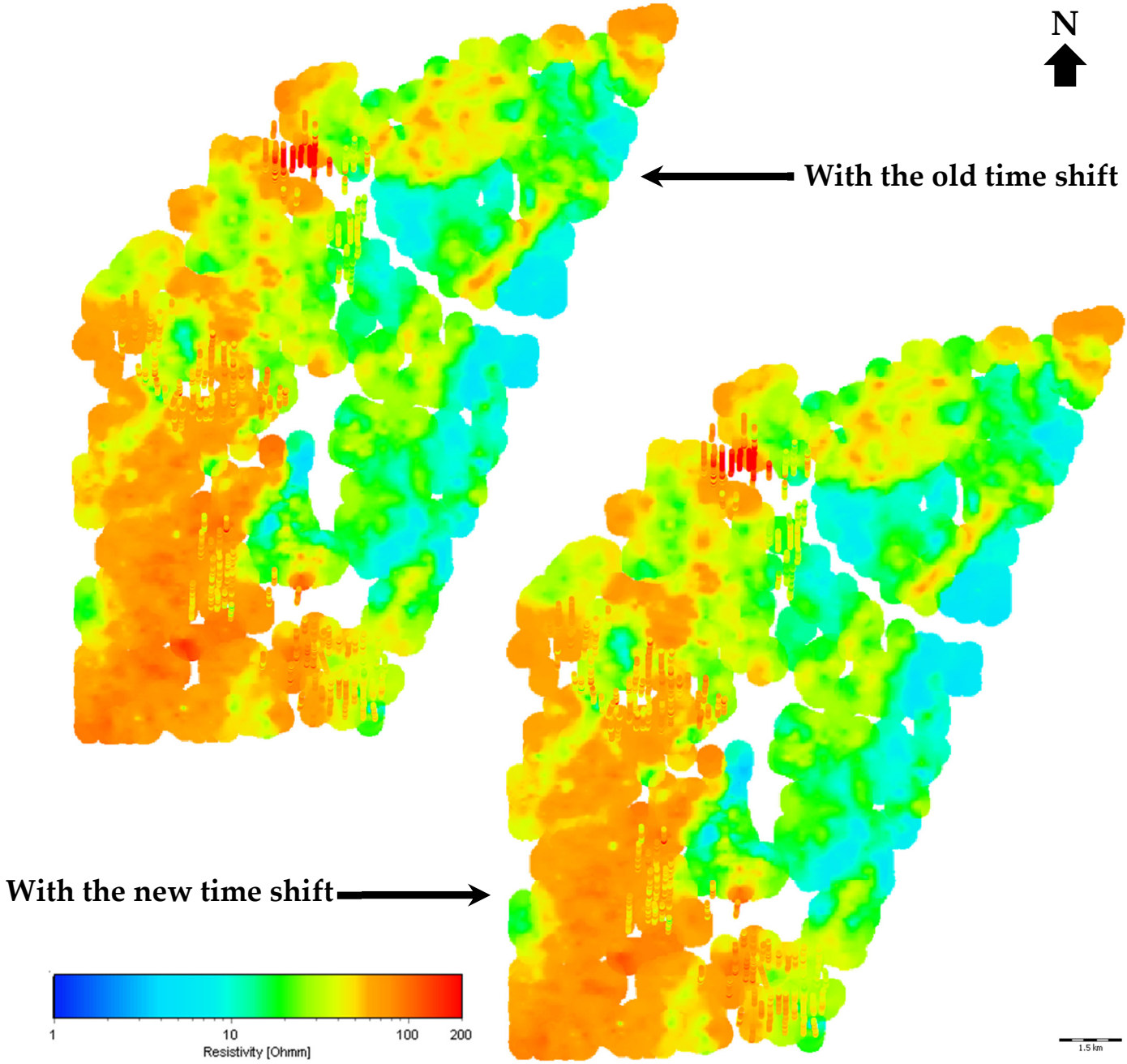

Figure 43. Mean resistivity map for depth 50-55 m - SCI smooth bias inversion on Sorø SkyTEM data with the old and the new time shifts. Inversion parameters: vertical constraint = 2, lat. const.=1.35, starting model of 100 Ωm, and first gate 5. The colored points correspond to the mean resistivity obtain from a SCI smooth inversion of ERT data.

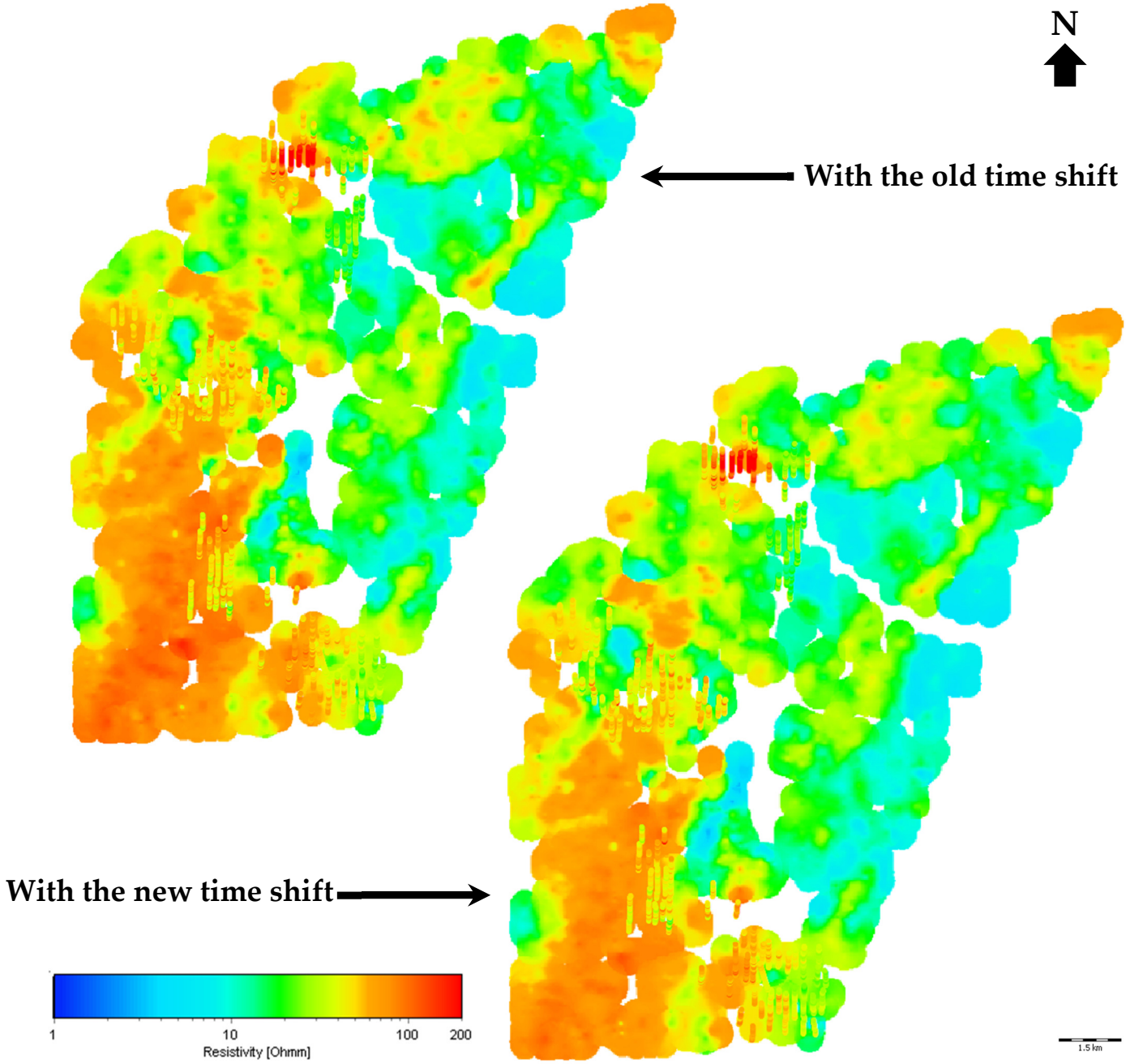

Figure 44. Mean resistivity map for depth 55-60 m - SCI smooth bias inversion on Sorø SkyTEM data with the old and the new time shifts. Inversion parameters: vertical constraint = 2, lat. const.=1.35, starting model of 100 Ωm, and first gate 5. The colored points correspond to the mean resistivity obtain from a SCI smooth inversion of ERT data.

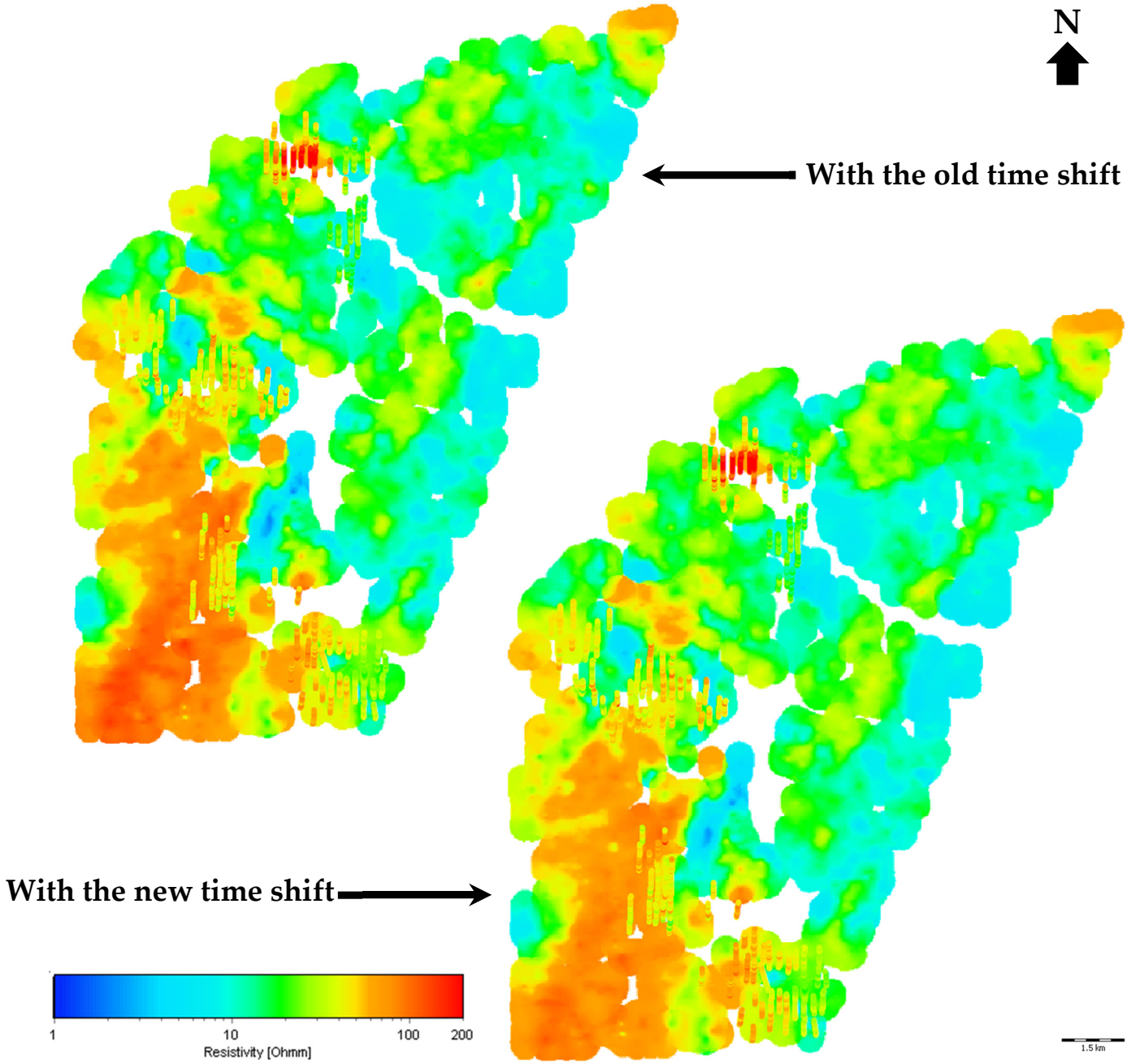

Figure 45. Mean resistivity map for depth 60-65 m - SCI smooth bias inversion on Sorø SkyTEM data with the old and the new time shifts. Inversion parameters: vertical constraint = 2, lat. const.=1.35, starting model of 100 Ωm, and first gate 5. The colored points correspond to the mean resistivity obtain from a SCI smooth inversion of ERT data.

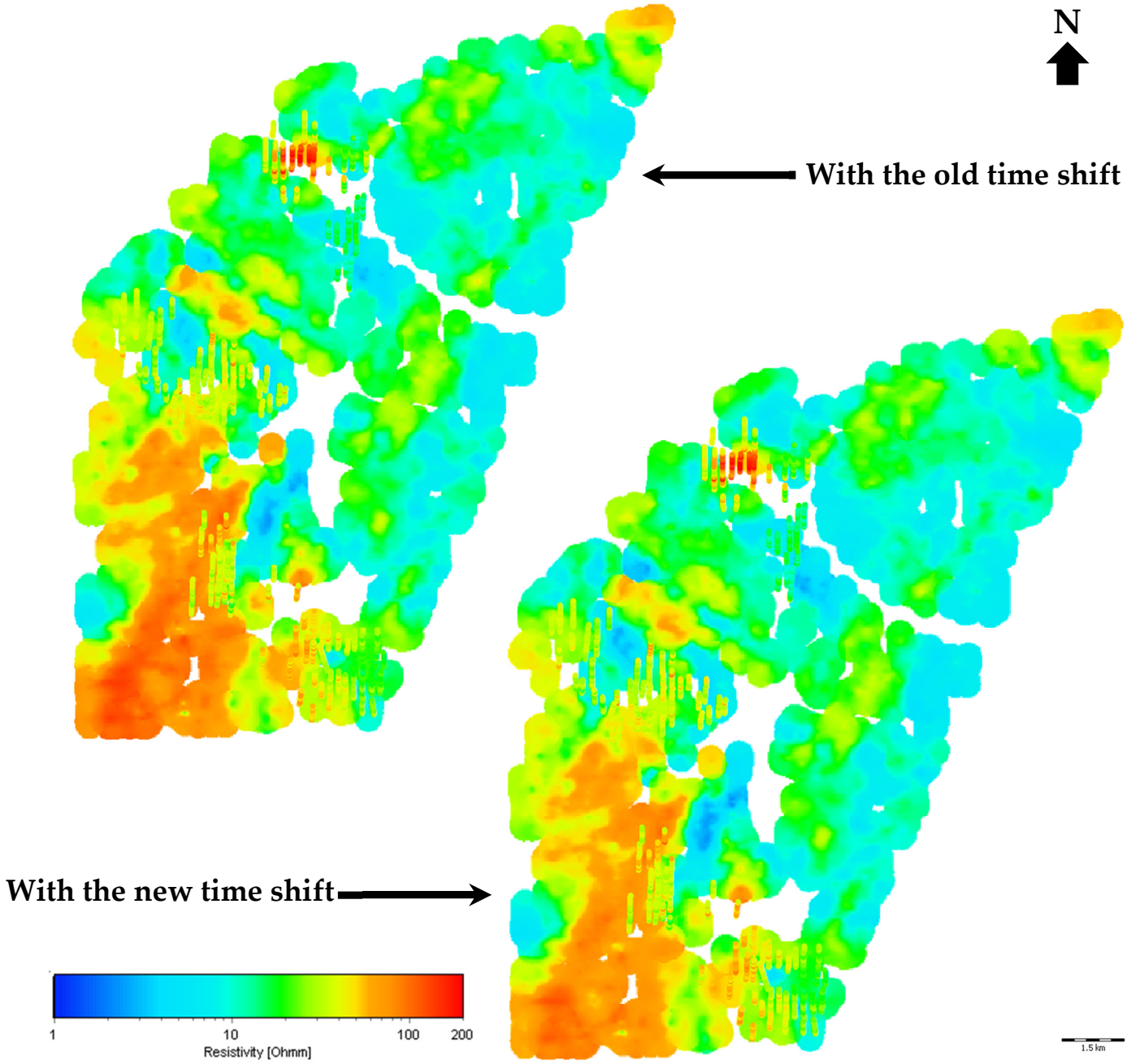

Figure 46. Mean resistivity map for depth 65-70 m - SCI smooth bias inversion on Sorø SkyTEM data with the old and the new time shifts. Inversion parameters: vertical constraint = 2, lat. const.=1.35, starting model of 100 Ωm, and first gate 5. The colored points correspond to the mean resistivity obtain from a SCI smooth inversion of ERT data.

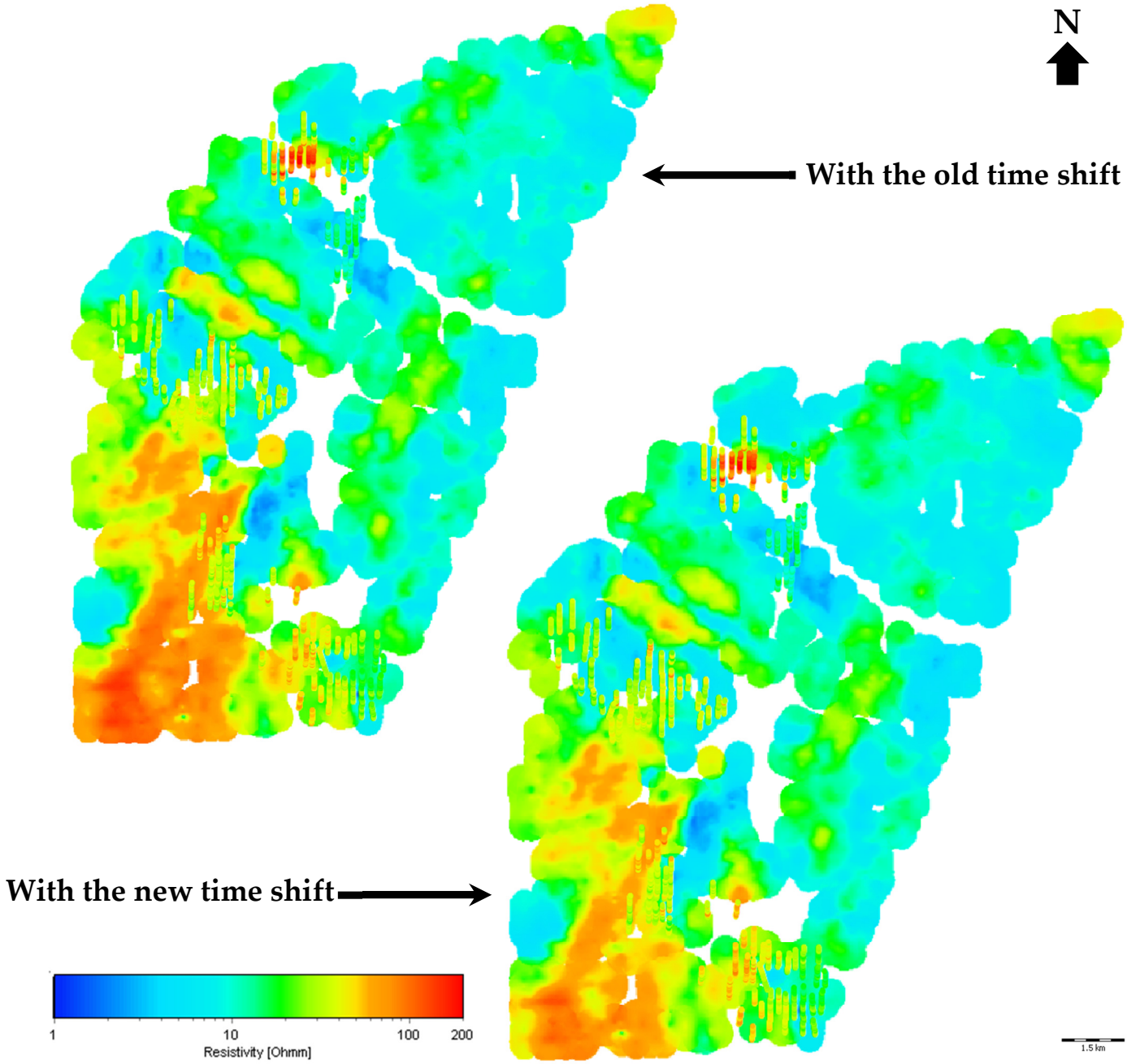

Figure 47. Mean resistivity map for depth 70-75 m - SCI smooth bias inversion on Sorø SkyTEM data with the old and the new time shifts. Inversion parameters: vertical constraint = 2, lat. const.=1.35, starting model of 100 Ωm, and first gate 5. The colored points correspond to the mean resistivity obtain from a SCI smooth inversion of ERT data.

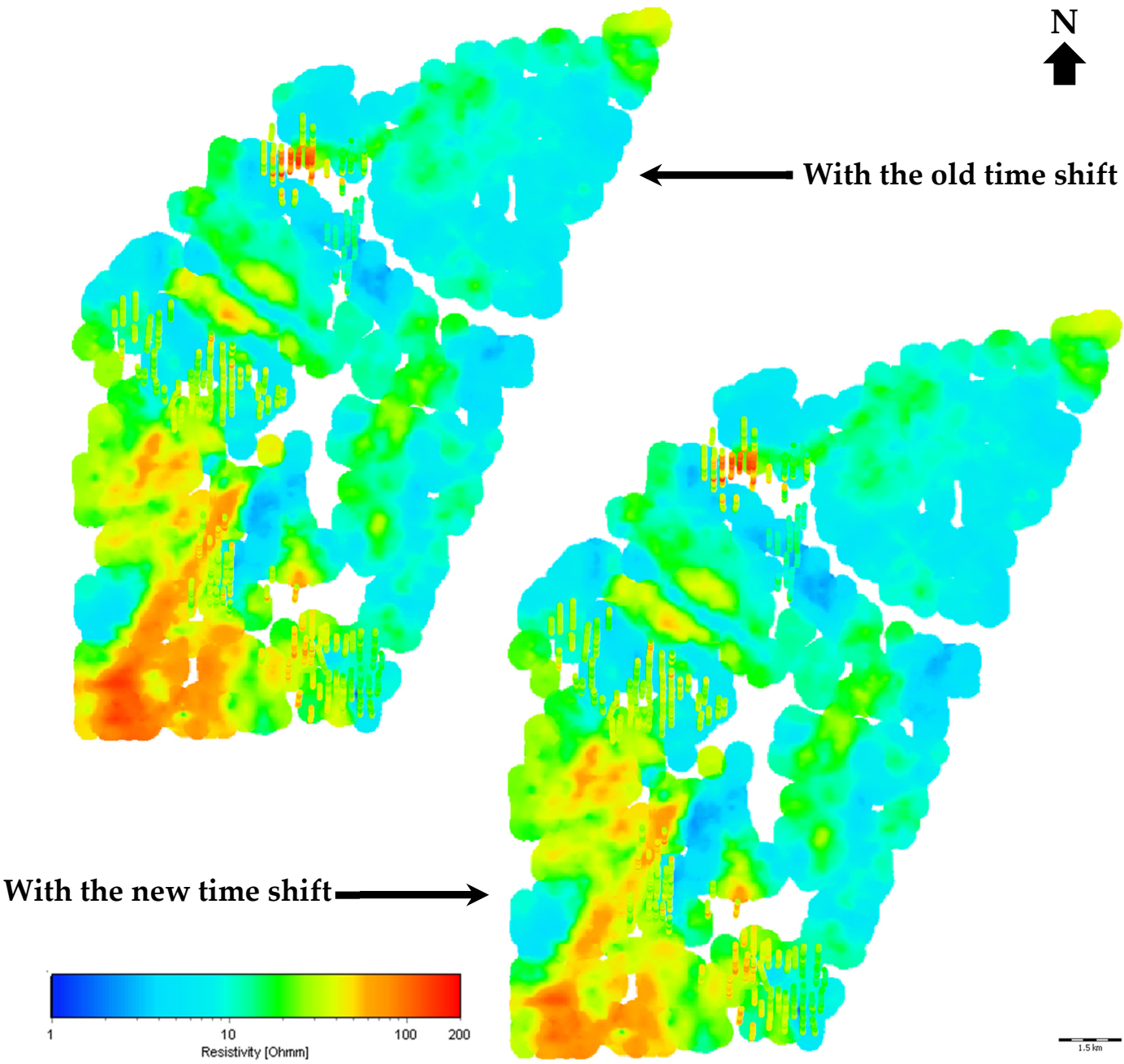

Figure 48. Mean resistivity map for depth 75-80 m - SCI smooth bias inversion on Sorø SkyTEM data with the old and the new time shifts. Inversion parameters: vertical constraint = 2, lat. const.=1.35, starting model of 100 Ωm, and first gate 5. The colored points correspond to the mean resistivity obtain from a SCI smooth inversion of ERT data.

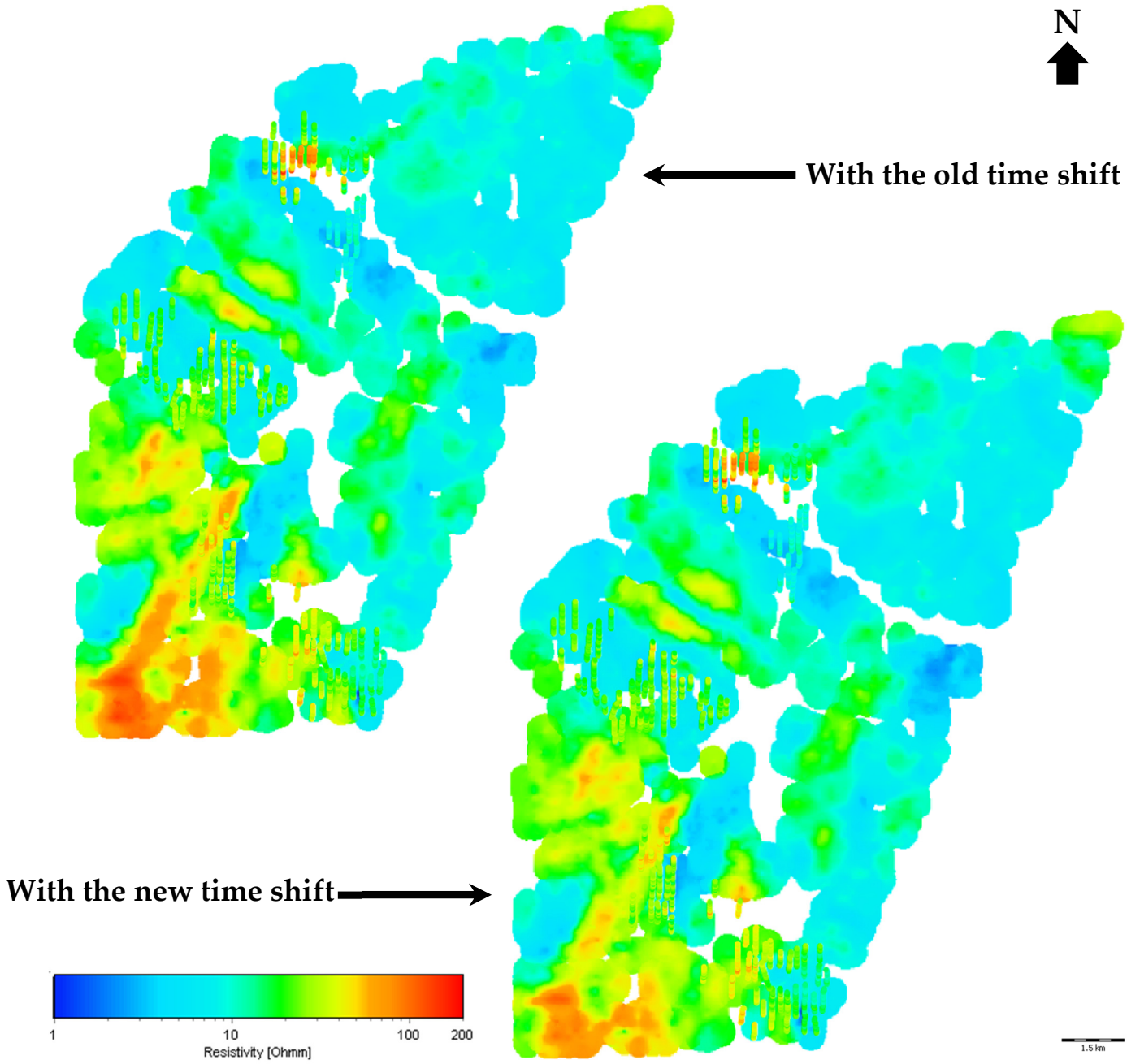

Figure 49. Mean resistivity map for depth 80-85 m - SCI smooth bias inversion on Sorø SkyTEM data with the old and the new time shifts. Inversion parameters: vertical constraint = 2, lat. const.=1.35, starting model of 100 Ωm, and first gate 5. The colored points correspond to the mean resistivity obtain from a SCI smooth inversion of ERT data.

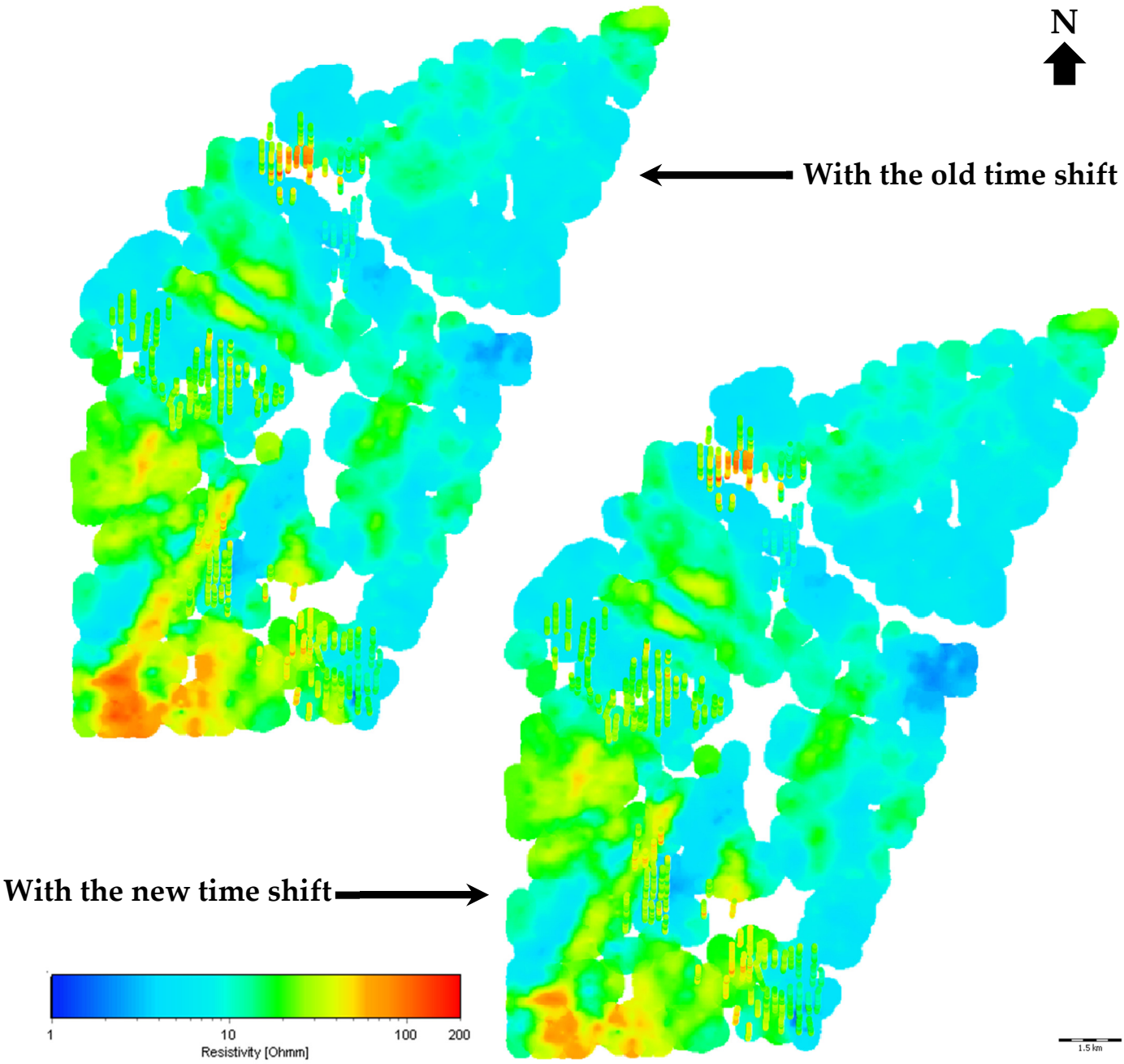

Figure 50. Mean resistivity map for depth 85-90 m - SCI smooth bias inversion on Sorø SkyTEM data with the old and the new time shifts. Inversion parameters: vertical constraint = 2, lat. const.=1.35, starting model of 100 Ωm, and first gate 5. The colored points correspond to the mean resistivity obtain from a SCI smooth inversion of ERT data.

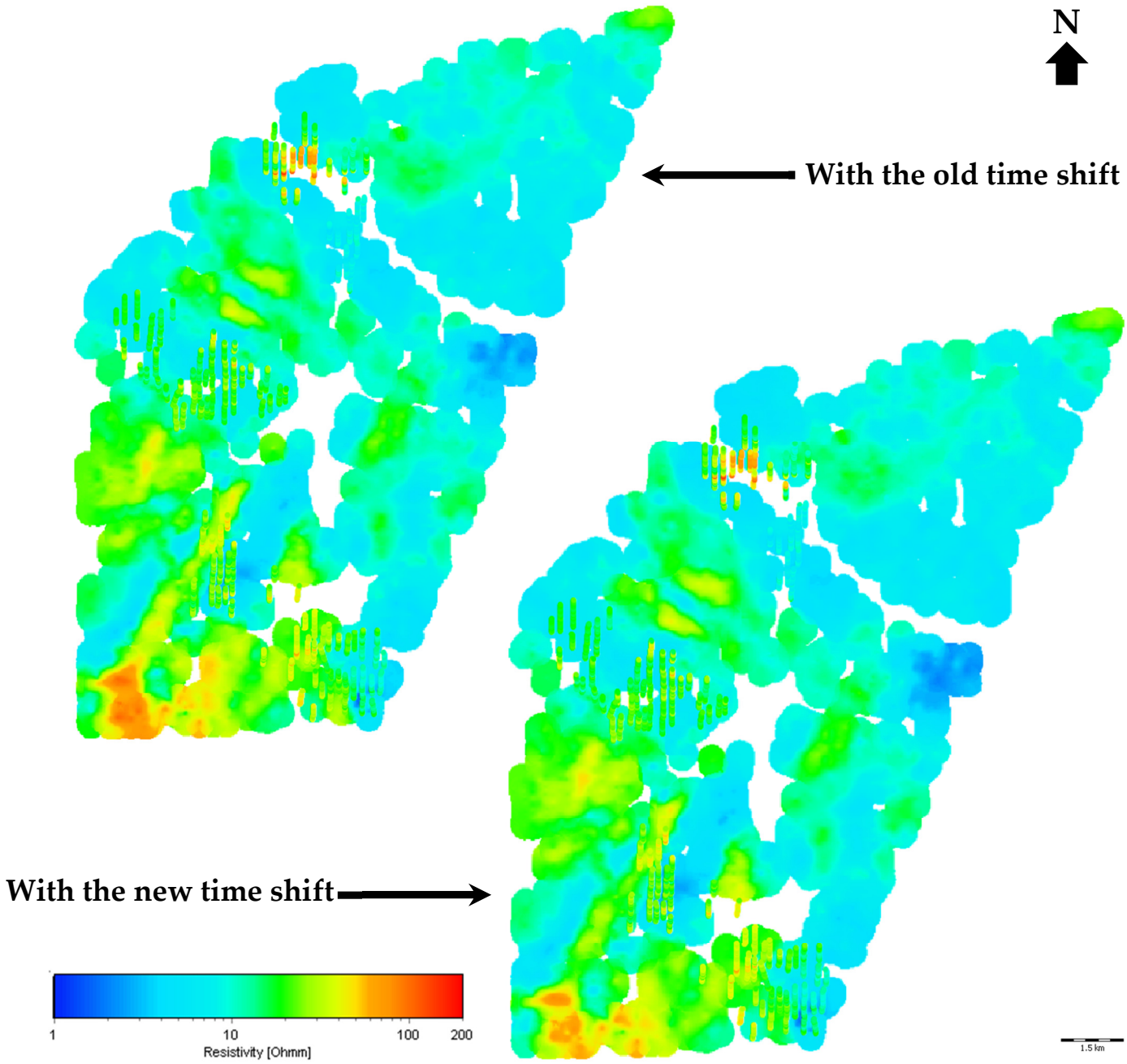

Figure 51. Mean resistivity map for depth 90-95 m - SCI smooth bias inversion on Sorø SkyTEM data with the old and the new time shifts. Inversion parameters: vertical constraint = 2, lat. const.=1.35, starting model of 100 Ωm, and first gate 5. The colored points correspond to the mean resistivity obtain from a SCI smooth inversion of ERT data.

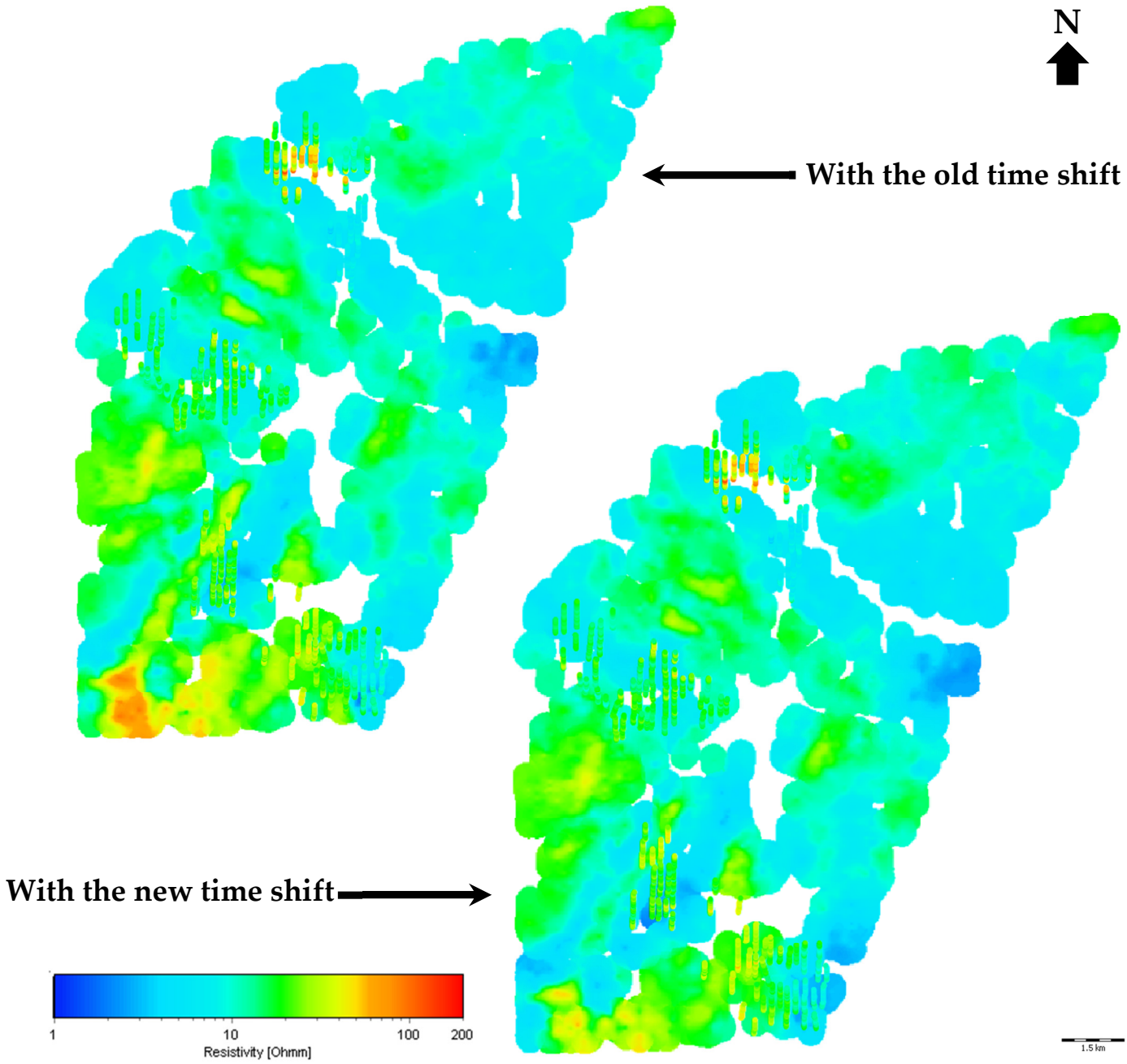

Figure 52. Mean resistivity map for depth 95-100 m - SCI smooth bias inversion on Sorø SkyTEM data with the old and the new time shifts. Inversion parameters: vertical constraint = 2, lat. const.=1.35, starting model of 100 Ωm, and first gate 5. The colored points correspond to the mean resistivity obtain from a SCI smooth inversion of ERT data.